

Aus dem Institut für Neuropathologie  
(Prof. Dr. med. Christine Stadelmann-Nessler)  
der Medizinischen Fakultät der Universität Göttingen

**Direct, indirect and longitudinal  
immunological effects of anti-CD20  
mediated B cell depletion in Multiple  
Sclerosis**

INAUGURAL-DISSERTATION

zur Erlangung des Doktorgrades  
der Medizinischen Fakultät der  
Georg-August-Universität zu Göttingen

vorgelegt von

**Nitzan Nissimov**

aus

Tel-Aviv, Israel

Göttingen 2021

Dekan: Prof. Dr. med. W. Brück

### **Betreuungsausschuss**

Betreuer: Prof. Dr. med. M. S. Weber

Ko-Betreuer: PD Dr. rer. nat. F. Lühder

### **Prüfungskommission**

Referent: Prof. Dr. med. M. S. Weber

Ko-Referent/in: .....

Drittreferent/in: .....

Datum der mündlichen Prüfung: .....

Hiermit erkläre ich, die Dissertation mit dem Titel „Direct, indirect and longitudinal immunological effects of anti-CD20 mediated B cell depletion in Multiple Sclerosis“ eigenständig angefertigt und keine anderen als die von mir angegebenen Quellen und Hilfsmittel verwendet zu haben.

Göttingen, den 10.02.2021

---

Nitzan Nissimov

Die Daten, auf denen die vorliegende Arbeit basiert, wurden teilweise publiziert:

**Nissimov N**, Hajyeva Z, Torke S, Grondey K, Brück W, Häusser-Kinzel S, Weber MS (2020): B cells reappear less mature and more activated after their anti-CD20-mediated depletion in multiple sclerosis. *Proc Natl Acad Sci U S A* 117, 25690–25699

## Table of contents

<b>List of figures .....</b>	<b>III</b>
<b>List of tables.....</b>	<b>V</b>
<b>Abbreviations .....</b>	<b>VI</b>
<b>1 Introduction .....</b>	<b>1</b>
1.1 Multiple sclerosis.....	1
1.1.1 MS in general .....	1
1.1.2 Etiology, pathogenesis, pathophysiology and neuropathology.....	1
1.1.3 Symptoms and diagnosis.....	8
1.1.4 MS therapies.....	10
1.2 Anti-CD20 antibodies (Rituximab, Ocrelizumab, Ofatumumab).....	11
1.2.1 Mechanism of action of anti-CD20 antibodies .....	11
1.2.2 Clinical trials in MS .....	12
1.3 Atacicept.....	12
1.4 Aims of the study .....	13
1.4.1 Direct effects of anti-CD20 depletion on CD20 <sup>+</sup> B and T cells .....	13
1.4.2 Indirect effects on other immune cell populations.....	13
1.4.3 Correlation with clinical parameters.....	13
<b>2 Materials and Methods .....</b>	<b>14</b>
2.1 Patients.....	14
2.2 Materials.....	15
2.3 Methods.....	19
2.3.1 PBMC isolation .....	19
2.3.2 Flow cytometry panels.....	20
2.3.3 Flow cytometry and gating strategy.....	27
2.3.4 TBNK classification .....	29
2.3.5 Statistical analysis.....	29
<b>3 Results.....</b>	<b>30</b>
3.1 Direct effects of anti-CD20 depletion on CD20 <sup>+</sup> B and T cells .....	30
3.1.1 Effects on B cells .....	30
3.1.2 Effects on CD20 <sup>+</sup> T cells.....	34
3.2 Indirect effects on other immune cell populations.....	39
3.2.1 Effects on CD20 <sup>-</sup> T cells.....	39
3.2.2 Effects on myeloid cells .....	44
3.3 Correlation with clinical parameters.....	50
<b>4 Discussion.....</b>	<b>56</b>
<b>5 Summary .....</b>	<b>62</b>

---

<b>6</b>	<b>Supplement .....</b>	<b>63</b>
6.1	Certificate – TBNK classification.....	63
6.2	Correlation between naïve and memory B cell frequencies and age.....	64
6.3	Data to different B cell activation, APC function and cytokine phenotype among the two patient groups .....	64
6.4	Data to different cell phenotypes among the two patient groups.....	66
6.4.1	Data to CD4 <sup>+</sup> T <sub>H</sub> cells.....	66
6.4.2	Data to CD8 <sup>+</sup> T <sub>C</sub> cells .....	67
6.4.3	Data to CD14 <sup>+</sup> myeloid cells.....	68
<b>7</b>	<b>References .....</b>	<b>71</b>

## List of figures

Figure 1. B cells targeted therapies.....	11
Figure 2. T cell maturation.....	22
Figure 3. Gating strategy.....	28
Figure 4. B cell frequency and cell count.....	30
Figure 5. B cell maturation phenotype.....	31
Figure 6. B cell activation phenotype.....	31
Figure 7. B cell APC phenotype.....	32
Figure 8. B cell cytokine phenotype.....	33
Figure 9. Overview of CD20 <sup>+</sup> cells population.....	34
Figure 10. CD20 <sup>+</sup> T cells frequencies.....	35
Figure 11. Time to detection of CD20 <sup>+</sup> cells' repletion.....	36
Figure 12. T4/T8 ratio.....	36
Figure 13. CD20 <sup>+</sup> CD4 <sup>+</sup> T <sub>H</sub> cells maturation and CD25 expression phenotype.....	37
Figure 14. CD20 <sup>+</sup> CD8 <sup>+</sup> T <sub>C</sub> cells maturation and CD25 expression phenotype.....	38
Figure 15. CD4 <sup>+</sup> T <sub>H</sub> cells frequency and cell count.....	39
Figure 16. CD4 <sup>+</sup> T <sub>H</sub> cells maturation phenotype.....	40
Figure 17. CD4 <sup>+</sup> T <sub>H</sub> cells' CD62L expression.....	41
Figure 18. CD8 <sup>+</sup> T <sub>C</sub> cells frequency and count.....	41
Figure 19. CD8 <sup>+</sup> T <sub>C</sub> cells maturation phenotype.....	42
Figure 20. CD8 <sup>+</sup> T <sub>C</sub> cells' CD62L expression.....	43
Figure 21. CD14 <sup>+</sup> myeloid cells frequency and monocytes' cell count.....	44
Figure 22. Myeloid cells' activation phenotype.....	45
Figure 23. Myeloid cells' APC phenotype I.....	46
Figure 24. Myeloid cells' APC phenotype II.....	47
Figure 25. Myeloid cells' IL-6 phenotype.....	48
Figure 26. Myeloid cells' IL-10 and TNF- $\alpha$ phenotype.....	49
Figure 27. Correlation between B cell frequency/count with age and sex.....	50
Figure 28. Correlation between naïve and memory B cell frequencies with EDSS score.....	51
Figure 29. Memory/balanced and naïve type.....	52
Figure 30. Correlation between the time to detection of CD20 <sup>+</sup> cells repletion and age.....	54
Figure 31. Correlation between frequencies of CD20 <sup>+</sup> T cells and age.....	55
Figure A1. Correlation between naïve and memory B cell frequencies and age.....	64
Figure A2. Differences in B cell activation phenotype between memory/balanced and naïve type.....	64
Figure A3. Differences in B cell cytokine phenotype between memory/balanced and naïve type.....	65
Figure A4. Differences in CD4 <sup>+</sup> T <sub>H</sub> cells maturation and CD62L expression phenotype between memory/balanced and naïve type.....	66
Figure A5. Differences in CD8 <sup>+</sup> T <sub>C</sub> cells maturation and CD62L expression phenotype between memory/balanced and naïve type.....	67
Figure A6. Differences in CD14 <sup>+</sup> myeloid cells activation and APC phenotype between memory/balanced and naïve type.....	68

---

Figure A7. Differences in CD14 <sup>+</sup> myeloid cells cytokine phenotype between memory/balanced and naïve type I .....	69
Figure A8. Differences in CD14 <sup>+</sup> myeloid cells cytokine phenotype between memory/balanced and naïve type II.....	70

---

## List of tables

Table 1: McDonald criteria.....	9
Table 2: Characteristics of patient cohort .....	14
Table 3: Human monoclonal antibodies for flow cytometry .....	15
Table 4: List of reagents.....	17
Table 5: List of buffers and cell culture media .....	18
Table 6: List of consumables.....	18
Table 7: List of devices and softwares .....	19
Table 8: Flow cytometry panels I .....	20
Table 9: Flow cytometry panels II.....	20
Table 10: Flow cytometry panels III.....	21
Table 11: Stimulation regimes .....	25
Table 12: Differences in immune cell phenotype after anti-CD20 depletion between patients with memory/balanced and naïve B cell phenotype pre-depletion.....	53

## Abbreviations

ADCC	antibody dependent cytotoxicity
APC	antigen presenting cell
APRIL	a proliferation-inducing ligand
AQP	aquaporin
ARR	annualized relapse rate
BAFF	B cell activating factor
BBB	blood brain barrier
BCR	B cell receptor
BLyS	B lymphocyte stimulator
BSA	bovine serum albumin
CCR	CC-chemokine receptor
CD	cluster of differentiation
CDC	complement dependent cytotoxicity
CIS	clinically isolated syndrome
CNS	central nervous system
CpG	cytosine-phosphate-guanine
CSF	cerebrospinal fluid
CXCL	chemokine (C-X-C motif) ligand
DC	dendritic cells
ddH <sub>2</sub> O	double-distilled water
DIS	dissemination in space
DIT	dissemination in time
DMEM	Dulbecco's Modified Eagle's medium
DMF	dimethyl fumarate
DMSO	dimethyl-sulfoxide
DNA	deoxyribonucleic acid
EAE	experimental autoimmune encephalomyelitis
EBNA	Epstein Barr nuclear antigen
EBV	Epstein-Barr virus

---

EDSS	expanded disability status scale
EDTA	ethylene diamine tetraacetic acid
FACS	fluorescence-activated cell sorting
FCS	fetal calf serum
FDA	Food and Drug Administration
HLA	human leukocyte antigen
i. m.	intramuscularly
i. v.	intravenously
ICD-10	International Classification of Diseases, 10 <sup>th</sup> version
IFN	interferon
IgG	immunoglobulin G
IL	interleukin
IMSGC	International Multiple Sclerosis Genetics Consortium
LPS	lipopolysaccharide
LT	lymphotoxin
mAb	monoclonal antibody
MBP	myelin basic protein
MFI	mean fluorescence intensity
MHC	major histocompatibility complex
MOG	myelin oligodendrocyte glycoprotein
MRI	magnetic resonance imaging
MS	multiple sclerosis
Na <sub>v</sub>	voltage-gated sodium channels
NF- $\kappa$ B	nuclear factor kappa-light-chain-enhancer of activated B cells
NK cells	natural killer cells
OCB	oligoclonal bodies
p. o.	per os
PBMC	peripheral blood mononuclear cells
PBS	phosphate buffered salt solution
PFA	paraformaldehyde

---

PKC	protein kinase C
PLP	proteolipid protein
PMA	phorbol 12-myristate 13-acetate
PPMS	primary progressive multiple sclerosis
PRMS	progressive relapsing multiple sclerosis
PTPRC	protein tyrosine phosphatase receptor type C
rpm	revolutions per minute
RPMI-1640	Roswell park memorial institute-1640
RRMS	relapsing remitting multiple sclerosis
s. c.	subcutaneously
SPMS	secondary progressive multiple sclerosis
TB NK	T, B, NK cells
T <sub>C</sub> cells	cytotoxic T cells
T <sub>CM</sub>	central memory T cells
TCR	T cells receptor
T <sub>EM</sub>	effector memory T cells
T <sub>EMRA</sub>	terminally differentiated effector memory T cells
T <sub>H</sub> cells	T helper cells
TLR	toll-like receptor
TMB	tetramethylbenzidine
T <sub>N</sub>	naïve T cells
TNF	tumor necrosis factor
T <sub>reg</sub>	regulatory T cells
T <sub>TD</sub>	terminally differentiated T cells

# 1 Introduction

## 1.1 Multiple sclerosis

Multiple sclerosis (MS, disseminate encephalomyelitis, ICD-10: G35) is a chronic primarily inflammatory disease of the central nervous system (CNS) in which myelin and axons are damaged due to focal lymphocytes' infiltration (Compston and Coles 2008). MS is a common neurological disorder and in some regions the lead cause of nontraumatic neurological disability in young adults (Browne et al. 2014).

### 1.1.1 MS in general

Epidemiology: as of 2007, approximately 1.3 million people worldwide were diagnosed with MS, in 2008 2.1 and in 2013 2.3, and is estimated at 2.5 million in 2018 (Dua et al. 2008; Browne et al. 2014). The incidence peak lays between 25-35 years, even though up to 3-5% develop the disease before the age of 18. MS is more common in the United States, Europe, Canada, Australia and New Zealand, and is, on the other hand, rare in Asia and in tropical and subtropical areas. Women are twice to thrice more affected than men (lifetime risk of 1 in 200 women) (Ascherio and Munger 2016).

### 1.1.2 Etiology, pathogenesis, pathophysiology and neuropathology

#### 1.1.2.1 Genetic susceptibility and environmental factors

Multiple sclerosis has a familial recurrence rate of approximately 20%, whereas the risk in white northern Europeans is 0.3%. Various genetic variations could be accounted for approximately 30% of overall disease risk, and more than 100 specific genetic regions were identified as associated with MS, explaining approx. one third of the entire genetic component, though non genetic factors have a larger contribution to the heterogeneity of the disease (International Multiple Sclerosis Genetics Consortium (IMSGC) et al. 2013; Brodin et al. 2015). An association between MS and the alleles of the human leukocyte antigens (*HLA*-) *DR15* and *DQ6* and the corresponding genotypes *DRB1\*1501*, *DRB5\*0101*, *DQA1\*0107*, and *DQB2\*0602* is described, and strongest in northern Europe. In other groups, MS is associated with *HLA-DR4* and the genotypes *DRB1\*0405*, *DQA1\*0301* and *DQB1\*0302*. On the other hand, the loci *HLA-C554* and *HLA-DRB1\*11* are suggested to have a protective effect (Olerup and Hillert 1991; Marrosu et al. 1992; Ramagopalan et al. 2007).

Epstein-Barr virus (EBV) infection and high anti-Epstein-Barr nuclear protein 1 (anti-EBNA1) IgG titers were suggested as a possible cause for MS (see below). A mechanism of molecular mimicry between *DRB5\*0101*-EBV peptide complex and *DRB1\*1501*-restricted myelin basic protein (MBP) was discussed to enlighten these findings.

*HLA-DRB1\*1501* can present MBP to CD4<sup>+</sup> T helper cells (CD4<sup>+</sup> T<sub>H</sub> cells), and is the strongest known genetic risk factor for MS (Sawcer et al. 2014). The T cell receptor (TCR) is in fact not antigen specific, but epitope specific, meaning that a TCR could recognize many different antigens, that are often but not always, similar, a phenomenon called receptor degeneracy or polyspecificity (Wucherpfennig and Sethi 2011). A resemblance between the two complexes at the surface presented to the TCR leads to a failed recognition of MBP by CD4<sup>+</sup> T<sub>H</sub> cells, leading to autoimmunity (Lang et al. 2002).

The hygiene hypothesis says, that multiple infections in childhood reduce the risk to develop autoimmune and allergic diseases in adolescence, by modulating the balance between CD4<sup>+</sup> T helper 1 (CD4<sup>+</sup> T<sub>H1</sub>) and CD4<sup>+</sup> T<sub>H2</sub> immunity, the dominant one at birth (Bach 2002). EBV is often mentioned in this context. Epstein-Barr virus is an enveloped  $\gamma$  herpes virus, which infects more than 90% of the world's population, and persists in B lymphocytes. EBV is related to nasopharyngeal carcinoma, Burkitt lymphoma, and Hodgkin lymphoma, but its connection to autoimmune diseases remains unclear. An EBV infection in childhood is usually milder than a fully manifested infectious mononucleosis in adolescents. The epidemiology of infectious mononucleosis in adolescents and adults and of MS suggests that MS could be the result of an EBV infection in adolescents and adults (Ascherio et al. 2001). On the one hand, an early EBV infection is suggested to have a protective effect on the development of MS. A comparison between individuals who could recall an EBV infection and seronegative individuals or individuals who could not recall the infection led to an odds ratio of MS of 2.9% (Martyn et al. 1993). On the other hand, anti-EBNA negative individuals have the lowest risk of MS, but when infected in adolescence, manifesting as infectious mononucleosis, their risk increases sharply, suggesting that individuals raised in a hygienic environment have an increased risk of MS only after EBV infection (Ascherio and Munger 2007; Levin et al. 2010). In a related context it was mentioned, that stress and infections double the risk for relapse because of an increased immune response (Buljevac et al. 2003).

Several epidemiological studies have shown, that vitamin D (25[OH]D) has a protective role in reducing MS risk, especially in childhood and adolescence, and that MS patients do suffer from insufficiency. When corrected, MS patients show a beneficial outcome, clinically and in magnetic resonance imaging (MRI). The mechanism of the above-mentioned is not yet understood, but can be supported by immunomodulatory effects of vitamin D, which increases interleukin (IL-)17 and induces regulatory T (T<sub>reg</sub>) cells (Cantorna et al. 2015; Hayes et al. 2015; Ascherio and Munger 2016).

As another possible environmental factor, the gut microbiome was discussed. Experimental autoimmune encephalomyelitis (EAE, and see 1.1.2.2) studies have shown, that changes in the gut microbiome could alter the severity and incidence of CNS inflammation. Nevertheless, a direct link between the gut microbiome and MS has yet to be discovered (Berer et al. 2011).

Another risk factor known is cigarette smoking. Smoking individuals have an increased risk to develop MS, and passive exposure by parental smoking for example increases the risk to develop pediatric MS (Hernan et al. 2001; Mikaeloff et al. 2007).

#### 1.1.2.2 Pathogenesis

Though the cause of MS is still unknown, there are many theories regarding the pathogenesis of MS, which can be divided into four main categories. In the first, only inflammation is the pathogenic factor, neurodegeneration follows. In the second the neurodegeneration happens first, the inflammation follows. In the third inflammation and neurodegeneration both lead independently to the clinical state. And in the fourth, inflammation reveals an existing predisposition for neurodegeneration, that leads to axonal vulnerability and cumulative injury (Compston and Coles 2008). From those four theories two main models are nowadays discussed: the extrinsic and the intrinsic model.

In the extrinsic model, autoreactive T cells activated in the periphery, most likely through processes of molecular mimicry (see EBV), migrate in the CNS alongside with activated B cells and monocytes, inducing inflammation, even though the CNS was earlier considered to be an immune privileged region, in which peripheral immune cells are largely not allowed to enter. EAE is an animal model based on that theory. In this model, emulsified CNS antigens are injected alongside with immune stimulants, encouraging the stimulation of pathogenic CD4<sup>+</sup> T<sub>H</sub>1 cells and pro-inflammatory T<sub>H</sub>17 cells in draining lymph nodes, which then enter the circulation and fulfil their effector function in the CNS through crossing the blood brain barrier (BBB) (Münz et al. 2009).

In the intrinsic model, the disease is triggered by intra-CNS events. Lymphocyte migration and activation of autoreactive lymphocytes are secondary. Those intra-CNS events still remain unclear, but CNS viral infection was suggested as a hypothesis (Ransohoff and Engelhardt 2012). In the context of microglia activation, it is suggested, that high concentrations of pro-inflammatory cytokines due to a peripheral immune reaction could result in transfer of cytokines across the BBB, inducing perivascular macrophage activation, which in turn causes pro-inflammatory microglial activation. Meaning microglia-dependent neurodegeneration could be the result of indirect activation, without the need of autoreactive T cells (Dantzer et al. 2008).

#### 1.1.2.3 Pathophysiology

Physiologically, mature oligodendrocytes synthesize myelin in order to better isolate the axons of nerve cells in the white matter in the CNS to allow rapid transmission of the action potential impulses. They build elongated processes which contact the nearby axons and cycle them, and so isolate the electrical impulses, preventing ion loss through saltatory conduction (Compston et al. 2006). In chronic inflammation different kinds of reactive species (for example reactive oxygen or nitrogen species) are produced at inflamed regions, and are suspected to promote mitochondrial damage, and mitochondrial DNA mutations. This leads

to mitochondrial insufficiency and ultimately to energy deficiency of the neurons, which have a high energy need in order to maintain a functional protein biosynthesis, neuroaxonal function and ionic homeostasis, which is crucial to the function of the neurons. Different compensatory mechanisms, among others voltage-gated sodium channels ( $\text{Na}_v1.2$  and  $\text{Na}_v1.6$ ), try to maintain a balanced ionic homeostasis, however fail also due to excess accumulation of glutamate, the most common neurotransmitter in the CNS, which is excessively released during neuronal injury, promoting ionic imbalance. This axonal damage can spread anterograde, meaning in the distal axon terminal (known as “Wallerian degeneration”), possibly effecting the postsynaptic neurons, or retrograde effecting the perikaryon (“neuronal dying back”), and could possibly lead to neuronal necrosis or apoptosis (Friese et al. 2014).

This loss of axonal isolation after demyelination reduces the speed of action potential impulses through the axons enormously. Depolarization could go through the lesion, but at an extreme low velocity, explaining the delay in evoked potential and fatigue, both characteristic for MS. Depending on the location of the demyelinated lesions symptoms vary (Compston and Coles 2008). In addition, there is axonal transport disturbances and axonal transections in lesions that finally lead to significant axonal loss within the lesions (Kuhlmann et al. 2002).

#### 1.1.2.4 Neuropathology

Robert Carswell described in 1838 the pathological anatomy and clinical features of MS as “a remarkable lesion of the spinal cord accompanied with atrophy” (Carswell 1838). The end stage of a demyelinating disease is the formation of a sclerotic plaque, and represents a long process including inflammation, demyelination, remyelination, oligodendrocyte loss and astrocytosis, leading to neuronal and axonal degeneration, which in turn leads to disruption of neuronal signaling.

In the histology one could identify four types of early MS lesions. Tissue injury associated with T cell infiltrates and macrophages (pattern 1), oligodendrocytes and myelin targeted immune reaction via complement activation or antibodies (pattern 2), hypoxia like injury via impaired mitochondrial function, as a result of inflammation-induced vascular damage or macrophage toxins (pattern 3), and possibly genetic dependent oligodendrocytes’ predisposition to immune reaction (pattern 4) (Lucchinetti et al. 1996; Lucchinetti et al. 2000; Mahad et al. 2009).

#### 1.1.2.5 Role of T cells

Already in early stages of MS, T cells can be detected in CNS lesions. As described in 1.1.2.1 above, an association between MS and different HLA alleles is suggested, and could in fact reflect the possible presentation of autoantigens to autoreactive T cells. In the neuropathology of MS, demyelination is the key factor. A theory is that myelin proteins or certain myelin peptides might be encephalitogenic, and therefore the target of those T cells.

MBP, proteolipid protein (PLP) and myelin oligodendrocyte glycoprotein (MOG) are known to be recognized by circulating CD4<sup>+</sup> T<sub>H</sub> cells of MS patients, but also of healthy individuals. This could be explained due to the fact that CNS antigens aren't presented to the differentiating T cells in the thymus as a part of the negative selection in the central tolerance. Therefore, autoimmune T cells could survive this selection. Nevertheless, not all individuals with MBP/PLP/MOG specific CD4<sup>+</sup> T<sub>H</sub> cells develop MS, which raises the question: what causes these cells to migrate into the CNS and act upon their autoimmunity. In addition, only a minority of MS patients show anti-MBP or anti-MOG antibodies, which reinforces the active role of T cells (Hellings et al. 2001; Bielekova et al. 2004).

The most studied model of MS is EAE in mice. In this model, the major players are CD4<sup>+</sup> T<sub>H</sub> cells, which after peripheral activation in lymph nodes migrate into the CNS, and are reactivated there by antigen-presenting cells (APCs), among others CD11c<sup>+</sup> dendritic cells (DCs), leading to an inflammatory response, which in turn recruits monocytes and naïve CD4<sup>+</sup> T cells into the CNS, fueling the inflammation (Quintana et al. 2014; Mundt et al. 2019). Those myelin reactive CD4<sup>+</sup> T cells are mainly T<sub>H</sub>1 cells and T<sub>H</sub>17 cells, expressing CC-chemokine receptor 6 (CCR6) and secreting interferon- $\gamma$  (IFN- $\gamma$ ) and IL17-A respectively. An intermediate type was also detected in lesions, secreting both cytokines (Kebir et al. 2009; Cao et al. 2015).

An interest in the role of CD8<sup>+</sup> cytotoxic (T<sub>C</sub>) cells and of B cells (see 1.1.2.7 below) came from observations of human MS. CD8<sup>+</sup> T<sub>C</sub> cells are histologically the dominant T lymphocytes in white matter and in grey matter cortical demyelinating lesions, and their presence approximately correlates with axonal damage, indicating a key role (Frischer et al. 2009). Even in CD4<sup>+</sup> T<sub>H</sub> cell driven EAE model autoreactive CD8<sup>+</sup> T<sub>C</sub> cells are activated via cross presentation by monocytes or DCs in the CNS (Ji et al. 2013). Exact analysis of the TCRs of those CD8<sup>+</sup> T<sub>C</sub> cells shows a local expansion of migrating T<sub>C</sub> cells, indicating an active role in the lesion formation. Different EAE models were developed in order to decipher the role of the CD8<sup>+</sup> T<sub>C</sub> cells in MS lesions. Some models show a cytotoxic CD8<sup>+</sup> T<sub>C</sub> cell function, causing glial apoptosis, others show a regulatory function, or even a cytotoxic function against the pathogenic CD4<sup>+</sup> T<sub>H</sub> cells (Hohlfeld et al. 2016).

In context of anti-CD20 mediated therapies, a small population of CD4<sup>+</sup> and CD8<sup>+</sup> cells co-expressing CD20 (which was earlier considered to be a specific B cell marker) was also described. These cells can be depleted via anti-CD20 monoclonal antibody (-mAb), yet the difference in function to the CD20<sup>-</sup> T cell population remains unclear (Gingele et al. 2018).

#### 1.1.2.6 Role of myeloid antigen presenting cells

The dominant immune cells located in MS lesions in relapsing-remitting and in progressive phases are mononuclear phagocytes. Some differentiate from CNS originated microglia and some from peripheral monocytes, which migrate into the CNS during lesion formation. Those phagocytes can interact with other immune cells, such as T and B cells, and show two

main functions in MS lesions: myelin damage caused by pro-inflammatory tissue damage, known as M1 differentiation, and removal of damaged tissue (debris) or tissue repair, known as M2 differentiation. Moreover, phagocytes are seen often near damaged axons, correlating with the extent of acute axonal destruction, indicating an active role in inducing inflammation via oxidative stress, secretion of pro-inflammatory cytokines, such as IL-6 and tumor necrosis factor (TNF)- $\alpha$ , and matrix metalloproteinases, which in turn results in axonal damage in both grey and white matter (Lassmann et al. 1998; Trapp et al. 1998; Kouwenhoven et al. 2001; Kuhlmann et al. 2002; Bar-Or 2003). On the other hand, the phagocytes are suggested to have a necessary role in tissue repair mechanisms during lesion resolution among others via secretion of anti-inflammatory cytokines and growth factors, to promote oligodendrocyte differentiation. One speculates, that those two reversed roles may show the origin of said cells, suggesting that the monocyte derived phagocytes are the ones responsible for axonal damage, and that the microglia derived phagocytes are the ones assisting in tissue repair (Miron et al. 2013). Yet this theory has been recently disputed, showing that monocytes of MS patients respond to glucocorticoid therapy with a M2 differentiation (Fischer et al. 2019).

#### 1.1.2.7 Role of B cells

B cells function as APCs, show modulatory function by cytokine secretion and are the precursor of antibody secreting plasma cells. Those functions of the B cell in the immune response have both pro- and anti-inflammatory components. Their key role in MS pathogenesis was emphasized by the undeniable therapeutic efficiency of anti-CD20-mAb, which deplete mostly B cells and CD20<sup>+</sup> T cells, but not plasma cells, which are CD20<sup>-</sup>, hence not reducing antibody production (Hauser et al. 2008).

The presence of B cells and of oligoclonal immunoglobulins (Ig, also known as oligoclonal bands, OCB) in the CSF was first observed in the 1950's, is seen in most MS patients, and is therefore used as a diagnostic criterion (Kabat und Freedman 1950). Moreover, B cells can be found not only in the CSF of MS patients but also in the parenchyma and in follicle like structures in the meninges (Lucchinetti et al. 2000; Serafini et al. 2004). The CNS seems to present a nesting milieu for the persistence and activation of B cells due to secretion of different chemokines, such as B cell activating factor (BAFF) and chemokine (C-X-C motif) ligand (CXCL)-13, which seem to be secreted by microglia and activated astrocytes (Krumbholz et al. 2005; Krumbholz et al. 2006; Kowarik et al. 2012).

By close examination of the above-mentioned Ig it was shown, that they are produced by clonally expanding B cells intrathecally (by comparing proteome and transcriptome of CSF B cells), and close examination of the CSF B cells showed indications for somatic hypermutation, which in turn suggests antigen-driven affinity maturation. Yet the antigens recognized by said antibodies remain unclear (Qin et al. 1998; Obermeier et al. 2008; Weber et al. 2011; Beltran et al. 2014). Further histological studies show Ig and complement depositions in MS lesions, suggesting that Ig alone (ADCC – antibody dependent

cytotoxicity) or in combination with complement activation (CDC – complement dependent cytotoxicity) induce demyelination. As for possible targets for those Ig oligodendrocytes and myelin proteins such as MBP, PLP or MOG were suggested, but also neuroglial and astrocytic antigens (Genain et al. 1999; Elliott et al. 2012, and see 1.1.2.4 above). Whether the humoral reaction comes primary or secondary to CNS inflammation, remains unclear.

As for their function as APCs, B cells recognize foreign antigens via their B cell receptor (BCR), a membrane-bound Ig, which in turn are internalized and presented via constitutive expressed major histocompatibility complex class II (MHC-II) to the responding CD4<sup>+</sup> T<sub>H</sub> cells. Once activated B cells express the co-stimulatory molecules CD80/86 resulting in T cell activation and inflammation (Lanzavecchia 1985). This antigen presenting function of B cells was demonstrated in the EAE model, emphasizing the importance of B cells as APC for the pathogenesis of MS (Molnarfi et al. 2013).

As mentioned, B cells have a modulatory function on other immune cells by secretion of pro- and anti-inflammatory cytokines. For example, B cells secrete IL-6, a pro-inflammatory cytokine which promotes the differentiation of T<sub>H</sub>17 and blocks the differentiation to T<sub>reg</sub> cells, increasing inflammation. MS patients' B cells show an increased IL-6 and TNF- $\alpha$  secretion compared to healthy controls (Barr et al. 2012). At the same time, B and plasma cells are a source of anti-inflammatory cytokines such as IL-10 and IL-35. IL-10 downregulates the expression of T<sub>H</sub>1 cytokines, inhibits the differentiation of pro-inflammatory T<sub>H</sub>1 and T<sub>H</sub>17 cells, MHC-II, and costimulatory molecules on myeloid APCs, such as monocytes and DCs. IL-10 also blocks NF- $\kappa$ B activity, which in turn promotes the secretion of pro-inflammatory cytokines, nitric oxide, and eicosanoids (Moore et al. 2001). MS patients' B cells show a decreased IL-10 secretion compared to healthy controls (Duddy et al. 2007).

When looking closely at the different B cells subpopulations, a difference can be seen between the naïve (CD27<sup>-</sup>) and the memory (CD27<sup>+</sup>) B cells. Duddy et al. (2007) described the differences between these populations in MS patients, showing a different cytokine profile, indicating different roles. They confirmed that IL-10 is almost exclusively produced by naïve B cells, and that the pro-inflammatory cytokines TNF- $\alpha$  and lymphotoxin (LT) are largely produced by memory B cells. They also described a difference in their activation profile, showing that memory B cells can be easier activated than the naïve B cells, and produce thereafter more pro-inflammatory cytokines (TNF- $\alpha$ , LT) for a fulminant immune reaction, whereas the naïve B cells produce the anti-inflammatory cytokine IL-10, to prevent an undesired reaction.

### 1.1.3 Symptoms and diagnosis

Dependent on the CNS area in which the MS typical lesions develop, the symptoms can vary. A clinical manifestation indicates, in most patients, the involvement of visual, sensory, motor or autonomic system, or a combination of two or more (see 1.1.2.3 above). Hence very few symptoms are disease specific. On the other hand, two are characteristic for MS: Lhermitte's symptom (upon neck flexion runs an electrical sensation down the spine), and the Uhthoff phenomenon (symptom worsening when body temperature increases), which could help at diagnosis (Compston and Coles 2008).

The clinical course of the disease varies as well. It may include acute episodic periods of new neurological symptoms or worsening of pre-existing symptoms, known as relapses, a stable progressive deterioration of neurological functions in the absence of relapses, or a combination of both. Four possible clinical courses of MS were defined. Relapsing remitting (RR-) MS: episodes of acute worsening of neurological functions (relapses) followed by a variable recovery (complete or incomplete) with stable disease between the relapses. Primary progressive (PP-) MS: the disease progresses continuously from onset, i.e. gradual nearly steady worsening of neurological symptoms, occasional plateaus and temporary minor improvements may occur. Secondary progressive (SP-) MS: initial RRMS course of MS, followed by a progression. SPMS may or may not be associated with overlying relapses. Without treatment, approximately 50% of RRMS patients convert to SPMS within 15 years after disease onset (Weinshenker et al. 1989). Progressive relapsing (PR-) MS: a rare variant showing from the beginning a primarily disease progression combined with clear acute relapses (Lublin et al. 1996).

The clinical severity of the disease is quantified using the Kurtzke Expanded Disability Status Scale (EDSS). Developed by John F. Kurtzke, the score is based on a neurological examination by a clinician, and ranges between 0.0, i.e. normal neurological exam and 10.0, i. e. death due to MS, in 0.5 steps (Kurtzke 1983).

As mentioned, the clinic of MS is very heterogenous. The diagnosis of MS is nowadays based on criteria including clinical, imaging and laboratory (CSF analysis) findings. These so-called McDonald criteria (Thompson et al. 2018) were first introduced in 2001 and were revised over time, leading to the criteria shown in Table 1:

Table 1: McDonald criteria (Thompson et al. 2018)

<b>Clinical attacks</b>	<b>No. of lesions with objective clinical evidence</b>	<b>Additional data needed for a MS diagnosis</b>
≥ 2 clinical attacks	≥ 2	None
≥ 2 clinical attacks	1 (as well as clear-cut historical evidence of a previous attack involving a lesion in a distinct anatomical location)	None
≥ 2 clinical attacks	1	Dissemination in space demonstrated by an additional clinical attack implicating a different CNS site or by MRI (DIS)
one clinical attack	≥ 2	Dissemination in time demonstrated by an additional clinical attack or by MRI or demonstration of CSF-specific oligoclonal bands (DIT or OCB)
one clinical attack	1	DIS and DIT or OCB
Progressive course onset (PPMS)	See additional data	One year of disability progression (retrospectively or prospectively determined) independent of clinical relapse PLUS two of the following criteria: <ul style="list-style-type: none"> <li>• One or more T2-hyperintense lesions characteristic of multiple sclerosis in one or more of the following brain regions: periventricular, cortical or juxtacortical, or infratentorial</li> <li>• Two or more T2-hyperintense lesions in the spinal cord</li> <li>• Presence of CSF-specific oligoclonal bands</li> </ul>

### 1.1.4 MS therapies

The infiltration of peripheral immune cells in the CNS has been the main target of MS therapies. Those immunomodulatory drugs reduce, on the one hand, immune cell activity and migration into the CNS, and thus the relapse frequency as well, but often have side effects of immune suppression, such as increased sensitivity to viral infections, development of malignancies, or even a deadly opportunistic infections (Haghikia et al. 2013). Despite decreased relapse frequency it is well known, that the MS therapies do not fully stop disease progression, and neuroaxonal damage progresses, accumulates and becomes permanent, ensuring future physical disability (Feinstein et al. 2015). The exact pathophysiological mechanisms that cause progressive neurodegeneration are not yet exactly defined. Whether they are the same that cause relapses, whether they are bystander mechanisms of inflammatory demyelination or whether there is a specific attack towards the neuroaxonal compartment, is still open.

#### 1.1.4.1 General principles

Due to lack of knowledge of disease pathogenesis, MS patients are therapied according to the disease severity and progression. Twelve MS therapies approved by the Food and Drug Administration (FDA) can be divided into four major principals (Brück et al. 2013): (1) Immunosuppression: cladribine (per os; p. o.), mitoxantrone (intravenously; i. v.); (2) Immunomodulation: interferon beta (IFN- $\beta$ )-1a, IFN- $\beta$ -1b, peginterferon beta-1a, glatiramer acetate (GA; all subcutaneously/intramuscularly; s. c./i. m.), teriflunomide, dimethyl fumarate (DMF; both p. o.); (3) Migration inhibition: fingolimod (p. o.), natalizumab (anti- $\alpha_4$ -Integrin-mAb, i. v.); (4) Cell depletion: alemtuzumab (anti-CD52-mAb), ocrelizumab (anti-CD20-mAb)

As an example for an immunomodulation therapy, one can look at IFN- $\beta$ , GA or DMF. As described in 1.1.2.4 above, T<sub>H</sub>1 and T<sub>H</sub>17 are the main CD4<sup>+</sup> T<sub>H</sub> cells populations causing the disease. IFN- $\beta$ , GA and DMF shift the scale towards T<sub>H</sub>2 cell phenotypes, decreasing inflammation (Kozovska et al. 1999; Vieira et al. 2003; Zoghi et al. 2011).

The MS disease modifying therapy, according to current German guidelines (LL 31 2012 Diagnose und Therapie der Multiplen Sklerose), is chosen according to the disease activity of the patients, and can divided into four main indications (B cell depleting therapy with Ocrelizumab is approved for the treatment of RRMS and PPMS in Germany, but not yet included in the current guidelines): (1) MS as clinically isolated syndrome (CIS), mild/moderate disease activity: IFN- $\beta$ -1a, IFN- $\beta$ -1b, GA (class I evidence); (2) RRMS: (a) high disease activity: alemtuzumab, fingolimod, natalizumab; mitoxantrone (cyclophosphamide); clinical studies. (b) mild/moderate disease activity: DMF, GA, IFN- $\beta$ -1a, IFN- $\beta$ -1b, peginterferon beta-1a, teriflunomide (azathioprine); (3) SPMS: with relapses: IFN- $\beta$ -1a, IFN- $\beta$ -1b, mitoxantrone (cyclophosphamide); without relapses: mitoxantrone; (4) acute relapse therapy: methylprednisolone, plasmapheresis.

### 1.1.4.2 B cell targeted

Nowadays there are three main ways to target B cells in the MS therapy: anti-CD20-mAb depleting peripheral B cells (see 1.2 below), anti-CD19-mAb (MEDI-551) depleting all B and plasma cells, and BLYS (B Lymphocyte Stimulator)/BAFF and APRIL (a proliferation-inducing ligand) inhibitors (Atacicept). An overview of these therapies is shown in Figure 1:

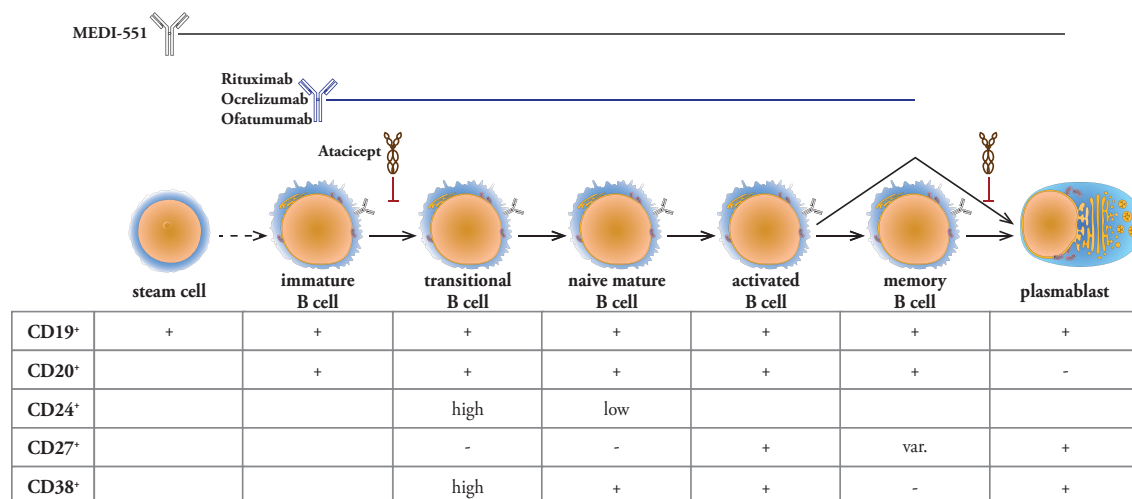


Figure 1. B cells targeted therapies. The figure shows the different B cell maturation phases and the therapeutic options for B cell inhibition/depletion (adapted from Bittner et al. 2017, with courtesy of Prof. Dr. med. Stefan Bittner).

## 1.2 Anti-CD20 monoclonal antibodies (Rituximab, Ocrelizumab, Ofatumumab)

Ocrelizumab as a new anti-CD20-mAb therapy is approved for the treatment of RRMS and PPMS. Rituximab as an anti-CD20-mAb therapy was often used as an off-label treatment for MS and in few clinical trials. Rituximab is a chimeric monoclonal anti-CD20-mAb depleting peripheral B cells, and has already been approved for treatment of B cell lymphoma and different autoimmune diseases (Gürçan et al. 2009). Ocrelizumab is a humanized IgG1 anti-CD20-mAb with decreased immunogenicity compared to rituximab, and binds to a different yet overlapping epitope on the CD20 molecule than rituximab. Ofatumumab is a fully humanized anti-CD20-mAb, which binds a different epitope than rituximab and ocrelizumab.

### 1.2.1 Mechanism of action of anti-CD20 monoclonal antibodies

All three antibodies deplete circulating CD20<sup>+</sup> cells almost completely, via a combination of antibody-dependent cellular cytotoxicity and complement-dependent cytotoxicity resulting in apoptosis (Reff et al. 1994), with a limited penetration of lymphoid tissues (Kamburova et al. 2013). Rituximab doesn't efficiently cross the BBB, but does deplete B cells in the CSF and CNS perivascular spaces. OCB changes after rituximab treatment are undetectable

(Cross et al. 2006; Martin et al. 2009). In comparison with rituximab, ocrelizumab shows increased antibody-dependent cellular cytotoxicity and reduced complement-dependent cytotoxicity, and ofatumumab has a higher binding affinity to CD20.

### 1.2.2 Clinical trials in MS

Four clinical trials with rituximab have been completed in MS (Barun and Bar-Or 2012). The most important of them, the HERMES trial, a randomized, placebo-controlled phase II trial in 104 patients with RRMS, has shown a 91% reduction of gadolinium enhancing lesions and a reduction of relapse rates by 49% after 48 weeks against placebo (Hauser et al. 2008). On the other hand, the OLYMPUS trial, a phase II/III trial in 439 patients with PPMS, failed to show a reduction in confirmed disease progression after 96 weeks (Hawker et al. 2009). Rituximab as off-label MS therapy is commonly administered i. v. either at a dose of 1000 mg on days 1 and 15, or 375 mg/m<sup>2</sup> in 4-weekly doses every 6–12 months (Kim et al. 2013; Melzer and Meuth 2014). Rituximab has shown in addition a successful depletion of B cells in the CSF and in the perivascular spaces (Martin et al. 2009). An intrathecal application in lower dosage was also investigated, presenting a depletion of peripheral B cells, but a moderate depletion of CSF B cells (Svenningsson et al. 2015).

The OPERA trials (I and II, both phase III trials) with ocrelizumab in 1656 RRMS patients showed a 47% reduction of annualized relapse rates (ARRs), a 95% reduction of gadolinium-enhanced T1 lesions and 40% reduction of confirmed disability compared with IFN- $\beta$ -1a after 96 weeks. Ocrelizumab was administered at 600 mg i. v. every 6 months (first cycle: twice 300 mg i. v. 2 weeks apart, then single dose 600 mg i. v.).

With regards to PPMS, ocrelizumab showed in a placebo-controlled phase III trial in 488 PPMS patients, the ORATORIO trial, in which it was administered at 300 mg i. v., 2 weeks apart, every 6 months, a 24% lower risk for confirmed disability progression after 12 weeks and after 24 weeks. T2-weighted lesion volumes were 3.4% lower than at baseline and brain volume loss was 17.5% lower than in placebo patients. Ocrelizumab was therefore the first treatment ever to show clinical efficacy in patients with PPMS (Sorensen and Blinkenberg 2016).

## 1.3 Atacicept

Atacicept is a human recombinant fusion protein blocking both BLyS/BAFF and APRIL, two regulatory ligands regulating B and plasma cell survival, T cell stimulation and antibody isotype switching (Schneider 2005). Atacicept is not approved for MS therapy and showed negative effects in clinical trials. RRMS patients injected weekly with atacicept in a placebo-controlled phase II trial (the ATAMS trial) had twice more relapses than the placebo group (Kappos et al. 2014).

## **1.4 Aims of the study**

B cell depletion as MS therapy is relatively new, and therefore immunological consequences and long-term (side) effects of this therapy are still unknown. MS was always considered to be driven by pathogenic T cells, but the significant effects of B cell depletion on relapses and MRI lesions point to a possibly greater role of B cells in the MS pathogenesis than thought. However, the long-term effects of B cell depletion, their phenotype during repletion and the effects of B cell depletion on other immune cell populations are largely unknown. Therefore, I aimed to identify and characterize B cell and other immune cell phenotypes and kinetics during B cell depletion and repletion phases. This work is also aiming at offering follow up and kinetic monitoring tools for treated patients with MS during B cell depletion treatments.

### **1.4.1 Direct effects of anti-CD20 depletion on CD20<sup>+</sup> B and T cells**

To detect differences in B cell maturation and activation phenotype, antigen presentation, co-stimulation and cytokine secretion capacities before B cell depletion and during repletion.

To detect differences between CD20<sup>+</sup> T cells before B cell depletion and during repletion and to identify repletion kinetics of CD20<sup>+</sup> cell populations.

### **1.4.2 Indirect effects on other immune cell populations**

Detection of changes in CD20<sup>-</sup> T cells maturation phenotype and migration potential.

Detection of altered myeloid cells' activation phenotype, of antigen presentation, co-stimulation and cytokine secretion capacities upon repletion compared to their pre-depletion state, with respect to pro- and anti-inflammatory phenotypes.

### **1.4.3 Correlation with clinical parameters**

Identification of the effects of B cell depletion on clinical outcomes (relapses, progression) and of long-term effects on other immune populations.

## 2 Materials and Methods

### 2.1 Patients

Blood samples were taken from 15 MS patients treated at the Department of Neurology at the University Medical Centre in Göttingen, Germany, all diagnosed with RRMS according to the McDonald criteria 2011. Blood was drawn before therapy induction with rituximab and sequentially afterwards, in various intervals. Blood samples were taken before a new dosage of rituximab was given. A total number of 95 samples has been collected and analyzed longitudinally, during the depletion and various repletion phases. Furthermore, clinical data were collected from all patients, as shown in Table 2. All participants did provide informed consent prior to study enrolment as approved by the Göttingen University ethics review board (#19/09/10 and #03/04/14).

Table 2: Characteristics of patient cohort

Characteristic	Patient cohort	
Age (years; mean $\pm$ SD)	40 $\pm$ 9.11	
Age at begin of study (years; mean $\pm$ SD)	35.73 $\pm$ 8.91	
Sex	8 f, 7 m	
EDSS score at start of the study (median $\pm$ IQR/range)	2.5 $\pm$ 3.5	
Time since multiple sclerosis diagnosis (years; mean $\pm$ SD)	10.76 $\pm$ 6.31	
Last treatment before Rituximab (cases)	Dimethylfumarate	2
	Fingolimod	6
	Glatiramer acetate	1
	Natalizumab	2
	Azathioprine	1
	None (i. e. treatment naïve)	3

Table 2: Characteristics of patient cohort

Previous treatments (cases)	Dimethylfumarate	2
	Fingolimod	9
	Glatiramer acetate	4
	Interferon beta-1a	6
	Interferon beta-1b	2
	Natalizumab	6
	Azathioprine	1
	Cortisone (in last six months before first anti-CD20 treatment)	4
Number of treatments before Rituximab (mean $\pm$ SD)	2.38 $\pm$ 1.12	
Antibody tests (cases, others unknown)	AQP4	6 negatives
	MOG	5 negatives
Rituximab since (years; mean $\pm$ SD)	2.68 $\pm$ 0.658	
Samples pro patient (mean $\pm$ SD)	6.33 $\pm$ 2.66	
Pre-/dep./early rep./late rep. (samples)	15/12/10/10	

## 2.2 Materials

Table 3: Human monoclonal antibodies for flow cytometry

Antigen	Fluorochrome	Clone	Dilution	Manufacturer
CD4	PE-Cy7	RPA-T4	1:100	BD Bioscience
CD8	PerCP-Cy5.5	RPA-T8	1:100	BD Bioscience
CD8a	PE	HIT8a	1:100	eBioscience
CD14	FITC	M5E2	1:100	BD Bioscience
CD14	PE-CF594	M $\phi$ P9	1:100	BD Bioscience
CD14	BV421	M $\phi$ P9	1:100	BD Bioscience

Table 3: Human monoclonal antibodies for flow cytometry

CD19	APC	HIB19	1:100	BD Bioscience
CD19	PerCp-Cy5.5	HIB19	1:100	BioLegend
CD19	FITC	HIB19	1:100	BD Bioscience
CD19	PE-Cy5	HIB19	1:100	BD Bioscience
CD20	APC-Cy7	L27	1:100	BD Bioscience
CD20	PE	REA780	1:100	Miltenyi
CD24	PerCp-Cy5.5	ML5	1:100	BioLegend
CD25	BV605	BC96	1:100	BioLegend
CD27	PacificBlue	O323	1:100	BioLegend
CD38	FITC	HIT2	1:100	BioLegend
CD40	PE/Dazzle™594	5C3	1:100	BioLegend
CD45RA	FITC	HI100	1:50	BD Bioscience
CD45RO	A700	UCHL1	1:100	BD Bioscience
CD62L	PE	DREG-56	1:100	BD Bioscience
CD69	FITC	FN50	1:100	BioLegend
CD80	PE-Cy7	L307.4	1:100	BD Bioscience
CD86	BV421	2331 (FUN-1)	1:100	BD Bioscience
CD95 (FAS)	PE	DX2	1:100	BioLegend
CD150	BV421	A12	1:100	BD Bioscience
MHCII	APC	Tü36	1:100	BioLegend
IL-6	FITC	MQ2-13A5	1:50	BD Bioscience
IL-10	PE-CF594	JES3-19F1	1:50	BD Bioscience
TNF- $\alpha$	A700	MAb11	1:50	BD Bioscience
Dead/Live	ZombieAqua™		1:500	BioLegend
Dead/Live	ZombieNIR™		1:500	BioLegend

Table 4: List of reagents

<b>Reagents</b>	<b>Manufacturer</b>
BD FACS Clean™	BD Biosciences
BD FACS Flow™	BD Biosciences
BD FACS Rinse™	BD Biosciences
BioColl separation solution	Biochrom
CpG oligodeoxynucleotides	Sigma Aldrich
Cytofix/Cytoperm™	BD Biosciences
DMEM (Dulbecco's Modified Eagle's medium)	Sigma Aldrich
DMSO (dimethyl-sulfoxide)	Sigma Aldrich
EDTA (ethylene diamine tetraacetic acid disodium salt dihydrate)	Carl Roth
Ethanol 100%	Merck Millipore
Fc-Block™	BioLegend
FCS (fetal calf serum)	Sigma Aldrich
GolgiPlug™	BD Biosciences
Ionomycin	Sigma Aldrich
L-glutamine	Sigma Aldrich
LPS (lipopolysaccharide)	Sigma Aldrich
PBS (phosphate buffered salt solution)	Sigma Aldrich
Perm/Wash™ buffer, 10x	BD Biosciences
PFA (para-formaldehyde)	Merck Millipore
PMA (phorbol 12-myristate 13-acetate)	Sigma Aldrich
RPMI-1640 (Roswell park memorial institute-1640)	Sigma Aldrich
Sodium pyruvate 100mM	Sigma Aldrich
TrypanBlue	Sigma Aldrich
β-mercaptoethanol	Sigma Aldrich

Table 5: List of buffers and cell culture media

<b>Solution</b>	<b>Composition</b>
RPMI <sub>complete</sub> (“whole-medium”)	0.5l RPMI-1640, 50 ml FCS, 5 ml sodium pyruvate, 5 ml L-glutamine, 0.5 ml $\beta$ -mercaptoethanol
Cryo-medium	60% RPMI <sub>complete</sub> , 20% FCS, 20% DMSO
FACS buffer	2% FCS in PBS

Table 6: List of consumables

<b>Product</b>	<b>Manufacturer</b>
96 well plates, flat bottom (flat-well)	Sarstedt
96 well plates, round bottom (U-well)	Sarstedt
FACS tubes, 5 ml	Sarstedt
Micro tubes (0.1 ml, 0.5 ml, 1 ml, 1.5 ml)	Eppendorf
Multistep pipettes, 1 ml	Eppendorf
Pipettes (10 $\mu$ l, 200 $\mu$ l, 1000 $\mu$ l)	Sarstedt
Pipettes (5 ml, 10 ml, 25 ml)	Sarstedt

Table 7: List of devices and softwares

<b>Device</b>	<b>Manufacturer</b>
BBD 6220 cell incubator	ThermoScientific
Centrifuge 5415R	Eppendorf
Centrifuge 5810R	Eppendorf
CKX41 light microscope	Olympus
FACS LSRII Fortessa	BD Biosciences
Neubauer chamber	Superior Marienfeld
SAFE 2020 clean bench	ThermoScientific
<b>Software</b>	<b>Manufacturer</b>
FACSdiva™ 6.1.2	BD biosciences
FlowJo™ 10.5.3	Tree Star Inc.
GraphPad Prism™ 7a	GraphPad software Inc.
Adobe™ Illustrator™ CS6 16.0.4	Adobe™

## 2.3 Methods

PBMC isolation, processing, cryopreservation and unfreezing subsequently were performed according to established protocols at the laboratory.

### 2.3.1 PBMC isolation

Blood was drawn via phlebotomy into EDTA tubes in order to prevent cell agglutination, and then transferred into sterile tubes and diluted with PBS (1:3). In order to create a “Ficoll gradient” in order to isolate the peripheral blood mononuclear cells, 20 ml BioColl™ were added to the blood-PBS suspension, which was then centrifuged for 35 minutes at 448 g and 21°C with low acceleration and without brake. After centrifugation, the PBMC were concentrated between the BioColl™ and the plasma layer. This layer was transferred into a new tube, diluted twice with DMEM, and centrifuged (10 minutes at 1250 rpm and 4°C) in order to remove unwanted residues. After resuspension with 5 ml DMEM the cells were counted under the microscope (see 2.3.2.2 below). For conservation, the cells were diluted to a count of  $4 \cdot 10^6 \cdot \text{ml}^{-1}$  in DMEM. The conservation tubes were filled with 500  $\mu\text{l}$  cell suspension and 500  $\mu\text{l}$  cryo-medium, achieving  $2 \cdot 10^6$  cells per tube. The tubes were frozen at  $-80^\circ\text{C}$  using an ethanol box, and so cooling slowly at  $1^\circ\text{K}$  per minute. The tubes were stored at  $-80^\circ\text{C}$ .

### 2.3.2 Flow cytometry panels

To answer the questions presented at the introduction, various flow cytometry stains under different stimulation regimes were used. This method had two leading limitations: the patients' samples, which were limited and not reproducible, and a potential spectral overlap of the fluorophores. The latter limits the number of fluorochromes to be used, without a too pronounced spectral overlap, which would lead in an unspecific signal. Therefore, the following panels were developed in order to achieve maximal knowledge per staining with the minimal number of panels needed. The final panels are presented in Tables 8-10:

Table 8: Flow cytometry panels I

<b>#1 B cell subset</b>		<b>#2B APC activation</b>		<b>#4 B cell activation</b>	
CD19	APC	CD14	FITC	CD19	PerCp-Cy5.5
CD20	APC-Cy7	CD19	PerCp-Cy5.5	CD25	BV605
CD24	PerCp-Cy5.5	CD40	PE/Dazzle™594	CD40	PE/Dazzle™594
CD27	PacificBlue	CD80	PE-Cy7	CD69	FITC
CD38	FITC	CD86	BV421	CD80	PE-Cy7
Dead/Live	ZombieAqua™	MHC-II	APC	CD86	BV421
		CD95 (FAS)	PE	MHC-II	APC
		Dead/Live	ZombieNIR™	CD95 (FAS)	PE
				Dead/Live	ZombieNIR™

Table 9: Flow cytometry panels II

<b>#3 major immune cell populations</b>		<b>#5 cytokine secretion</b>	
CD4	PE-Cy7	CD14	BV421
CD8a	PE	CD19	PE-Cy5
CD14	PE-CF594	IL-6	FITC
CD19	FITC	IL-10	PE-CF594
CD150	BV421	TNF- $\alpha$	A700
MHC-II	APC	Dead/Live	ZombieNIR™
Dead/Live	ZombieAqua™		

Table 10: Flow cytometry panels III

#2 T cell subset		#6 CD20 <sup>+</sup> T cell subset	
CD4	PE-Cy7	CD4	PE-Cy7
CD8	PerCP-Cy5.5	CD8	PerCP-Cy5.5
CD20	APC-Cy7	CD14	PE-CF594
CD45RA	FITC	CD19	APC
CD45RO	A700	CD20	PE
CD62L	PE	CD25	BV605
Dead/Live	ZombieAqua™	CD45RA	FITC
		CD45RO	A700
		Dead/Live	ZombieAqua™

Panel #1, B cell subset allows the characterization of following maturation phases through surface antigens (and see Figure 1): transitional immature B cells (CD24<sup>high</sup>, CD27<sup>-</sup>, CD38<sup>high</sup>); mature naïve B cells (CD27<sup>-</sup>, CD38<sup>+</sup>); activated B cells (CD27<sup>+</sup>, CD38<sup>+</sup>); memory B cells (CD27<sup>var</sup>, CD38<sup>-</sup>); plasmablasts (CD20<sup>-</sup>, CD27<sup>+</sup>, CD38<sup>+</sup>).

Panel #2 and #6, T cell subsets, allow the general characterization of T cell maturation phases (an accurate characterization requires the analysis of six surface antigens) and of CD20<sup>+</sup> T cells, those through the following surface antigens: CD45: also known as Protein tyrosine phosphatase receptor type C (PTPRC), a type I transmembrane protein, that is present in various isoforms on all differentiated hematopoietic cells (except erythrocytes and plasma cells), and an essential regulator of T and B cell antigen receptor signaling, either via extracellular co-stimulation or via intracellular activation of various kinases required for the antigen receptor signaling (Holmes 2006). CD45 has two main isoforms: (1) CD45RA: typical for naïve T cells; (2) CD45RO: the shortest CD45 isoform, expressed by activated and memory T cells. These CD45RO<sup>+</sup> cells are rare in neonates and progressively accumulate with age. CD62L: also known as L-selectin, is a cell adhesion molecule found on leukocytes. CD62L acts as a docking molecule, allowing lymphocytes to enter secondary lymphoid tissues via high endothelial venules, which in turn express the passing ligands. Through the adhesion the lymphocytes' circulation speed slows down, allowing entry into secondary lymphoid organs. CD62L is commonly found on the surface of T cells (Cotran et al. 1999).

Figure 2 shows the T cell maturation phases as analyzed in the study:

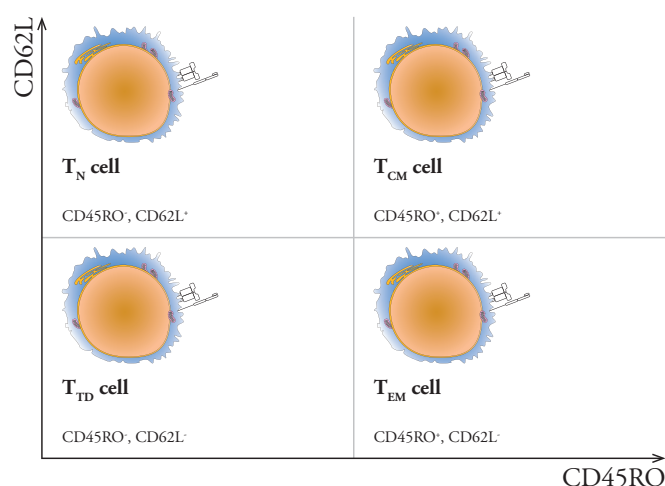


Figure 2. T cell maturation. The figure shows the four main T cell maturation phases, naïve T cells ( $T_N$ ), central memory T cells ( $T_{CM}$ ), effector memory T cells ( $T_{EM}$ ) and terminally differentiated T cells ( $T_{TD}$ ), differentiated through CD45RO and CD62L (own representation based on Sallusto et al. 2004; Holmes 2006; Mahnke et al. 2013).

Naïve T cells ( $T_N$ ) leave the thymus epitope specific after undergoing positive and negative selection, and migrate into the periphery as a part of an immune response after antigen encounter. After antigen elimination, more than 95% of the effector T cells die, the rest differentiate into long-living memory T cells.

The  $CD45RO^+$  memory T cells can be divided into two groups. Central memory T cells ( $T_{CM}$ ) and effector memory T cells ( $T_{EM}$ ) both express CD45RO, but differ in their cytokine profile and their function.  $T_{CM}$  produce IL-2 (a T cell differentiation promoting cytokine, which promotes the differentiation into  $T_{reg}$  and into  $T_{CM}$  and  $T_{EM}$  (Liao et al. 2011; Arenas-Ramirez et al. 2015) and lack immediate killing activity, while  $T_{EM}$  produce mostly IFN- $\gamma$  and TNF- $\alpha$ , but not IL-2, and are capable of immediate cytotoxicity.

Studies have shown, that in humans some memory T cells, terminally differentiated T cells ( $T_{TD}$ , also known as terminally differentiated effector memory T cells [ $T_{EMRA}$ ]), re-express naïve T cell surface antigen CD45RA, and down-regulate the expression of CD62L, representing a terminal stage of effector differentiation (Sallusto et al. 2004; Surh and Sprent 2008; Sathaliyawala et al. 2013).

As Figure 2 shows,  $T_N$  and  $T_{CM}$  express CD62L as they need to enter secondary lymph nodes, either to encounter their antigen, or to re-enter secondary lymphoid organs to proliferate upon antigen re-encountering.  $T_{EM}$  and  $T_{TD}$  do not express CD62L, as they circulate in the periphery and have immediate effector functions upon encountering antigen (Kohn et al. 2012).

Panels #2B and #4, APC and B cell activation allow the characterization of following surface antigen related to antigen presentation and to general activation: MHC-II: a surface antigen used to present internalized antigens to the corresponding  $CD4^+$  T cells (Owen et al. 2013).

CD40: a type I glycoprotein involved in B cell differentiation, co-stimulation, isotype class-switching and protection of B cells from apoptosis. CD40 is important for the B cell-T cell interaction by binding CD40 ligand (CD40L) on T cells (Kawabe et al. 1994). CD80/CD86: a type I glycoprotein also known as B7-1/2 and are expressed on antigen-presenting cells. An interaction with CD28 is used as a co-stimulatory signal to activate the passing T cell (Owen et al. 2013). CD25: a type I transmembrane glycoprotein found on activated mononuclear immune cells, in association with CD122 and CD132 it forms the IL-2 receptor complex (Sakaguchi et al. 1995; Buckner 2010). CD69: this type II transmembrane protein is a member of the C-type lectin family and is involved in early lymphocyte activation. Among other functions: signal-transmitting receptor in platelets and natural killer (NK) cells (Ziegler et al. 1994; Cambiaggi et al. 1992). CD95 (FAS): a type I transmembrane protein, also known as FAS receptor or apoptosis antigen 1. Binding FAS ligand (CD178) induces cell apoptosis which plays a role in the maintenance of the peripheral tolerance. One assumes, that CD95 might be involved in the development of autoimmune diseases. CD95 expression is regulated by NF- $\kappa$ B and is high-regulated in activated T and B cells (Wajant 2002; Liu et al. 2012).

Panel #3 gives a complementary view of myeloid cells' activation to panel #2B through the analysis of CD150: also known as signaling lymphocytic activation molecule (SLAM), a type I transmembrane molecule, is expressed by mature dendritic cells and activated monocytes, exclusively after in vitro stimulation by bacteria-derived ligands, and not by cytokine stimulation. The bacteria produce flagellin, a TLR5 activator, which in turn induces CD150 on monocytes (Farina et al. 2004). In MS brain lesion, monocytes do not usually known to express CD150 (Theil et al. 2005).

Panel #5 completes the B cell and myeloid cells' phenotypes by giving a view of their cytokine secretion phenotype, which could indicate a pro- or anti-inflammatory phenotype. Three major cytokines in MS were analyzed: IL-6: a pro-inflammatory cytokine. IL-6 is an important mediator of fever, achieved through crossing the BBB and initiating PGE<sub>2</sub> synthesis in the hypothalamus, changing the body's temperature setpoint, and of the acute phase response, stimulating acute phase protein synthesis such as CRP, as well as the production of neutrophil granulocytes in the bone marrow (Banks et al. 1994; Bastard et al. 1999). TNF- $\alpha$ : a pro-inflammatory cytokine, involved in systemic inflammation, is mainly produced by activated macrophages, but can be produced by other cell population such as lymphocytes, NK cells mast cells and others. TNF- $\alpha$  is an endogenous pyrogen, which induces fever, apoptotic cell death, cachexia and inflammation. IL-10: an anti-inflammatory cytokine, produced mainly by monocytes and, to less extent, by T<sub>H</sub>2 cells, mast cells, T<sub>reg</sub> and certain subsets of activated T and B cells. IL-10 has diverse effects in immunomodulation and inflammation, such as down-regulation of T<sub>H</sub>1 cytokines, MHC-II surface antigen and co-stimulatory molecules on macrophages, reducing antigen presentation and T cell activation. In addition, IL-10 prolongs B cell survival, proliferation, and antibody production (Mosser and Zhang 2008).

### 2.3.2.1 Stimulation regimes

Some surface markers and cytokines are up regulated, respectively synthesized only upon cell activation. Therefore, cells were incubated with the following substances to simulate a stimulation. CpG: cytosine triphosphate deoxynucleotide ("C") followed by a guanine triphosphate deoxynucleotide ("G") is unmethylated a frequent DNA sequence in microbial genome, and a rarity in vertebrate genome (Gardiner-Garden and Frommer 1987). As such it is an activator of TLR9 (CD289), which is mostly expressed by B cells and dendritic cells. Once activated, TLR9 is internalized and then activates MyD88, which continues the signaling pathway. TLR9 signal pathway leads to a pro-inflammatory response and to secretion of cytokines such as type-I interferon, IL-6, TNF- $\alpha$ , IFN- $\alpha$ , and IL-12 (Ramirez-Ortiz et al. 2008; Agrawal and Gupta 2011). LPS: Lipopolysaccharides are large molecules consisting of a lipid and a polysaccharide fraction, which are found in the outer membrane of Gram-negative bacteria (Rothfield and Pearlman-Kothencz 1969). LPS binds the CD14/TLR4/MD2 receptor complex in many cell types, but especially in monocytes, dendritic cells and macrophages, and by doing so activating the signal pathway NF- $\kappa$ B, which promotes the secretion of pro-inflammatory cytokines, nitric oxide, and eicosanoids (Underhill and Ozinsky). Ionomycin: an ionophore produced by the bacterium *Streptomyces conglobatus*. Ionomycin is commonly used to raise the intracellular level of calcium ( $\text{Ca}^{2+}$ ) and so to stimulate the intracellular production of various cytokines, such as interferon, perforin, IL-2, and IL-4; usually in conjunction with PMA (Ai et al. 2013). PMA: phorbol 12-myristate 13-acetate, a di-ester of phorbol and a potent tumor promoter often used to activate the signal transduction enzyme protein kinase C (PKC) (Niedel et al. 1983). PMA is also commonly used together with ionomycin to stimulate T-cell activation, proliferation, and cytokine production, and is used in protocols for intracellular staining of these cytokines (Ai et al. 2013).

The used stimulating regimes are presented in Table 11:

Table 11: Stimulation regimes

<b>Panel</b>	<b>Stimulation</b>
#1 B cell subset	Unstimulated
#2 T cell subset	Unstimulated
#2B APC activation	Unstimulated
#3 major immune cell populations	22 h with LPS stimulated [100 pg/ml]
#4 B cell activation	22 h with CpG stimulated [2 µg/ml]
#5a cytokine secretion	22 h with CpG stimulated [1 µg/ml]
#5b cytokine secretion	20 h unstimulated + 2 h with LPS stimulated [500 pg/ml]
#5c cytokine secretion	22 h unstimulated
#6 CD20 <sup>+</sup> T cell subset	Unstimulated

+ 2 h Golgi Plug  
 + 2 h Ionomycin / PMA  
 [500 ng/ml / 20 ng/ml]

### 2.3.2.2 Sample preparation

The frozen cells in the cryo-medium were stored at -80°C. Due to the fact that the cryo-medium is toxic for living cells, a fast defrost was required, as well as a dilution of the cryo-medium in whole-medium in order to dilute the DMSO, the toxic part. Therefore, the samples were shortly warmed by hand, only until the still frozen sample could be transferred in a tube containing 30 ml whole-medium. In order to properly dilute the cryo-medium no more than three cryo-tubes were defrosted in the same tube. All tubes were centrifuged (1250 rpm, 4°C, 10 minutes) and the supernatants were removed. In case more than three cryo-tubes were needed, all cells of the same sample were resuspended in 10 ml whole-medium and transferred into one tube. That tube was again centrifuged and the supernatants were removed. All samples were then resuspended in 1 ml whole-medium, and the cell count was determined.

In order to do so a Neubauer chamber was used. To exclude dead cell from the count, 10 µl cell suspension was stained with 10 µl TrypanBlue suspension (prediluted 1:10 in PBS), making a dilution factor (*dil. fac.*) of two. 10 µl of that mixture was counted using the counting chamber. The cells in the four 1 mm<sup>2</sup> squares were counted, representing a total volume of 0,1 µl each, and the mean cells count was calculated. The total cell count of the sample was then calculated as following:

$$cell\ count = mean\ cells \cdot 10^4 \cdot dil.\ fac. \cdot volume[ml]$$

The cell suspension was then further diluted with whole-medium to a concentration of 500,000 cells/1 ml. 100  $\mu$ l of cell suspension, containing 50,000 cells, was given to a 96 well plate. Unstimulated panels were stained on the same day with a 96 U-well plate (panels #1, 2, 2B), stimulated panels were stimulated in 96 flat-well plate (panels #3, 4, 5a, 5b, 5c), to ensure an equal stimulation. To the stimulated panels #3, 4, 5a, 5b, 5c were added 100  $\mu$ l of 200 pg/ml LPS, 4  $\mu$ g/ml CpG, 2  $\mu$ g/ml CpG, 80  $\mu$ l whole-medium and 100  $\mu$ l whole-medium respectively, which resulted in a further dilution of the stimulants with the factor two (and so achieving the goal concentrations). The cells were incubated at 37°C, 5% CO<sub>2</sub> for 22 hours. To panel #5b 20  $\mu$ l of 5,000 pg/ml LPS were added after 20 hours incubation (after dilution 500 pg/ml) and the panel was then further incubated for 2 hours (37°C, 5% CO<sub>2</sub>). Panels #5a, b and c were then further treated as described in 2.3.2.6 below.

After incubation the plates were centrifuged (1250 rpm, 4°C, 10 minutes) and the supernatants were frozen at -20°C for a subsequent analysis.

#### 2.3.2.3 Dead/Live stain

In order to exclude dead cells from the analysis, the cells were stained with the fixable Zombie™ dye (ZombieAqua™/ZombieNIR™ as shown in Tables 8-10, BioLegend). The Zombie™ dyes react with primary amine groups on proteins. Living cells exclude the dye, resulting only in a surface stain, while dead cells with a compromised cell membrane don't. This results in an entry of the dye into the cytoplasm, and so increasing significantly the amount of stained proteins. Hence dead cells are significantly Zombie™ brighter than living cells, and can be distinguished (BioLegend).

Prior to staining, the cells were washed twice (resuspension in 170  $\mu$ l PBS followed by centrifugation [1250 rpm, 4°C, 7 min] and removal of supernatants, *wash in PBS*). Afterwards 30  $\mu$ l of the compatible Zombie™ dye (1:500 in PBS) were given into the sample wells and the Zombie™ single staining, followed by 10 minutes at room temperature incubation in the dark. Following the cells were washed in FACS buffer.

#### 2.3.2.4 Fc-block

Some immune cell populations bear Fc receptors on their surface, which may falsely bind and lead to non-specific staining of the antibodies. Therefore, a blockage of those Fc receptors was required in order to ensure a specific and accurate stain. After washing all cells were incubated with 30  $\mu$ l Fc-Block™ (50  $\mu$ g/ml in FACS buffer) for 10 minutes on ice in the dark. After incubation the cells were washed in FACS buffer.

#### 2.3.2.5 Surface stain

Before the surface stain can be performed, several preparations were required. The samples needed to be stained with all fluorophore labelled antibodies, whether the single staining samples only with one, in order to create a compensation. Therefore an “antibodies-mix”

containing all fluorophore labelled antibodies of a panel (diluted 1:100 in FACS buffer), as well as single antibody solutions (1:100 in FACS buffer) for the single stainings needed to be made. Samples were given with 30  $\mu$ l of antibody-mix, single stainings with 30  $\mu$ l of the single antibody solutions, and incubated for 10 minutes on ice in the dark. After incubation, the cells were washed in FACS buffer twice and then resuspended in 100  $\mu$ l FACS buffer for transfer into 5 ml FACS tubes for the flow cytometry analysis.

#### 2.3.2.6 Intracellular stain

In order to ensure a proper cytokine accumulation in the cells that can be stained and furthermore detected, the Golgi apparatus needs to be stopped. Therefore, 10  $\mu$ l GolgiPlug<sup>TM</sup> (pre-diluted 1:10 in whole-medium) were added to the “cytokine secretion” panels (panels #5a, b, c) after stimulation, followed by a two hours incubation (37°C, 5% CO<sub>2</sub>). To further increase the cytokine synthesis 50  $\mu$ l Ionomycin [3000 ng/ml] and 50  $\mu$ l PMA [300 ng/ml] were added [500 ng/ml respectively 20 ng/ml after in well dilution] and incubated for two more hours (37°C, 5% CO<sub>2</sub>). After incubation the cells were centrifuged (1250 rpm, 4°C, 10 minutes) and the supernatants were frozen at -20°C for a subsequent analysis. The cells to be stained were resuspended in PBS and a surface stain as described in 2.3.2.3 above was performed.

To perform an intracellular stain of the cells, the cell membrane needed to be fixed and permeabilized, achieved by adding 50  $\mu$ l Fix/Perm<sup>TM</sup> to each well followed by a 30 minutes incubation in room temperature in the dark. Afterwards the cells were washed in 200  $\mu$ l Perm/Wash<sup>TM</sup> (prediluted 1:10 in ddH<sub>2</sub>O) and then given 50  $\mu$ l of prepared intracellular fluorophore labelled antibody-mix respectively single antibody solutions (1:50 in Perm/Wash<sup>TM</sup>; as explained in 2.3.2.5 above). The cells were then incubated with the antibodies for 16 hours at 4°C covered with aluminum foil. On the next day the cells were wash in FACS buffer twice, resuspended in 100  $\mu$ l FACS buffer, transferred into a 5 ml FACS tube and analyzed.

### 2.3.3 Flow cytometry and gating strategy

The fluorophore-labelled stained cells were analyzed by flow cytometry using the LSRII Fortessa FACS machine (manufacturer: BD Biosciences). To ensure accurate and reliable results all samples were stained in duplicates. Each sample was acquired for 75 seconds (time required for 100  $\mu$ l sample to be fully acquired). Due to the large number of samples, they could not be processed and measured at the same time, though all samples of the same patient were always analyzed at the same time. In every repetition the PBMCs of the same healthy control were also analyzed, to ensure the stain's successfulness, and to analyze all samples similarly. The cells for the single stainings of the fluorophores also came from the healthy control. Even though all stains were performed identically, minor changes could not be avoided (such as antibody residue on the pipette end, causing a slightly brighter

fluorescence for example), which resulted in a slightly different compensation. In order not to neglect these minor differences, but rather address them, every stain was analyzed with its compensation and gated with its control.

The data obtained was analyzed using the FlowJo™ 10.5.3.

In order to identify the living cells in the sample, pre-gating was performed in all panels as shown in Figure 3A. Only those cells were then analyzed according to the goals of the panel. For some surface markers are ubiquitous expressed by all cells of a population, the mean fluorescence intensity (MFI) was used to semi quantify their expression, as shown in Figure 3B.

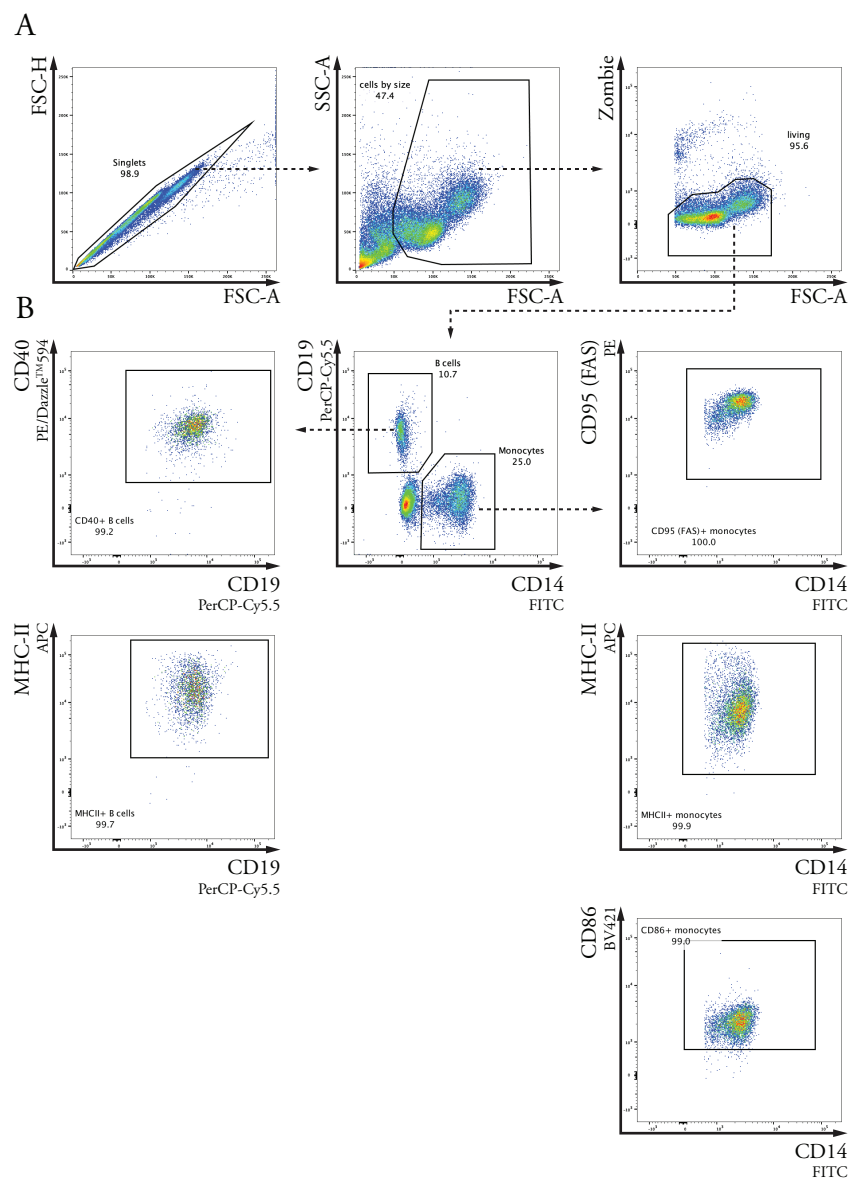


Figure 3. Gating strategy. The figure shows the three pre-gates that proceeded to every analysis (A) and a few examples of ubiquitous expressed surface antigens (B).

### 2.3.4 TBNK classification

The TBNK classification is a flow cytometry-based analysis of not agglutinated whole blood samples (EDTA blood). This classification was performed by the central laboratory of the University Medical Centre in Göttingen Germany. The certificate of the laboratory for this analysis is attached in supplements (see 6.1 below).

### 2.3.5 Statistical analysis

GraphPad Prism<sup>TM</sup> 7a was used for all statistical analysis. The patients' data were tested for Gauss distribution with the Shapiro-Wilk normality test and the Kolmogorov-Smirnov normality test. Data were analyzed as Gauss distributed when both tests were positive. For two longitudinal samples with Gauss distribution the paired t-test was used, without Gauss distribution the Wilcoxon matched-pairs signed rank test. As not all patients had samples for all time points, an ANOVA could not be performed. Therefore, paired t-tests respectively Wilcoxon matched-pairs signed rank tests were used and the  $\alpha$ -value was corrected with the Bonferroni-Holm method. For possible correlations linear regression was used, for interval scale Spearman  $r$ , for rational scale Pearson  $r$ . A  $p$ -value  $< 0.05$  was considered statistically significant, and  $p < 0.05$  (\*),  $p < 0.005$  (\*\*),  $p < 0.0005$  (\*\*\*),  $p < 0.0001$  (\*\*\*\*), were defined.

### 3 Results

#### 3.1 Direct effects of anti-CD20 depletion on CD20<sup>+</sup> B and T cells

##### 3.1.1 Effects on B cells

B cells are the target of anti-CD20 depletion, and the effects of their elimination were of great interest in this project. Therefore, it was necessary to ensure that the B cells were successfully eliminated. Figure 4 shows the B cell frequencies and counts in four time points for every patient (for differences between early and late repletion see 3.1.2 below). The figure shows, that the B cells, starting at a mean frequency of 10% and mean counts of 154 cells per  $\mu\text{l}$  blood before depletion, are successfully depleted at the “depletion” time point, and first reappear at the “late repletion” time point. A sample was considered repleted, when the CD19<sup>+</sup> cell frequency of all living PBMCs was greater than 1%.

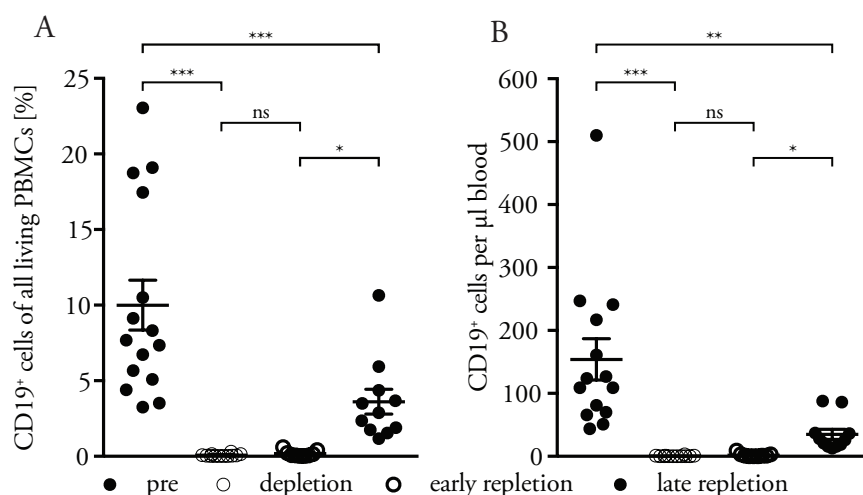


Figure 4. B cell frequency and cell count. The figure shows the frequencies of CD19<sup>+</sup> cells expressed as % of all living PBMCs unstimulated (A) and the B cell counts determined in a TBNK classification of whole blood (B) in four time points for every patient. Data is presented as mean  $\pm$  standard error of mean ( $n = 15/12/10/10$ ; Wilcoxon matched-pairs signed rank test as stated in figure).

In order to further characterize the possible changes in the B cell maturation phenotype upon repletion, five main B cell maturation phases described in 1.1.4.2 above and shown in Figure 5 were analyzed before B cell depletion and during late repletion. The figure shows a shift in the B cell maturation phenotype. Before B cell depletion, peripheral B cells were mainly mature naïve and memory B cells. During late repletion this phenotype changes, and the majority of B cells are transitional and naïve B cells making together a total of 83.96% of all B cells. This reflects the migration of new maturing cells from the bone marrow into the peripheral blood. The plasmablasts' frequency is slightly elevated, since these cells are not depleted after anti-CD20 treatment.

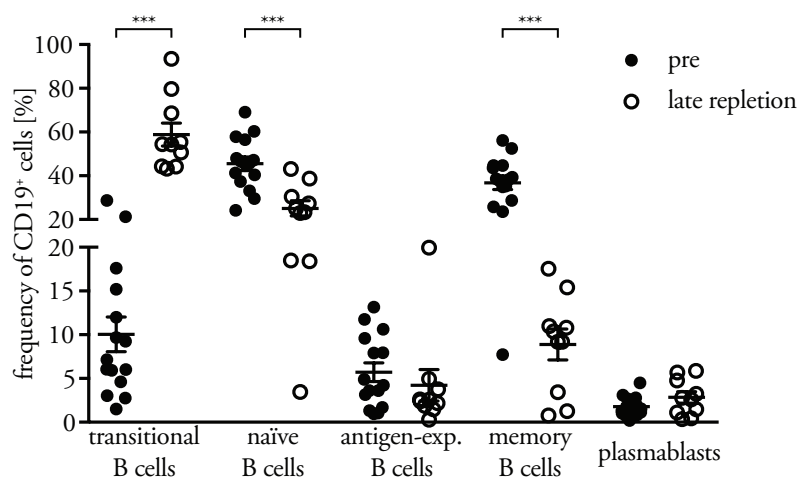


Figure 5. B cell maturation phenotype. The figure shows the frequencies of transitional, naïve, activated, memory B cells and plasmablasts expressed as % of CD19<sup>+</sup> cells before B cell depletion and during late repletion. Data is presented as mean  $\pm$  standard error of mean (n = 15/10; paired t-test/Wilcoxon matched-pairs signed rank test: ns unless otherwise stated).

As for the B cell activation phenotype, three key surface antigens were analyzed. As shown in Figure 6, the frequencies of CD25<sup>+</sup>, CD69<sup>+</sup> and CD95 (FAS)<sup>+</sup> B cells is significantly higher during late repletion than before therapy administration, indicating a more activated phenotype of the transitional and naïve B cells, the two major B cell populations at late repletion.

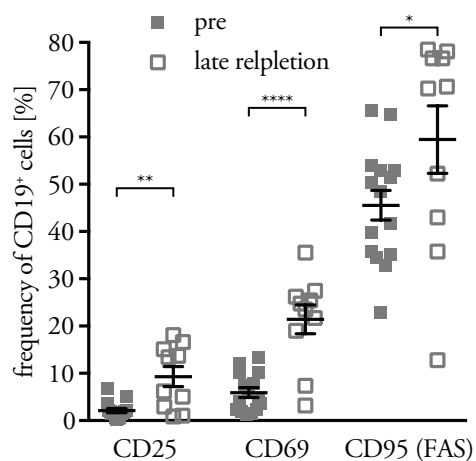


Figure 6. B cell activation phenotype. The figure shows the frequencies of CD25<sup>+</sup>, CD69<sup>+</sup>, and CD95 (FAS)<sup>+</sup> expressed as % of CD19<sup>+</sup> B cells upon CpG stimulation [2  $\mu$ g/ml] before B cell depletion and during late repletion. Data is presented as mean  $\pm$  standard error of mean (n = 15/10; paired t-test/Wilcoxon matched-pairs signed rank test: ns unless otherwise stated).

As B cells are professional APCs, their antigen presentation phenotype was analyzed. As shown in Figure 7, there seems to be a non-significant decrease in CD80<sup>+</sup> cells, however significantly more CD86<sup>+</sup> B cells were seen. The MFI of CD40 was slightly, yet significantly elevated, the MFI of MHC-II remained stable.

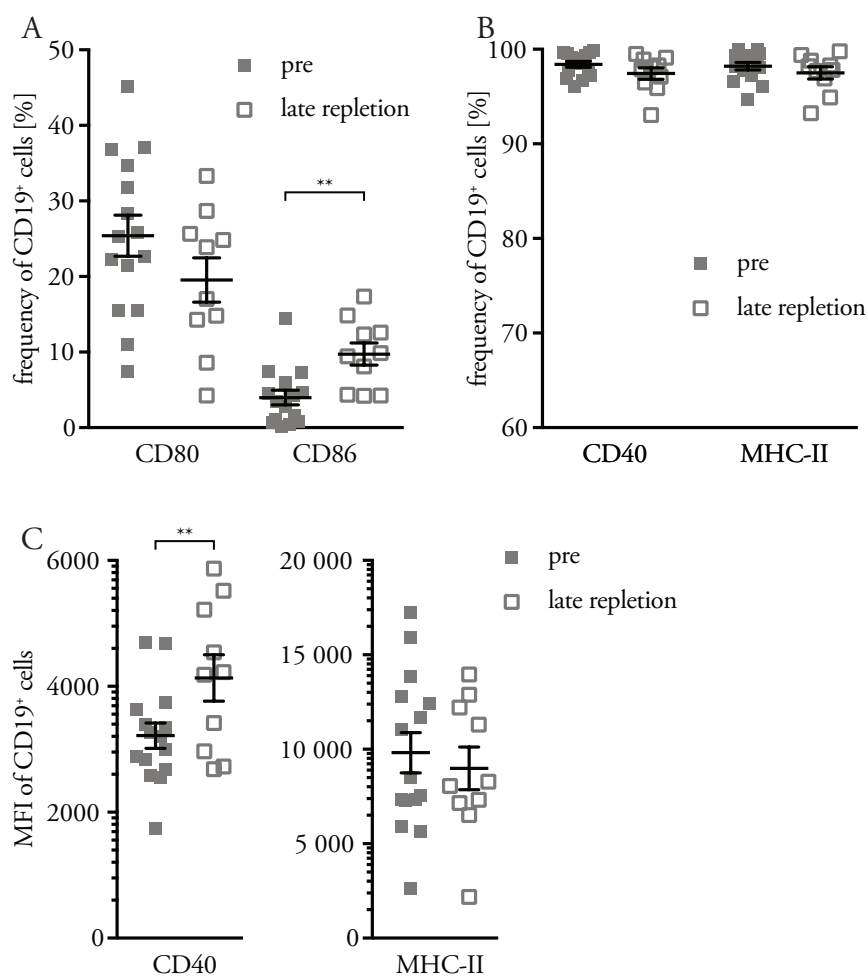


Figure 7. B cell APC phenotype. The figure shows the frequencies of (A) CD80<sup>+</sup>, CD86<sup>+</sup> and (B) CD40<sup>+</sup> and MHC-II<sup>+</sup> expressed as % of CD19<sup>+</sup> B cells and the (C) MFIs of CD40 and MHC-II of CD19<sup>+</sup> B cells upon CpG stimulation [2 µg/ml] before B cell depletion and during late repletion. Data is presented as mean ± standard error of mean (n = 15/10; paired t-test: ns unless otherwise stated).

The B cell expression of the surface antigens CD40, CD80, CD86, CD95 (FAS) and MHC-II was also analyzed unstimulated in panel #2B, an analysis which has shown similar differences as the results shown in Figures 6 and 7, and therefore are not shown here.

B cells have an immunomodulatory function, which they fulfil via cytokine secretion. IL-6, IL-10 and TNF- $\alpha$  are three of the cytokines that are known to have a key role in the pathogenesis of MS. The unstimulated B cell cytokine phenotype, as shown in Figure 8, shows a significant elevation in IL-6 production, a non-significant decrease in TNF- $\alpha$  production, and almost non-IL-10 production.

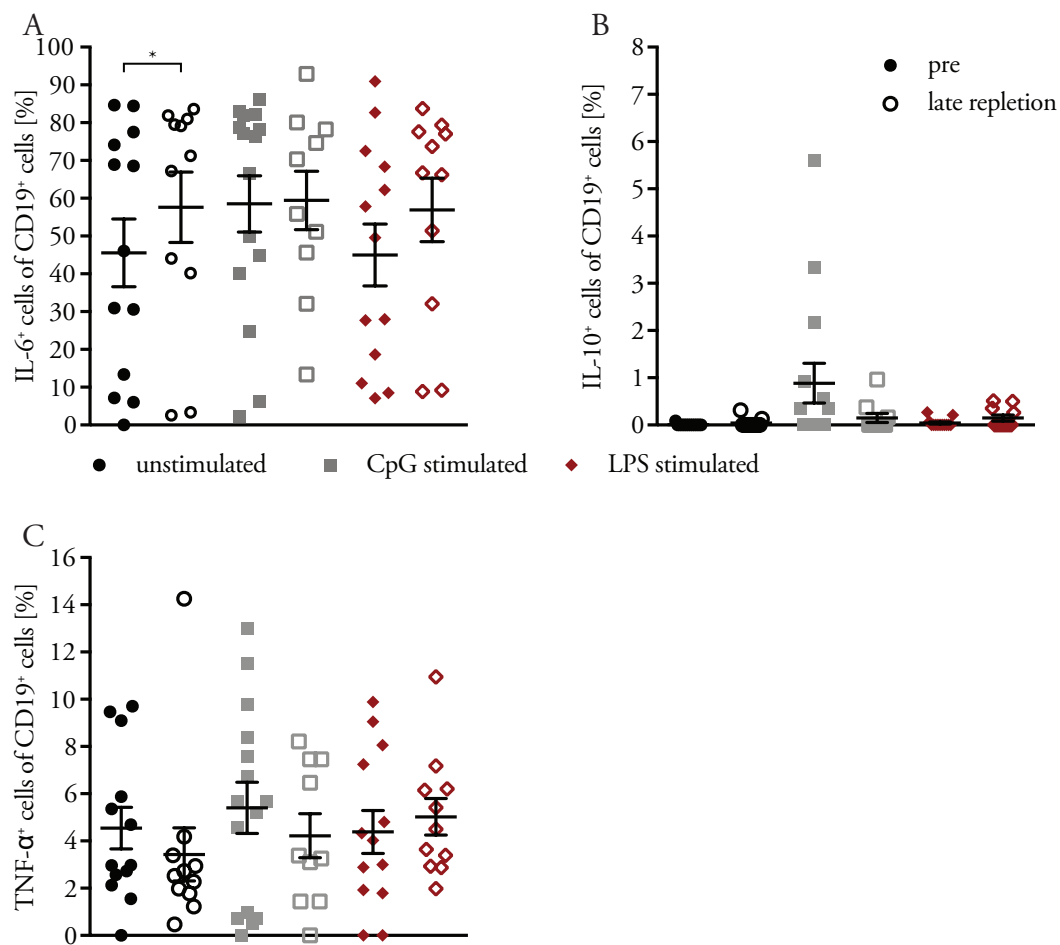


Figure 8. B cell cytokine phenotype. The figure shows the frequencies of IL-6<sup>+</sup> (A), IL-10<sup>+</sup> (B) and TNF-α<sup>+</sup> (C) cells expressed as % of CD19<sup>+</sup> B cells unstimulated, upon CpG [1 μg/ml] and LPS [500 pg/ml] stimulation as shown in Table 11 before B cell depletion and during late repletion. Data is presented as mean ± standard error of mean (n = 15/10; paired t-test/Wilcoxon matched-pairs signed rank test: ns unless otherwise stated).

### 3.1.2 Effects on CD20<sup>+</sup> T cells

T cells may express CD20, and therefore may be depleted after administration of anti-CD20-mAb. To characterize possible depletion and repletion of CD20<sup>+</sup> T cells and its kinetics, their frequencies were analyzed. The CD20<sup>+</sup> T cells replete earlier than the B cells. Figure 9 shows the four immunological states of the patients' samples. When comparing before therapy and at late repletion, the ratio between the frequencies of CD20<sup>+</sup> T<sub>H</sub>, T<sub>C</sub> and B cells is the same, all patients have very few CD20<sup>+</sup> T<sub>H</sub> cells, followed by CD20<sup>+</sup> T<sub>C</sub> cells (as they are a small subpopulation) and B cells. At depletion all three cell populations show a successful depletion. When comparing the differences at depletion and at early repletion, one could see a significant increase in CD20<sup>+</sup> T<sub>C</sub> cell frequency, a (after Bonferroni-Holm correction as stated in legend) non-significant increase in CD20<sup>+</sup> T<sub>H</sub> cell frequency, and a non-significant minor increase in B cell frequency, indicating the repletion of the CD20<sup>+</sup> T cells but not of the B cells.

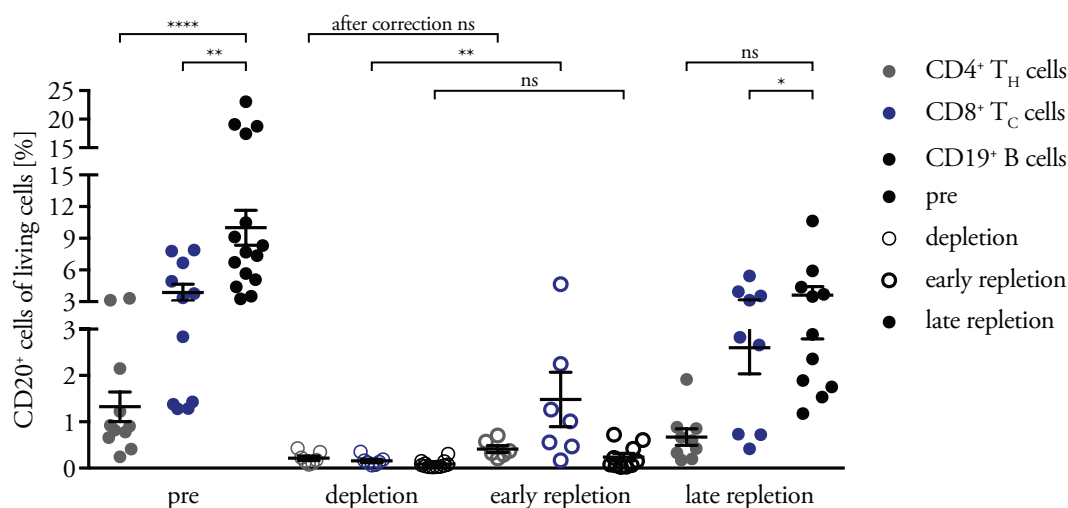


Figure 9. Overview of CD20<sup>+</sup> cells population. The figure shows the frequency of CD20<sup>+</sup> cell population expressed as % of all living PBMCs before anti-CD20 therapy (left), at depletion (2<sup>nd</sup> from left), at early, CD20<sup>+</sup> T cell, repletion (2<sup>nd</sup> from right) and at late, B cell, repletion (right). Data is presented as mean  $\pm$  standard error of mean (n = 11,11,15/7,7,12/7,7,10/9,9,11; Wilcoxon matched-pairs signed rank test/Mann-Whitney-U-Test as stated in figure; CD4<sup>+</sup> depletion-early repletion p = 0.0379, after Bonferroni-Holm correction: ns).

Figure 10 shows the frequencies of CD20<sup>+</sup> T cells in four time points for every patient. One could see, that the CD20<sup>+</sup> T cells, starting at mean frequency of 9% (all T cells) 5.8% (CD4<sup>+</sup>) and 16.3% (CD8<sup>+</sup>) are successfully depleted at the “depletion” time point, and start to replete at the time point “early repletion”, with a mean frequency of 2.85% (all T cells) 1.16% (CD4<sup>+</sup>) and 4.6% (CD8<sup>+</sup>) whereas the B cells, as shown in Figure 4, do not yet replete at that timepoint. A sample was considered repleted, when the CD20<sup>+</sup> cell frequency of CD4<sup>+</sup> respectively CD8<sup>+</sup> cells was greater than 1%.

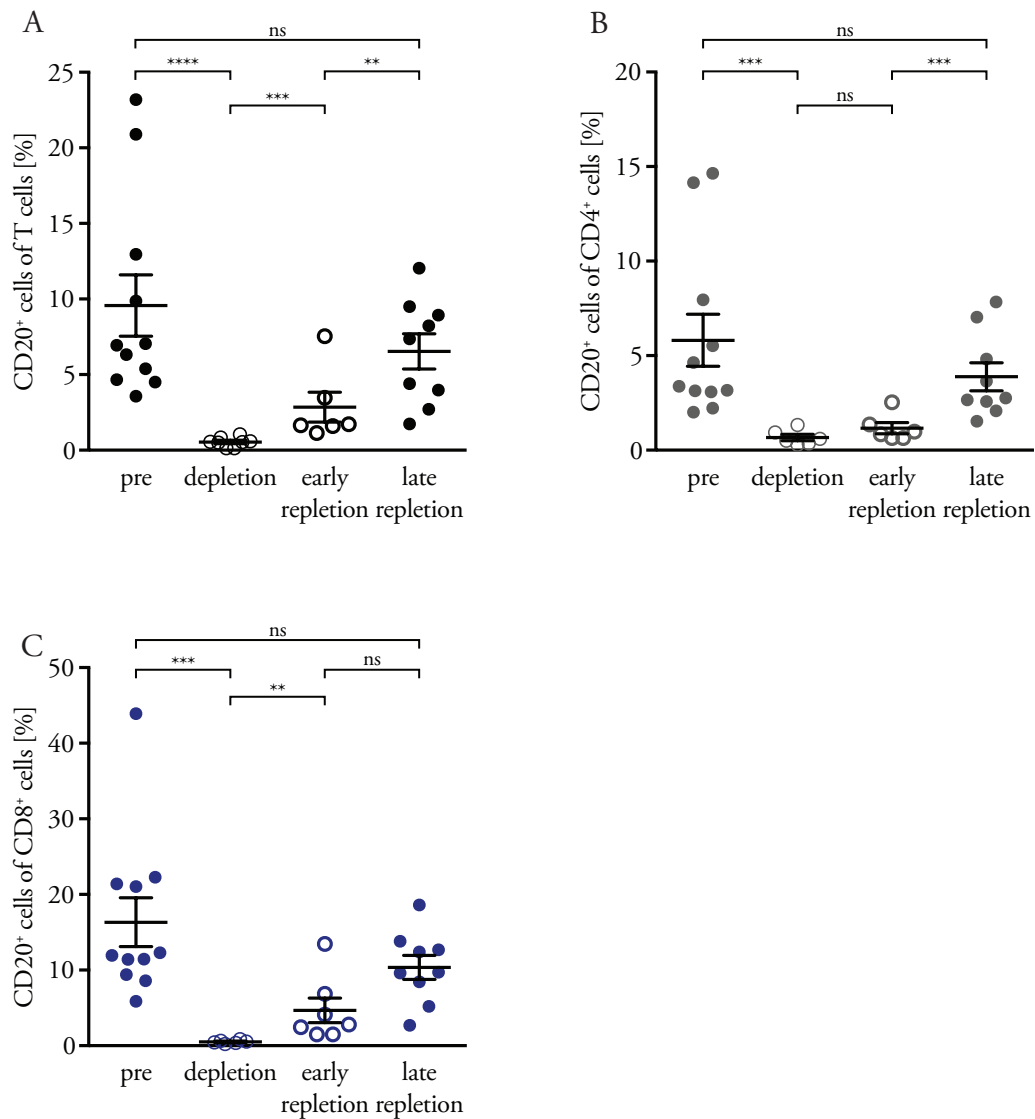


Figure 10. CD20<sup>+</sup> T cells frequencies. The figure shows the frequencies of CD20<sup>+</sup> cells expressed as % of all T cells (A) CD4<sup>+</sup> T<sub>H</sub> cells (B) and of CD8<sup>+</sup> T<sub>C</sub> cells (C) in four time points for every patient. Data is presented as mean ± standard error of mean (n = 11/6/7/9; Mann-Whitney-U-Test as stated in figure).

After observing that, the time difference between the repletion phases was of interest. Figure 11 shows the time difference between detection of repleting CD20<sup>+</sup> T cells (= early repletion), after a mean time of 191.81 days, compared to repleting CD20<sup>+</sup> B cells (= late repletion), that occurred after a mean time of 309.09 days. One could see through the lines connecting every patient's date, that the CD20<sup>+</sup> T cells replete earlier than the CD20<sup>+</sup> B cells individually for every patient.

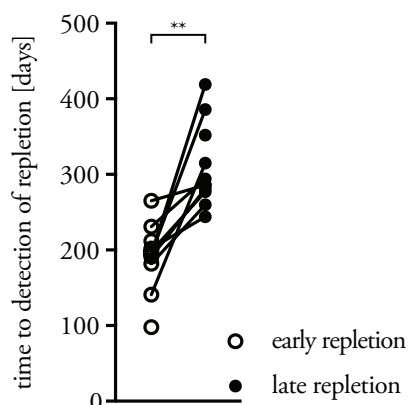


Figure 11. Time to detection of CD20<sup>+</sup> cells' repletion. The figure shows the time in days past between last anti-CD20 therapy administration and the detection of CD20<sup>+</sup> cells at early and late repletion phases. (n = 9, paired t-test).

As shown in Figure 10, the T<sub>C</sub> cells express more CD20 than T<sub>H</sub> cells, the T<sub>4</sub>/T<sub>8</sub> ratio (ratio between the frequencies of CD4<sup>+</sup> T<sub>H</sub> and CD8<sup>+</sup> T<sub>C</sub> of CD20<sup>+</sup> respectively CD20<sup>-</sup> of all living PBMCs) was also analyzed before the administration of anti-CD20 therapy. Figure 12A presents the frequencies of CD4<sup>+</sup> respectively CD8<sup>+</sup> cells of CD20<sup>+</sup> and of CD20<sup>-</sup> T cells, and shows that among the CD20<sup>-</sup> T cells, the frequencies of CD4<sup>+</sup> T<sub>H</sub> and CD8<sup>+</sup> T<sub>C</sub> cells are largely the same, explaining the mean ratio of 1 (the distribution of the ratios in Figure 12B shows that the frequencies within the CD20<sup>-</sup> cells compartment also varies, but as shown in figure non-significant). On the other hand, the figure shows that the frequency of CD8<sup>+</sup> T<sub>C</sub> cells among the CD20<sup>+</sup> T cell compartment is almost double than the frequency of the CD4<sup>+</sup> T<sub>H</sub> cells within this compartment, explaining the ratio of 0.5.

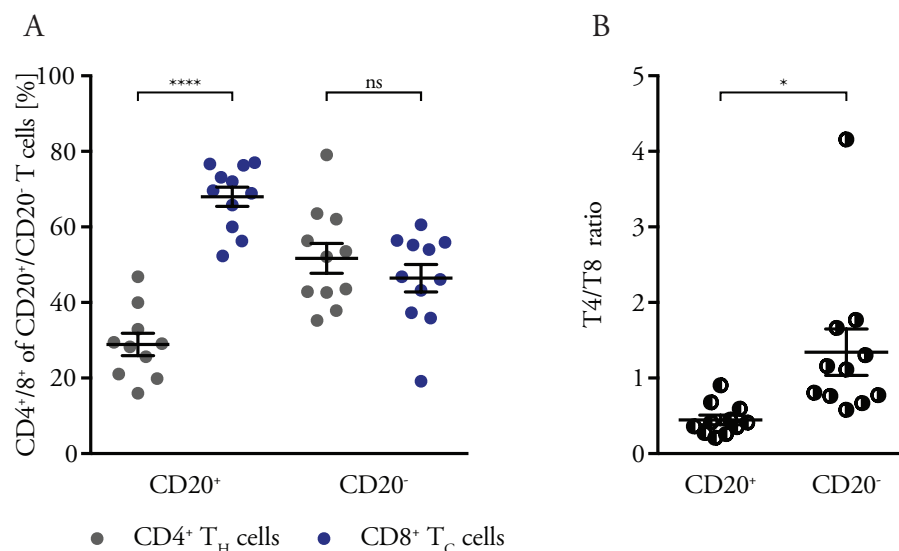


Figure 12. T<sub>4</sub>/T<sub>8</sub> ratio. The figure shows the (A) frequencies of CD4<sup>+</sup> T<sub>H</sub> and CD8<sup>+</sup> T<sub>C</sub> cells within the CD20<sup>+</sup> and CD20<sup>-</sup> T cell compartment before administration of anti-CD20 therapy expressed as % of all T cells. The figure also shows the (B) T<sub>4</sub>/T<sub>8</sub> ratio among the T cells in the compartment. Data is presented as mean ± standard error of mean (n = 11; paired t-test as stated in figure).

Furthermore, the detailed characterization of the CD20<sup>+</sup> T cells maturation phases (naïve and memory) and the CD25 expression was analyzed. The CD25 expression of the CD20<sup>+</sup> T cells did not differ from its expression among the CD20<sup>-</sup> T cells (data not shown).

Figure 13 shows the two maturation phases of the CD20<sup>+</sup> CD4<sup>+</sup> T<sub>H</sub> cells and their CD25 expression. Most CD20<sup>+</sup> T<sub>H</sub> cells were memory T cells before depletion and at early and late repletion. Their frequency slightly decreases at early repletion and increases at late repletion, all non-significant. The frequency of naïve CD20<sup>+</sup> T<sub>H</sub> cells, expressing CD45RA, remains mostly stable during the three time points. It increases at early repletion, and stays constant at late repletion, all non-significant. The CD25 expression of these cells remains constant through all time points (besides one patient).

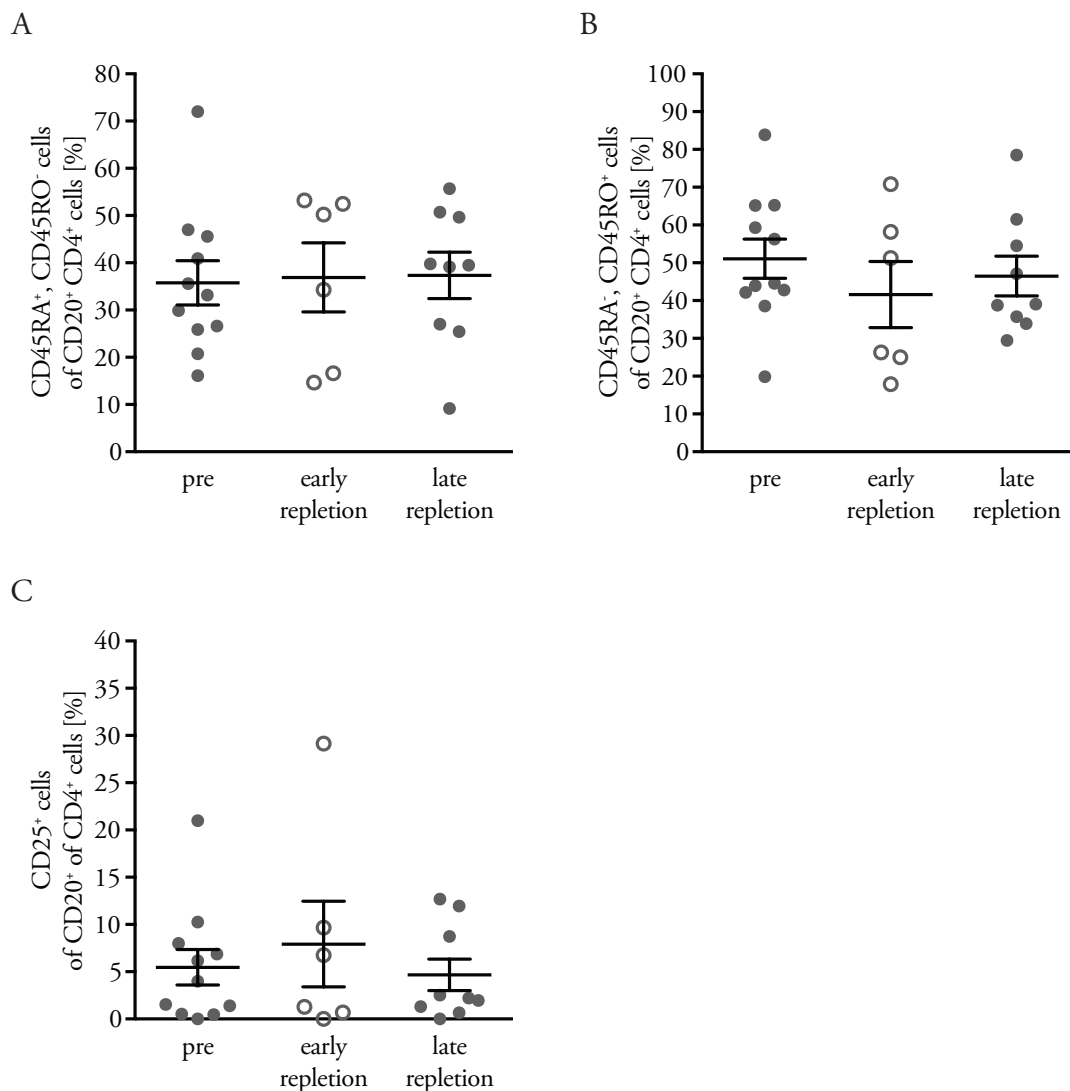


Figure 13. CD20<sup>+</sup> CD4<sup>+</sup> T<sub>H</sub> cells maturation and CD25 expression phenotype. The figure shows the frequencies of naïve (A) and memory (B) CD20<sup>+</sup> T<sub>H</sub> cells expressed as % of CD20<sup>+</sup> CD4<sup>+</sup> cells as well as the CD25<sup>+</sup> (C) CD20<sup>+</sup> T<sub>H</sub> cells expressed as % of CD20<sup>+</sup> CD4<sup>+</sup> cells through three time points for every patient. Data is presented as mean ± standard error of mean (n = 11/6/9; paired t-test/Wilcoxon matched-pairs signed rank test: ns unless otherwise stated).

Figure 14 shows the three maturation phases of the CD20<sup>+</sup> CD8<sup>+</sup> T<sub>C</sub> cells and their CD25 expression. Most CD20<sup>+</sup> T<sub>C</sub> cells were naïve before depletion and at early and late repletion. The transient CD20<sup>+</sup> T<sub>C</sub> cells, expressing both CD45RA and CD45RO, remain through all time points constant at approx. 22%. On the other hand, the frequency of memory CD20<sup>+</sup> T<sub>C</sub> cells, expressing CD45RO, increases non-significantly at early repletion, and then significantly decreases at late repletion. The CD25 expression of these cells remains constant through all time points (besides one patient, but not the same one as in Figure 13).

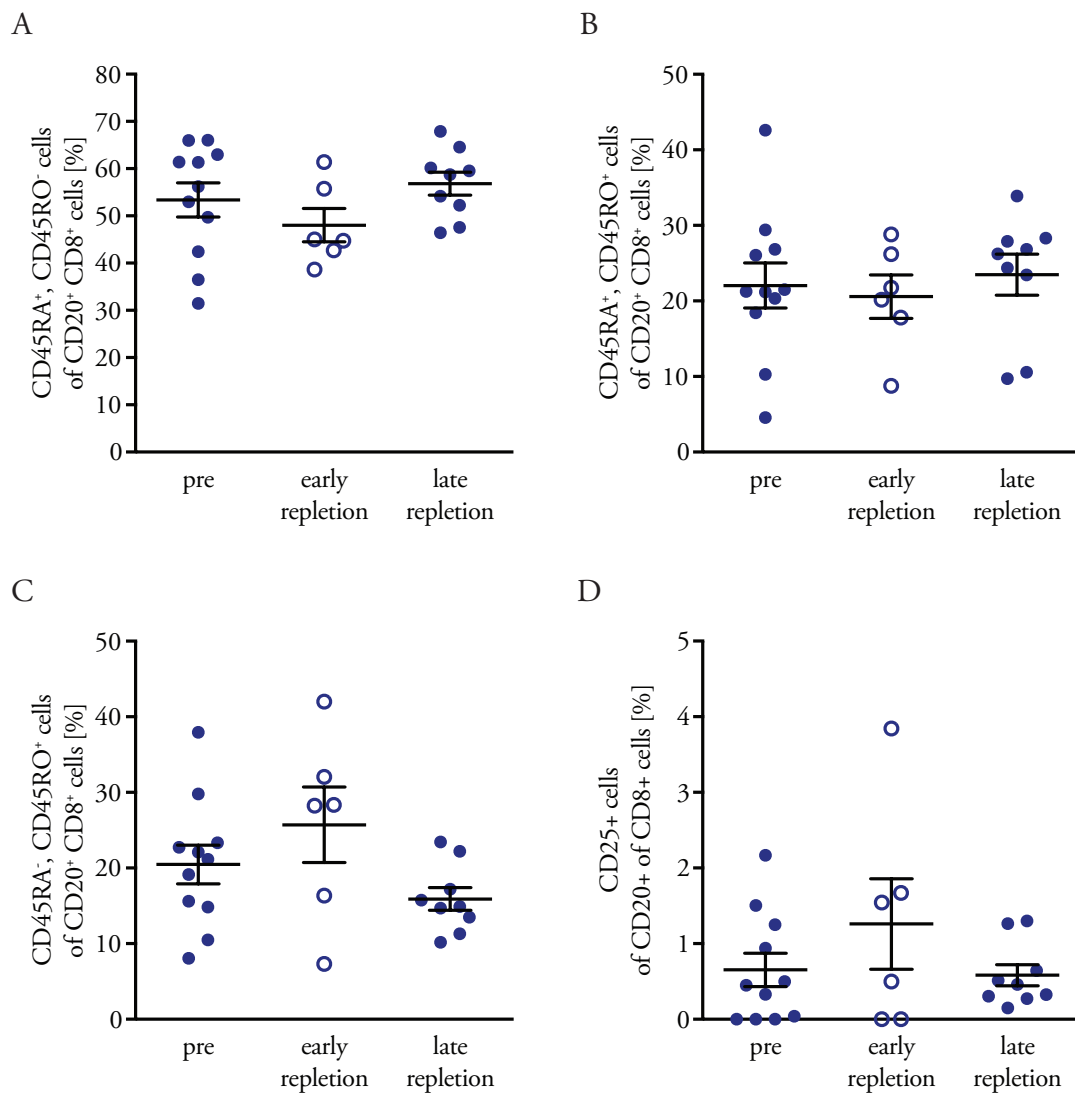


Figure 14. CD20<sup>+</sup> CD8<sup>+</sup> T<sub>C</sub> cells maturation and CD25 expression phenotype. The figure shows the frequencies of naïve (A), transient (B) and memory (C) CD20<sup>+</sup> T<sub>C</sub> cells expressed as % of CD20<sup>+</sup> CD8<sup>+</sup> cells as well as the CD25<sup>+</sup> (D) CD20<sup>+</sup> T<sub>C</sub> cells expressed as % of CD20<sup>+</sup> CD8<sup>+</sup> cells through three time points for every patient. Data is presented as mean ± standard error of mean (n = 11/6/9; paired t-test/Wilcoxon matched-pairs signed rank test: ns unless otherwise stated).

## 3.2 Indirect effects on other immune cell populations

### 3.2.1 Effects on CD20<sup>+</sup> T cells

As they play different roles in the immune reaction and interact differently with B cells, it is necessary to differentiate between CD4<sup>+</sup> T<sub>H</sub> cells and CD8<sup>+</sup> T<sub>C</sub> cells.

#### 3.2.1.1 Effects on CD4<sup>+</sup> T<sub>H</sub> helper cells

In the classical EAE model of MS, the disease is driven by autoreactive CD4<sup>+</sup> T<sub>H</sub> cells. Therefore, it was of great interest to examine the influence of anti-CD20 therapy on this immune population. Figure 15 shows the CD4<sup>+</sup> T<sub>H</sub> cells' frequencies and cell counts in the four time points for every patient. One could see a significant increase in the frequency of T<sub>H</sub> cells at depletion, representing the loss of CD20<sup>+</sup> cells, which then normalizes, reflecting the CD20<sup>+</sup> cell depletion and the successive repletion of CD20<sup>+</sup> T cells and of B cells. On the other hand, the cell count hardly changes.

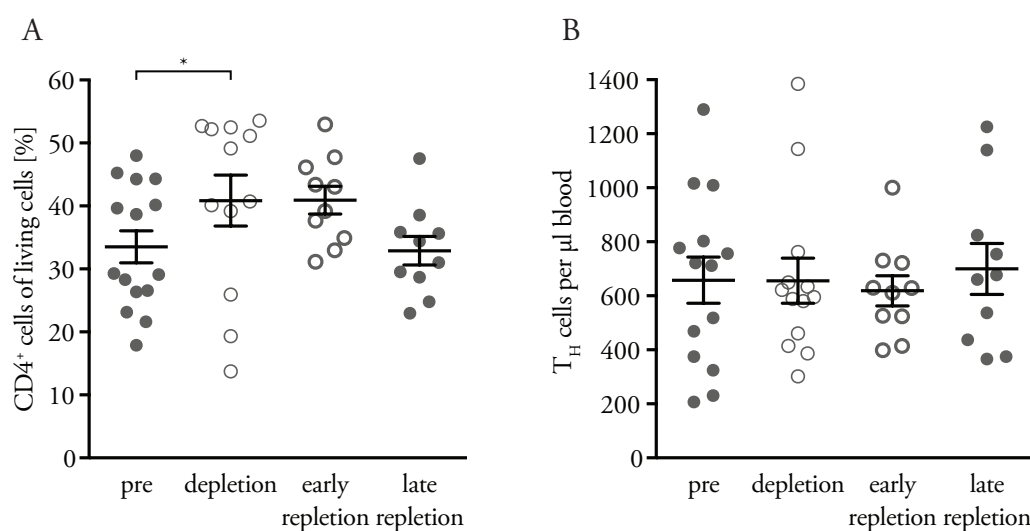


Figure 15. CD4<sup>+</sup> T<sub>H</sub> cells frequency and cell count. The figure shows the frequencies of CD4<sup>+</sup> cells expressed as % of all living PBMCs unstimulated (A) and the T<sub>H</sub> cell counts determined in a TBNK classification of whole blood (B) in four time points for every patient. Data is presented as mean  $\pm$  standard error of mean ( $n = 15/12/10/10$ ; Wilcoxon matched-pairs signed rank test: ns unless otherwise stated).

As mentioned above, the CD4<sup>+</sup> T<sub>H</sub> cells maturation phenotype through the four time points was of great interest, for changes could affect the disease progression. The CD4<sup>+</sup> T<sub>H</sub> cells maturation phenotype as presented in Figure 16 shows a majority of T<sub>TD</sub> (47.2%) followed by T<sub>EM</sub> (13.4%), T<sub>CM</sub> (11.9%) and T<sub>N</sub> (11.8%). A significant increase in T<sub>N</sub>, T<sub>CM</sub>, and T<sub>EM</sub> frequencies between pre-treatment and late depletion can be seen to 18.4%, corresponding 18.6% and a corresponding significant decrease in T<sub>TD</sub> from 47.2% to 34.4%, which doesn't change the order, but reducing the difference between the populations' frequencies. Moreover, T<sub>CM</sub> and T<sub>EM</sub> frequencies show a characteristic trend: slightly increasing at depletion, decreasing at early repletion and again increasing at late repletion.

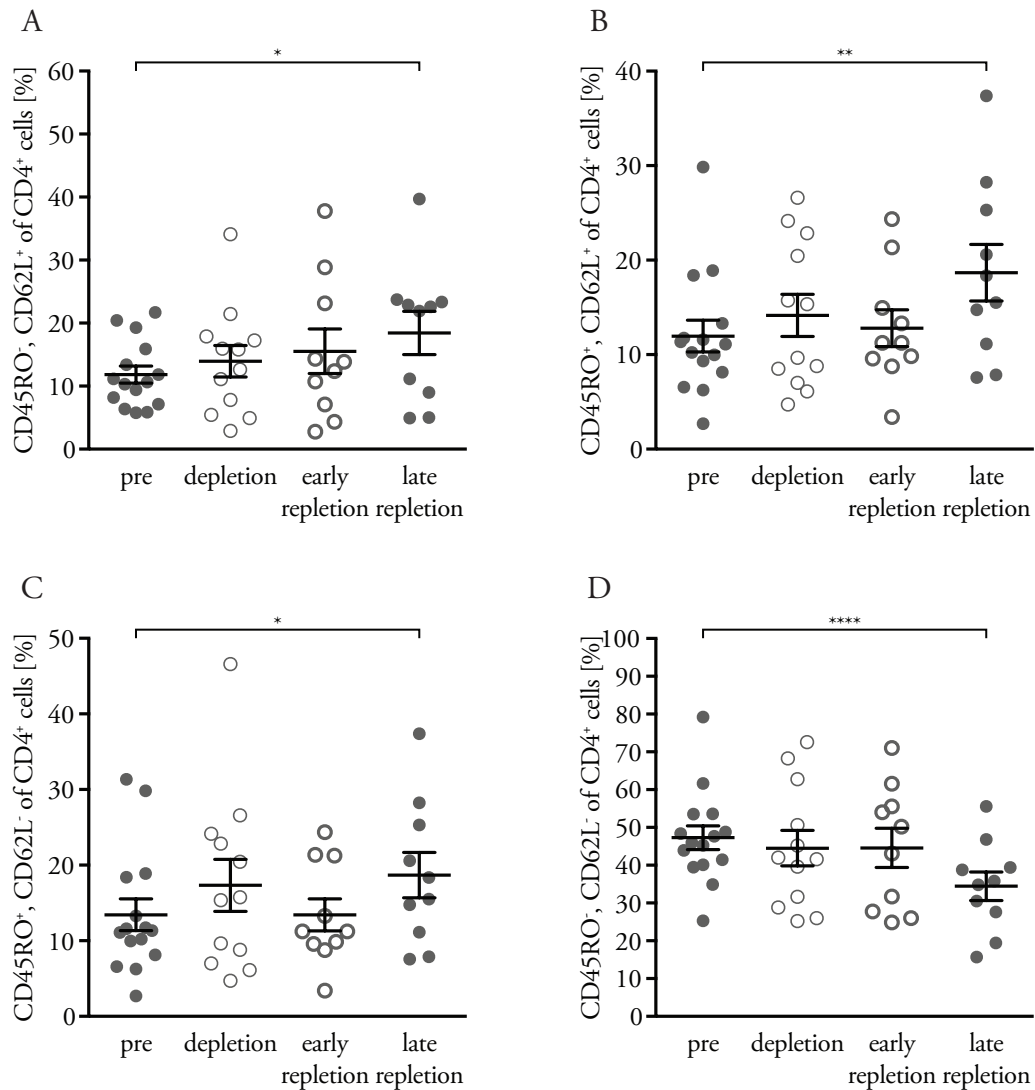


Figure 16. CD4<sup>+</sup> T<sub>H</sub> cells maturation phenotype. The figure shows the frequencies of naïve (A), central memory (B), effector memory (C) and terminally differentiated (D) T<sub>H</sub> cells expressed as % of CD4<sup>+</sup> cells through four time points for every patient. Data is presented as mean ± standard error of mean (n = 15/12/10/10; paired t-test/Wilcoxon matched-pairs signed rank test: ns unless otherwise stated).

As CD62L is a surface antigen used to migrate through the blood vessels in the periphery, its overall expression was of interest. Figure 17 shows the increasing overall CD62L expression by CD4<sup>+</sup> T<sub>H</sub> cells through all time points, showing a significance only between the time points before therapy and the transition between early and late repletion. This corresponds to the trends shown in Figure 16, an increase in T<sub>N</sub> and T<sub>CM</sub> (expressing CD62L) and a decrease in T<sub>TD</sub>.

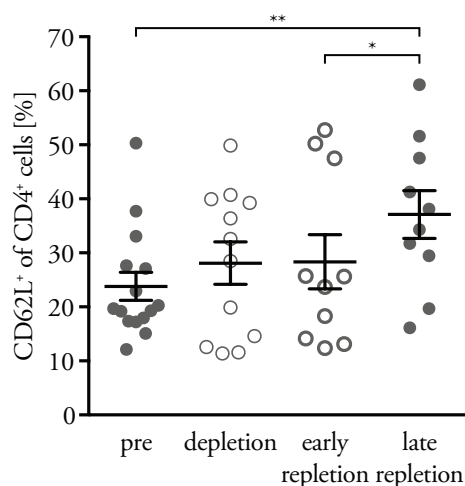


Figure 17. CD4<sup>+</sup> T<sub>H</sub> cells' CD62L expression. The figure shows the frequencies of CD62L<sup>+</sup> T<sub>H</sub> cells expressed as % of CD4<sup>+</sup> cells through four time points for every patient. Data is presented as mean  $\pm$  standard error of mean (n = 15/12/10/10; Wilcoxon matched-pairs signed rank test: ns unless otherwise stated).

### 3.2.1.2 Effects on CD8<sup>+</sup> cytotoxic T<sub>C</sub> cells

CD8<sup>+</sup> T<sub>C</sub> cells are the dominant cell population in MS lesions. Therefore, it was of great interest to examine the influence of anti-CD20 therapy on this immune cell population. Figure 18 shows, that the CD8<sup>+</sup> T<sub>C</sub> cells' frequencies and cell counts in the four time points for every patient hardly change. A slight non-significant decrease in cell count can be seen upon CD20 depletion, which could be contributed to the fact, that 16.3% of CD8<sup>+</sup> T<sub>C</sub> cells are CD20<sup>+</sup> as shown in Figure 10.

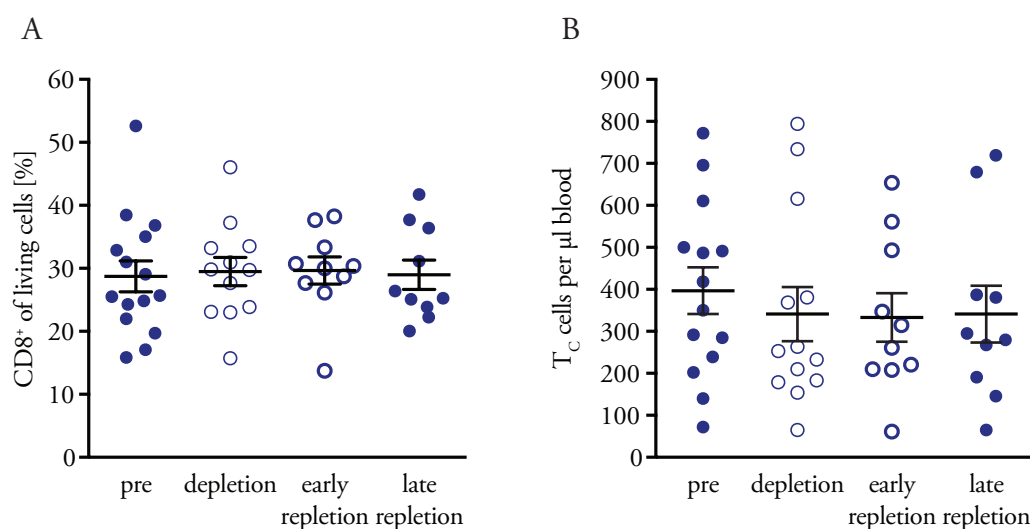


Figure 18. CD8<sup>+</sup> T<sub>C</sub> cells frequency and count. The figure shows the frequencies of CD8<sup>+</sup> cells expressed as % of all living PBMCs unstimulated (A) and the T<sub>C</sub> cell counts determined in a TBNK classification of whole blood (B) in four time points for every patient. Data is presented as mean  $\pm$  standard error of mean (n = 15/12/10/10; Wilcoxon matched-pairs signed rank test: ns unless otherwise stated).

As previously mentioned, the CD8<sup>+</sup> T<sub>C</sub> cells maturation phenotype through the four time points was of great interest, for changes could affect the disease progression. The CD8<sup>+</sup> T<sub>C</sub> cells maturation phenotype, as presented in Figure 19, shows a majority of T<sub>TD</sub> (53.7%) followed by T<sub>EM</sub> (25.9%), T<sub>N</sub> (12.4%) and T<sub>CM</sub> (7.95%) before depletion, corresponding to the CD4<sup>+</sup> T<sub>H</sub> cells. A small, yet significant, increase in T<sub>N</sub> (16.7%) and T<sub>CM</sub> (10.1%) in comparison to a corresponding decrease in T<sub>TD</sub> (49.14%) and T<sub>EM</sub> (23.8%) can be seen at late repletion. In addition, a trend corresponding to the frequency changes in CD4<sup>+</sup> T<sub>CM</sub> and T<sub>EM</sub> can be seen: increased frequencies of T<sub>N</sub> and T<sub>CM</sub> at depletion, decreased frequencies at early repletion (CD20<sup>+</sup> T cells repletion) and increased frequencies at late repletion. T<sub>EM</sub> and T<sub>TD</sub> do the opposite, T<sub>TD</sub> significant, T<sub>EM</sub> non-significant

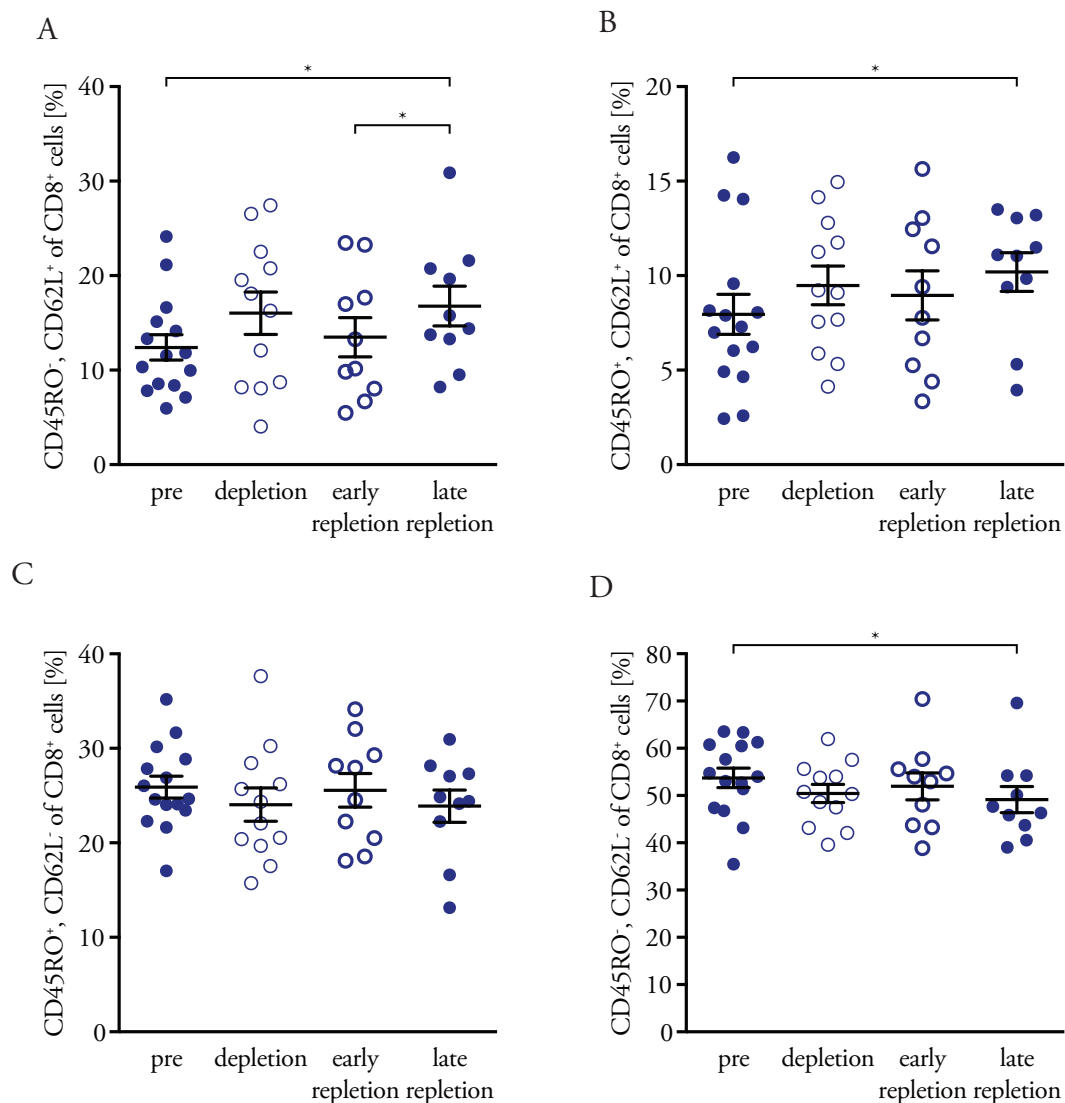


Figure 19. CD8<sup>+</sup> T<sub>C</sub> cells maturation phenotype. The figure shows the frequencies of naïve (A), central memory (B), effector memory (C) and terminally differentiated (D) T<sub>C</sub> cells expressed as % of CD8<sup>+</sup> cells through four time points for every patient. Data is presented as mean ± standard error of mean (n = 15/12/10/10; paired t-test: ns unless otherwise stated).

As CD62L is a surface antigen used to migrate through the blood vessels in the periphery, its overall expression was of interest. Figure 20 shows, that the overall CD62L expression by

CD8<sup>+</sup> T<sub>C</sub> cells slightly increases from 20.3% before depletion to 25.5% at depletion, decreasing to 22.5% at early repletion and again increasing to 27% at late repletion, corresponding to the trend seen in the frequencies of T<sub>N</sub>, T<sub>CM</sub> and T<sub>TD</sub> (Figure 19).

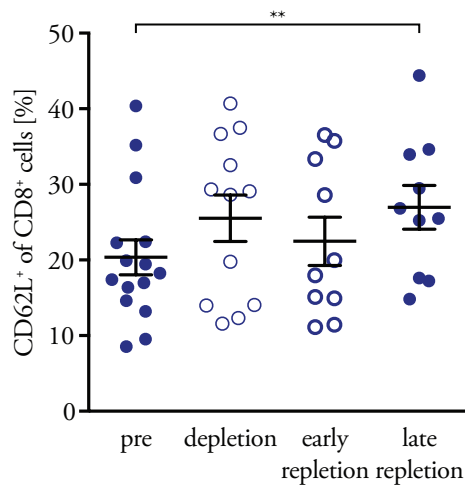


Figure 20. CD8<sup>+</sup> T<sub>C</sub> cells' CD62L expression. The figure shows the frequencies of CD62L<sup>+</sup> T<sub>C</sub> cells expressed as % of CD8<sup>+</sup> cells through four time points for every patient. Data is presented as mean ± standard error of mean (n = 15/12/10/10; Wilcoxon matched-pairs signed rank test: ns unless otherwise stated).

### 3.2.2 Effects on myeloid cells

The interaction between myeloid APCs and T cells is of great interest, since myeloid cells could, on the one hand, stimulate the T cells through antigen presentation or through pro-inflammatory cytokine secretion, but on the other hand, reduce the immune reaction through anti-inflammatory cytokines. As Figure 21 shows, the CD14<sup>+</sup> myeloid cells' frequencies increase relatively through the four time points, even though the monocytes' cell counts in the four time points don't change.

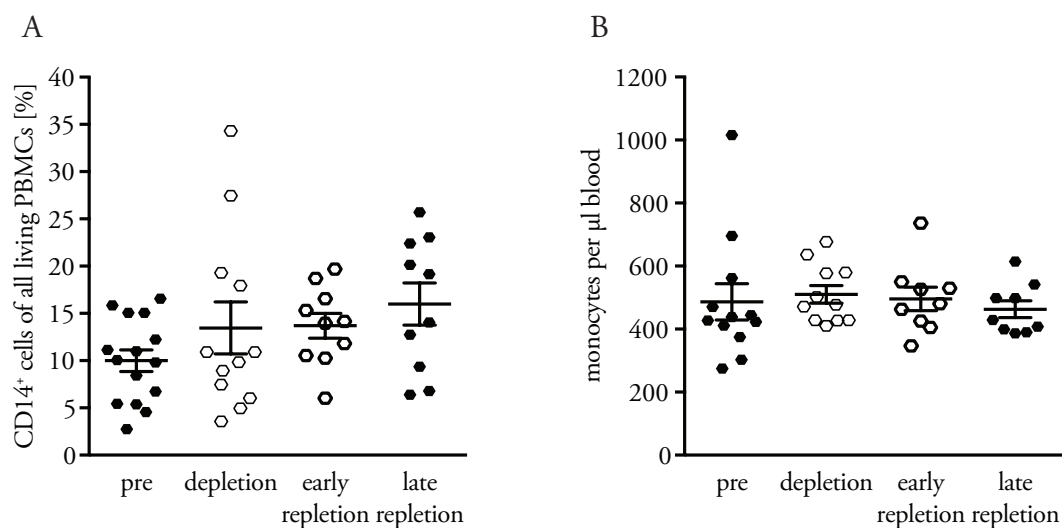


Figure 21. CD14<sup>+</sup> myeloid cells frequency and monocytes' cell count. The figure shows the frequencies of CD14<sup>+</sup> cells expressed as % of all living PBMCs unstimulated (A) and the monocytes' cell counts calculated from hemogram (B) in four time points for every patient. Data is presented as mean  $\pm$  standard error of mean ( $n = 15/12/10/10$ ; Wilcoxon matched-pairs signed rank test: ns unless otherwise stated).

In the myeloid cells' activation panel, the expressions of CD95 (FAS) and CD150, were analyzed. Figure 22 shows, that the myeloid cells' low CD150 expression, which varied before depletion, becomes unanimous at depletion. It then decreases at early repletion and varies again at late repletion, all non-significant. The overall expression of CD150 hardly changes. The figure also shows the myeloid cells' ubiquitous expression of CD95 (FAS), and the changes in its MFI. The CD95 (FAS) expression stays at three of the time points constant, yet increases significantly at early repletion, when compared to the expression before therapy.

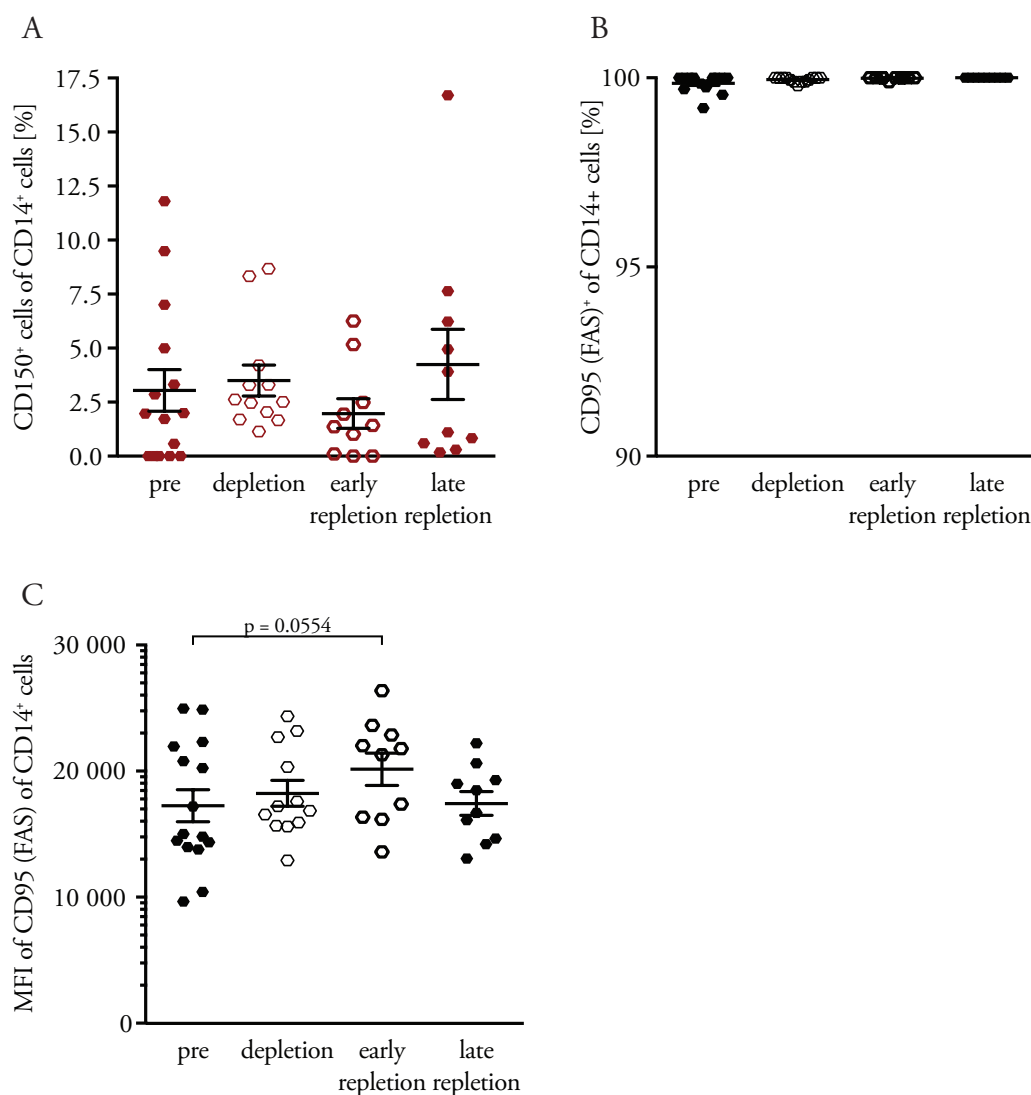


Figure 22. Myeloid cells' activation phenotype. The figure shows the (A) frequencies of CD150<sup>+</sup> myeloid cells expressed as % of CD14<sup>+</sup> cells upon LPS stimulation [100 pg/ml], as shown in Table 11, (B) the frequencies of CD95 (FAS)<sup>+</sup> myeloid cells expressed as % of CD14<sup>+</sup> cells and (C) MFI of CD95 (FAS) of CD14<sup>+</sup> cells through four time points for every patient. Data is presented as mean  $\pm$  standard error of mean (n = 15/12/10/10; Wilcoxon matched-pairs signed rank test/paired t-test: ns unless otherwise stated).

Like B cells, myeloid cells are professional APCs, and as such, they could interact with T cells. With the potential to take over the B cells' function as APCs, the myeloid cells' APC phenotype was of great interest. Figures 23 and 24 show the myeloid cells' APC phenotype. The myeloid cells' CD40 expression slightly increases, reaching a maximum at late repletion, but at B cell repletion decreases to its original level, all non-significant. The same trend can be seen in the MFIs of this surface antigen, showing a significantly increased expression at early repletion compared with the expression before therapy. At late repletion the expression decreases to its original level. The MHC-II expression acts the same, increasing at depletion and at early repletion and sinking, this time below its original level at late repletion. One could see through the MHC-II expression, that the myeloid cells' reaction

to the anti-CD20 depletion differs from patient to patient. Though the mean of said surface antigen only slightly changes, the variability changes at early repletion.

The myeloid cells' CD80 expression almost doesn't change throughout the different time points, and their CD86 expression shows a similar trend to the T<sub>C</sub> and T<sub>H</sub> cells, increasing at depletion, slightly decreasing at early repletion and again increasing at late repletion.

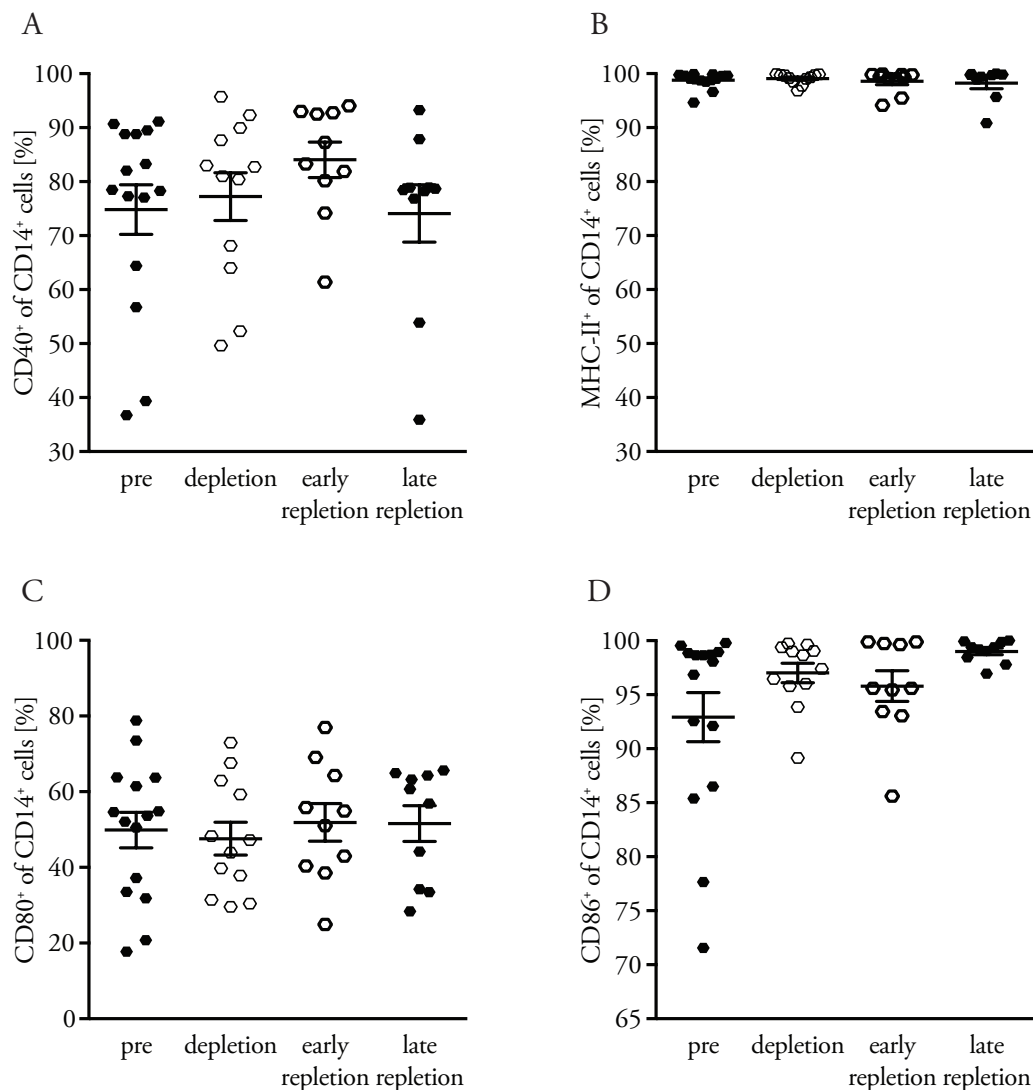


Figure 23. Myeloid cells' APC phenotype I. The figure shows the frequencies of CD40<sup>+</sup> (A), MHC-II<sup>+</sup> (B), CD80<sup>+</sup> (C) and CD86<sup>+</sup> (D) myeloid cells expressed as % of CD14<sup>+</sup> cells through four time points for every patient. Data is presented as mean  $\pm$  standard error of mean (n = 15/12/10/10; paired t-test/Wilcoxon matched-pairs signed rank test: ns unless otherwise stated).

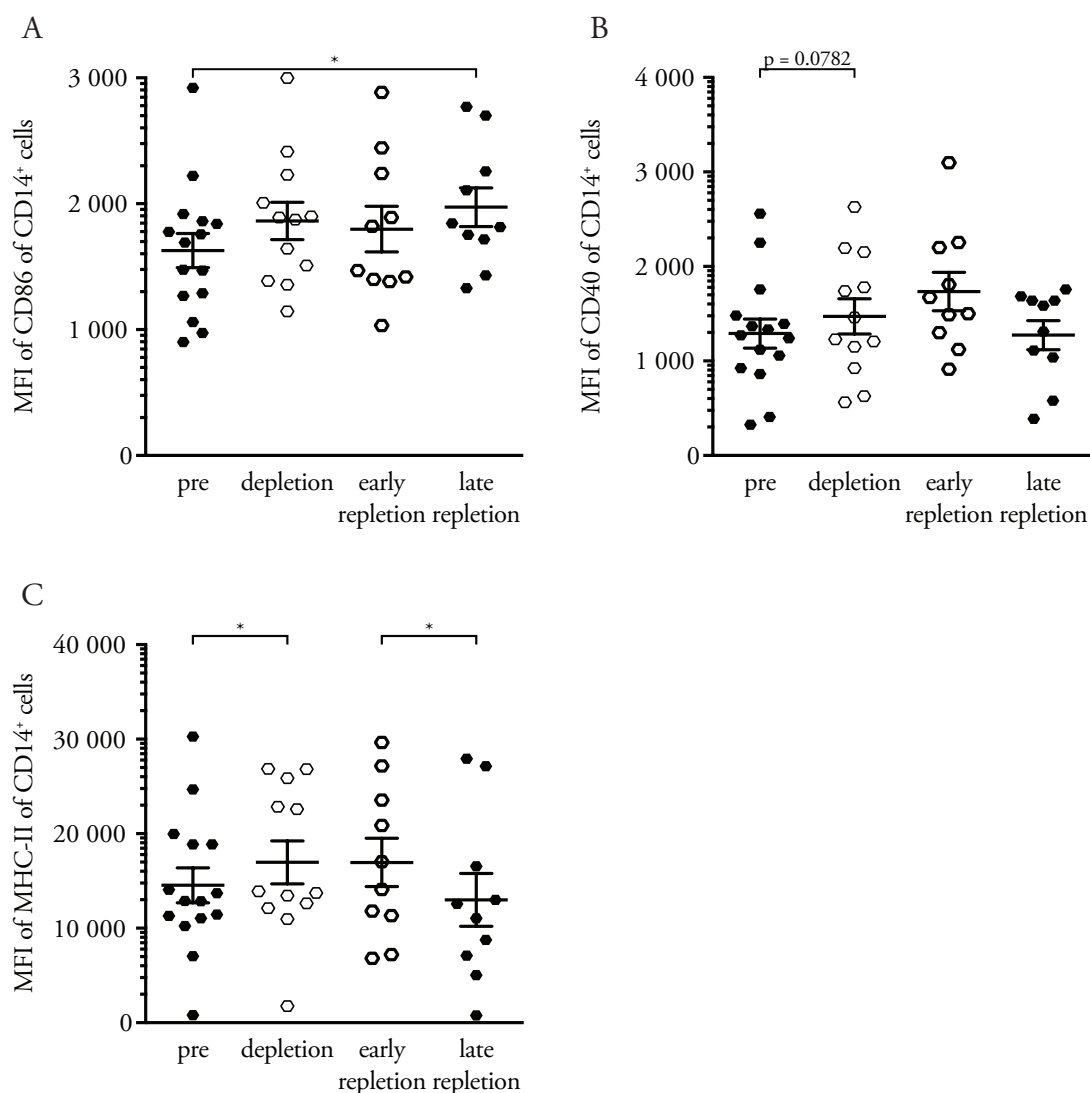


Figure 24. Myeloid cells' APC phenotype II. The figure shows the MFIs of CD86 (A), CD40 (B) and MHC-II (C) of CD14<sup>+</sup> cells through four time points for every patient. Data is presented as mean  $\pm$  standard error of mean ( $n = 15/12/10/10$ ; paired t-test/Wilcoxon matched-pairs signed rank test: ns unless otherwise stated).

The myeloid cells' cytokine secretion phenotype as a possible immune modulating factor was of great interest in the project. As shown in Figure 25, all myeloid cells produce IL-6, independent of the stimulation. Nevertheless, one could see in the MFIs, that unstimulated some myeloid cells produce more IL-6 at early repletion, and maintain that level at late repletion. The non-significant differences in the MFIs show again the difference in the variability of the myeloid cells at early repletion, which persists at late repletion as well. One could say, that overall the myeloid cells don't necessarily produce more IL-6 (no change in mean), but the range of their values increases, indicating that the single cells within the group vary. Upon CpG stimulation the myeloid cells' IL-6 production increases already at depletion, continues to increase at early repletion, and slightly sinks at late repletion. The difference in the variability can be seen here as well. This doesn't apply to the

LPS stimulation, where the myeloid cells' IL-6 production remains constant, and the variability doesn't change either.

Figure 26 shows the myeloid cells' IL-10 and TNF- $\alpha$  production. The IL-10 production remains mainly constant, but shows upon LPS stimulation a different trend than unstimulated and upon CpG stimulation. Unstimulated and upon CpG stimulation the IL-10 production slightly increases at depletion, again at early repletion and sinks below its original value at late repletion. Upon LPS stimulation the IL-10 production first significantly sinks at depletion, then, besides two patients, remains constant at early repletion, and increases at late repletion, but stays below original value.

The myeloid cells produce TNF- $\alpha$  upon CpG stimulation, unstimulated and upon LPS stimulation increasingly. Unstimulated myeloid cells' TNF- $\alpha$  production increases minimally at depletion, remains at that level at early repletion, and sinks at late repletion below original level. Upon CpG stimulation it increases again minimally at depletion, but sinks already at early repletion, and remains at that level at late repletion. Upon LPS stimulation it increases through depletion until early repletion, then sinks at late repletion slightly below original level. As shown in Figures 25 and 26 most changes are non-significant.

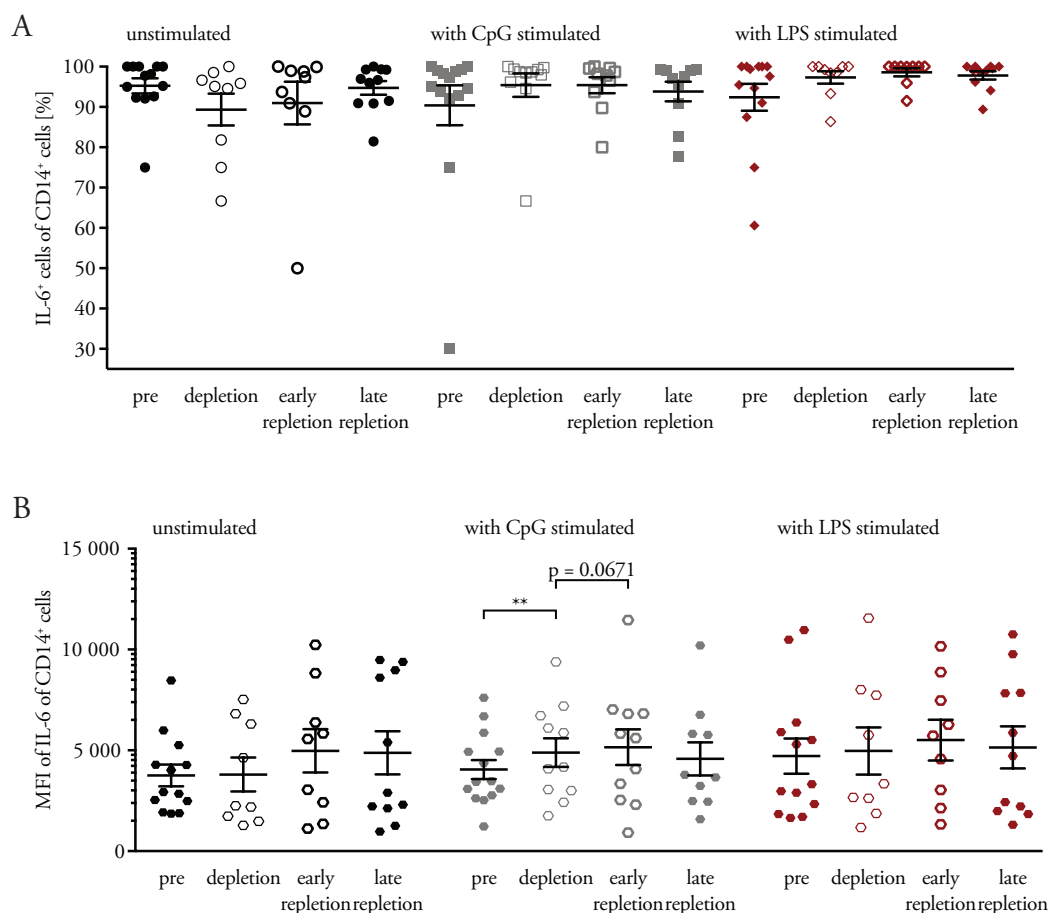


Figure 25. Myeloid cells' IL-6 phenotype. The figure shows the frequencies of IL-6<sup>+</sup> myeloid cells expressed as % of CD14<sup>+</sup> cells (A), and MFI of IL-6 of CD14<sup>+</sup> cells (B) unstimulated and upon CpG [1  $\mu$ g/ml] and LPS [500 pg/ml] stimulation, as shown in Table 11, through four selected samples

representing four selected time points for every patient. Data is presented as mean  $\pm$  standard error of mean ( $n = 15/9,11,9/9,10,9/10,11$ ; paired t-test/Wilcoxon matched-pairs signed rank test: ns unless otherwise stated).

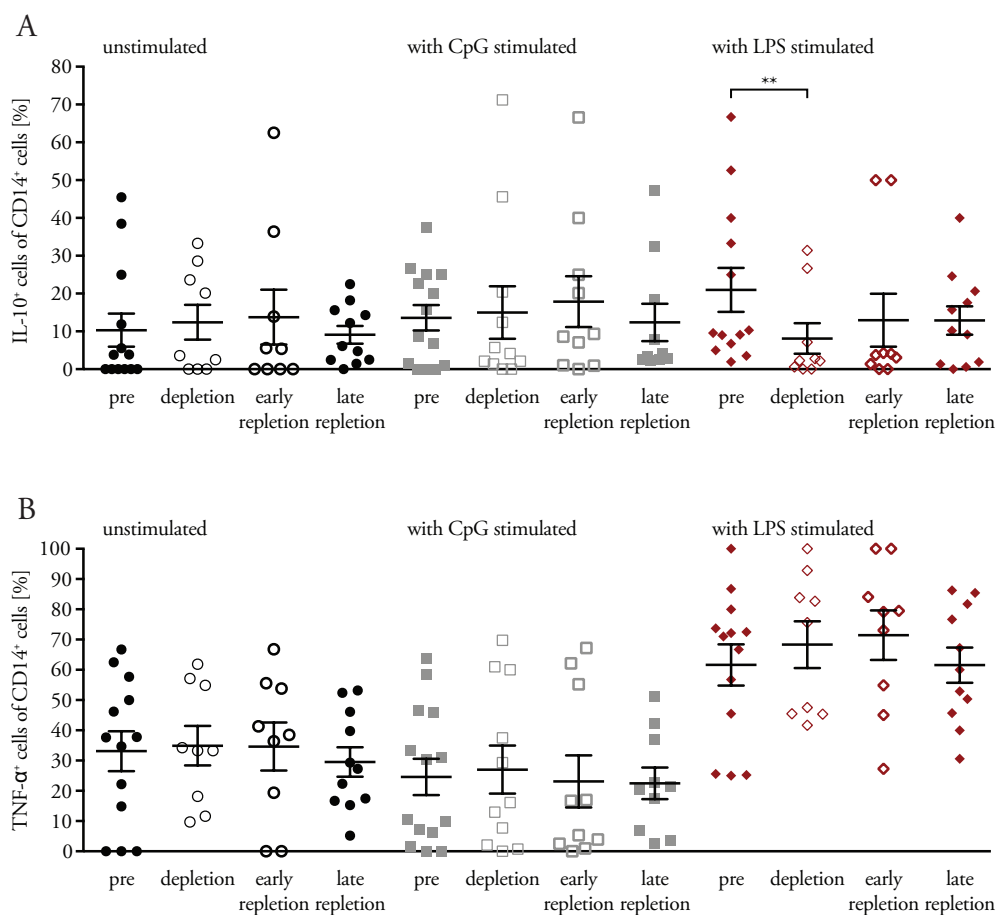


Figure 26. Myeloid cells' IL-10 and TNF- $\alpha$  phenotype. The figure shows the frequencies of IL-10<sup>+</sup> (A) and TNF- $\alpha$ <sup>+</sup> (B) myeloid cells expressed as % of CD14<sup>+</sup> cells unstimulated and upon CpG [1  $\mu$ g/ml] and LPS [500 pg/ml] stimulation, as shown in Table 11, through four selected samples representing four selected time points for every patient. Data is presented as mean  $\pm$  standard error of mean ( $n = 15/9,11,9/9,10,9/10,11$ ; paired t-test/Wilcoxon matched-pairs signed rank test: ns unless otherwise stated).

### 3.3 Correlation with clinical parameters

Anti-CD20 therapy shows significant clinical effects in MS therapy. This raises the question of the role of B cells in the pathogenesis. MS is also more common by women than men, and manifests usually between 25 and 35 years of age. As such, the correlations between patient's age, sex and B cell frequency, respectively count, were of great interest, and are shown in Figure 27. The figure shows, that with increasing age, the B cell frequency and the B cell counts increase significantly. When separating male and female patients, one can still see a significantly positive correlation only among the female patients.

It is important to mention, that I have only looked at 15 patients. Therefore, the results should be interpreted very carefully.

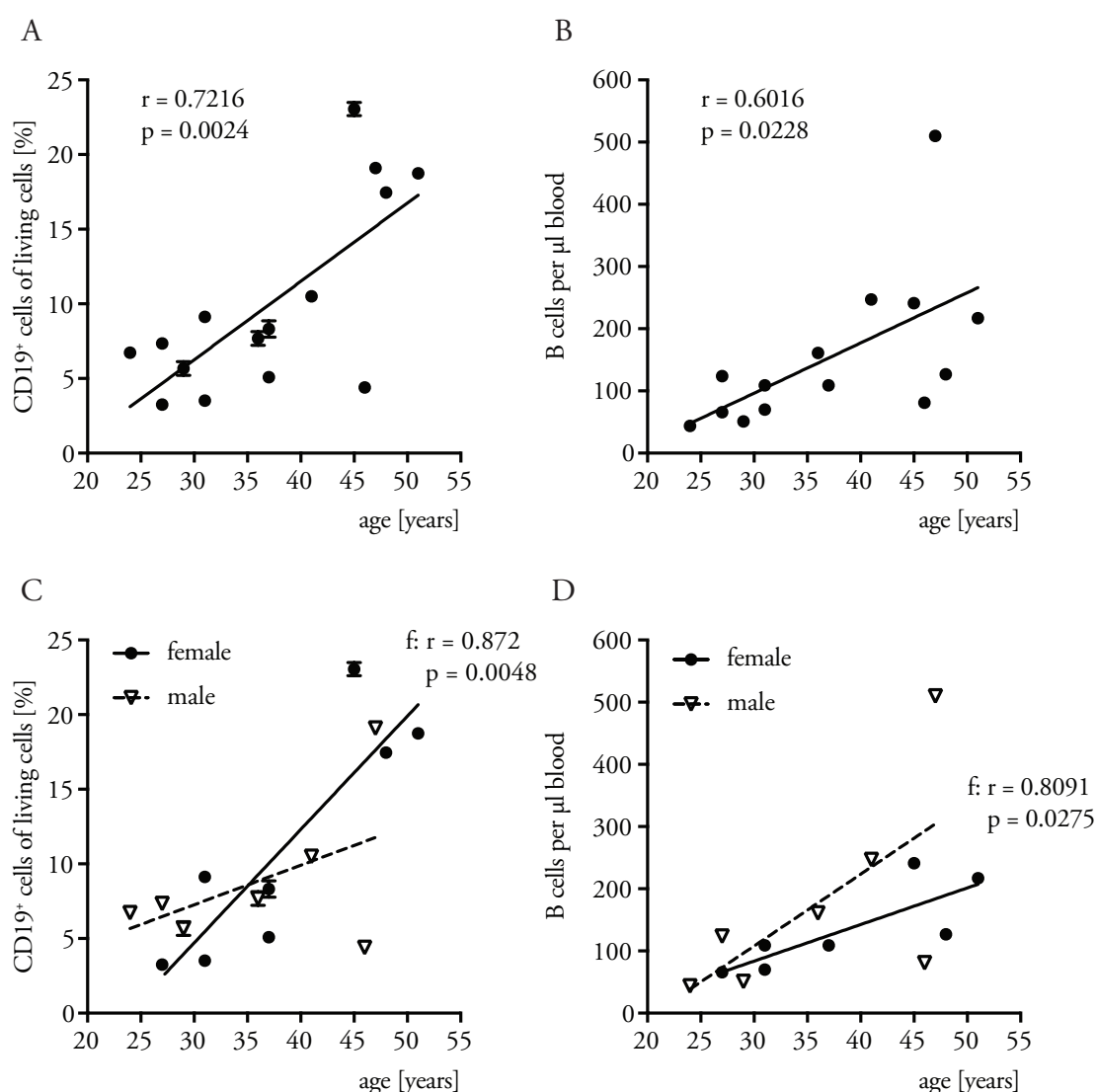


Figure 27. Correlation between B cell frequency/count with age and sex. The figure shows the frequency of CD19<sup>+</sup> cells expressed as % of all living PBMCs (A, C) and B cell counts determined in a TBNK classification of whole blood (B, D), both before depletion, and patients' age. Data is presented as mean  $\pm$  standard error of mean ( $n = 15$ ,  $f = 8$ ,  $m = 7$  (A, C)/ $n = 14$ ,  $f = 7$ ,  $m = 7$  (B, D), linear regression, Pearson  $r$ ; C – m:  $p = 0.2531$ , D – m:  $p = 0.1102$ , both not shown in figure).

In light of these findings and the efficacy of anti-CD20 therapy, the correlation between the patients' clinical EDSS score and the B cell frequency and count was also analyzed. A significant positive correlation between B cell frequency respectively B cell count and the patients' EDSS score was found, which could be explained due to the correlation with age ( $r = 0,5468$ ,  $p = 0,0368$ ; data not shown).

Naïve and memory B cells are the largest B cell populations circulating in peripheral blood (as shown in Figure 5), yet these population differ in their characteristics. Naïve B cells aren't antigen experienced, memory B cells are. Naïve B cells tend to have a more anti-inflammatory profile, whereas memory B cells a more pro-inflammatory one. Therefore, the correlations between the frequencies of these populations and the EDSS score of the patients were of interest, and are shown in Figure 28. One can see, that a strong correlation between all but one patient (in grey) was found with both frequencies. Figure 28 shows, that the EDSS score of all patients positively correlates with the naïve B cell frequency. The memory B cell frequency and EDSS score, on the other hand, correlates negatively (in all but the one patient in grey). The ratio naïve/memory B cells shows a positive correlation between in all patients (data not shown,  $r = 0.841$ ,  $p = 0.0003$ ; when  $n = 15$ :  $r = 0.539$ ,  $p = 0.0403$ ). A correlation of those three parameters with age was also analyzed to exclude a secondary correlation, and was not found (see Figure A1).

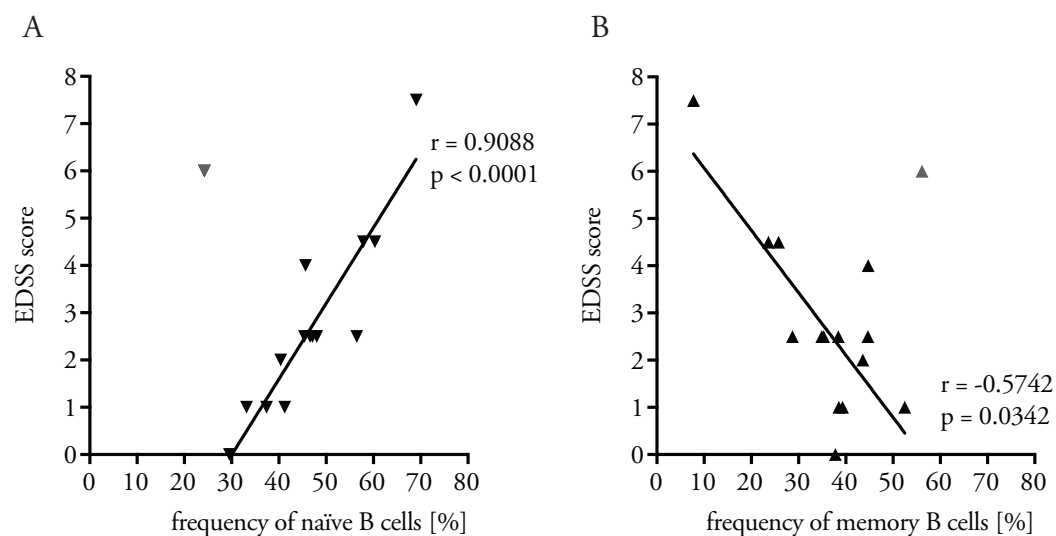


Figure 28. Correlation between naïve and memory B cell frequencies with EDSS score. The figure shows the frequency of naïve (A) and memory (B) B cells expressed as % of CD19<sup>+</sup> cells, both before depletion and patients' EDSS score at time of first administration of anti-CD20 therapy ( $n = 14$ , linear regression, Spearman  $r$ ; when  $n = 15$ : A:  $p = 0.0216$  (\*),  $r = 0.5938$ ; B:  $p = 0.2385$ ,  $r = -0.3234$  all not shown in figure).

In light of these findings it was interesting to determine, if one could identify patients who would more profit from an anti-CD20 therapy, based on the ratio between naïve and memory B cells. On the one hand as stated in 1.1.2.7 above the “good” anti-inflammatory are the naïve B cells and the “bad” pro-inflammatory are the memory B cells. On the other hand, as seen in Figure 28, the more naïve B cells a patient has, the worst the EDSS score is, and vice

versa with the memory B cells. Figure 29 shows a possible classification of all patients in memory/balanced type ( $n/m$  ratio  $\leq 1$ , in balanced type the difference between the frequencies of naïve and memory B cells must not exceed 5%) and in naïve type ( $n/m$  ratio  $> 1$ ). The patient that differed within the correlation to the EDSS score (Figure 28) is presented in gray.

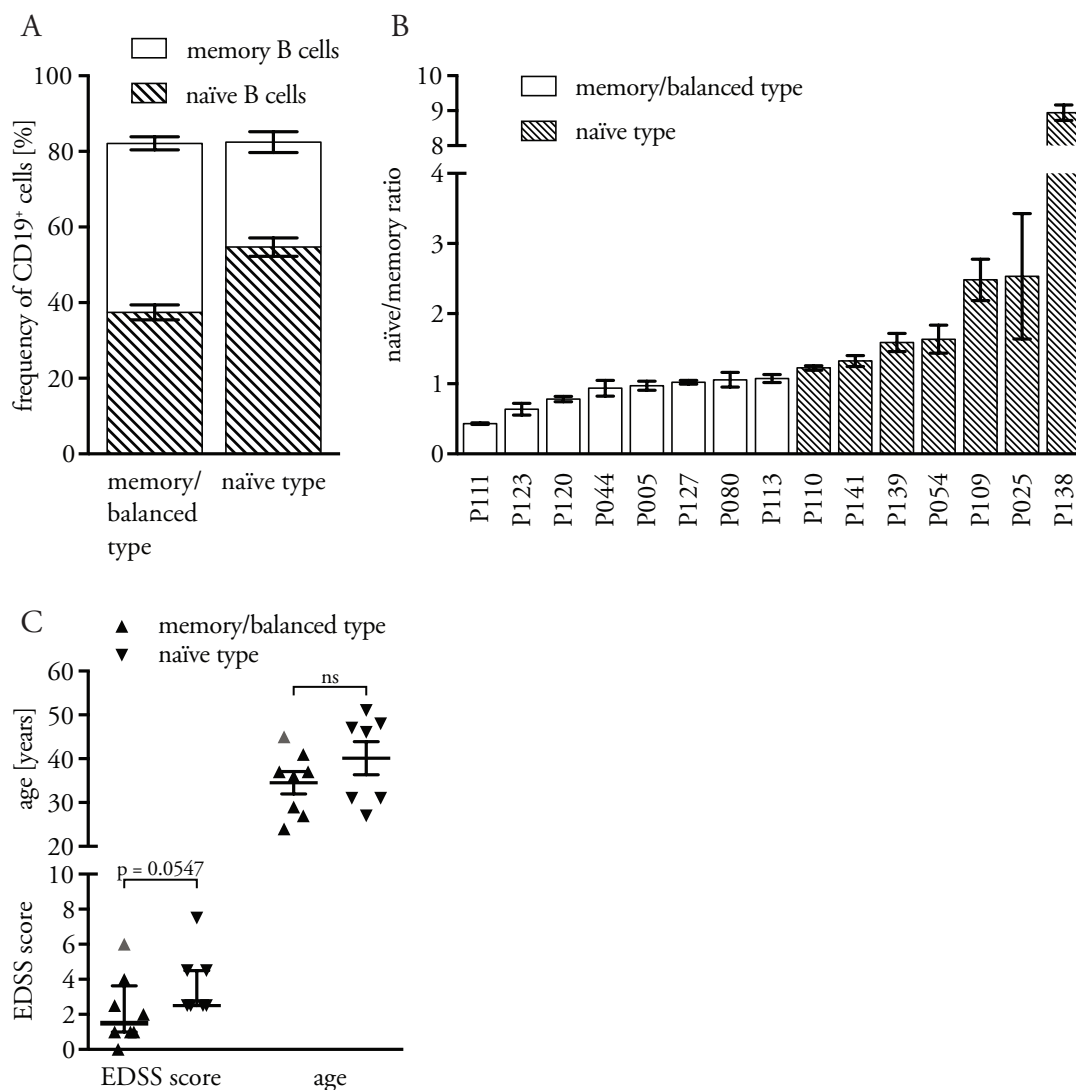


Figure 29. Memory/balanced and naïve type. The figure shows (A) the frequency of memory and naïve B cells expressed as % of CD19<sup>+</sup> cells, both before depletion, (B) the naïve/memory ratio of each patient and (C) the median EDSS score  $\pm$  IQR/range and mean age  $\pm$  standard error of mean of the patients in these groups. Data is presented as mean  $\pm$  standard error of mean (besides EDSS score;  $n = 8/7$ ; unpaired t-test/Mann-Whitney-U-Test as stated in figure)

After defining these two patient groups, I looked at their distribution within the different parameters measured in the study. The median EDSS score ( $\pm$  IQR/range) of these groups was: memory/balanced type:  $1.5 \pm 2.625$ , naïve type:  $2.5 \pm 2.5$ . The patients in those groups did not differ in age. Data to those differences is shown in 6.4 below, and is summarized in Table 12.

Table 12: Differences in immune cell phenotype after anti-CD20 depletion between patients with memory/balanced and naïve B cell phenotype pre-depletion.

<b>Cell population</b>	<b>Surface antigen</b>	<b>Memory/balanced B cell type</b>	<b>Naïve B cells type</b>
CD4 <sup>+</sup> T <sub>H</sub> cells	T <sub>N</sub>	low and increasing	low and constant
	T <sub>CM</sub>	low and increasing	low and constant
	T <sub>EM</sub>	low and increasing	low and constant
	T <sub>TD</sub>	high and decreasing	high and constant
	CD62L	high and increasing	high and constant
CD8 <sup>+</sup> T <sub>C</sub> cells	T <sub>N</sub>	low and increasing – decreasing – increasing	low and constant
	T <sub>CM</sub>	low and increasing – decreasing – increasing	low and decreasing
	T <sub>EM</sub>	low and decreasing – increasing – decreasing	low and increasing
	T <sub>TD</sub>	high and decreasing	high and increasing
	CD62L	low and increasing	high and constant
CD14 <sup>+</sup> myeloid cells	CD150	low and constant	low and constant
	CD95 (FAS) (MFI)	high and increasing	high and constant
	CD40 (MFI)	constant	increasing
	CD80	high and increasing	very high and decreasing
	CD86 (MFI)	high and increasing	high and constant
	MHC-II (MFI)	decreasing	increasing
	IL-6 (unstimulated)	increasing	decreasing
	IL-10 (unstimulated)	low and constant	low and increasing – decreasing
	TNF- $\alpha$ (unstimulated)	low and increasing	low and decreasing
EDSS	median $\pm$ IQR/range	1.5 $\pm$ 2.625	2.5 $\pm$ 2.5

All of the above shows that certain changes do occur in the different populations of the immune system after administration of anti-CD20 therapy. Those changes and their opposite happen in some patients, and balance each other in the overall population.

The role of CD20<sup>+</sup> T cells is still unknown, but their earlier repletion raises the question of origin. One is not entirely sure if those cells come from the bone marrow, suggesting a regulated population with a specific role in the immune system, or if T cells in the periphery start to re-express CD20. Figure 30 show the correlation between age and the time to detection of repletion. The time to detection of B cell repletion doesn't correlate with age, as a minimum of 250 days can be seen at all times, yet one could notice, that after 40 years of age this time interval prolongs. Nevertheless, the time do detection of CD20<sup>+</sup> T cell repletion decreases significantly with age.

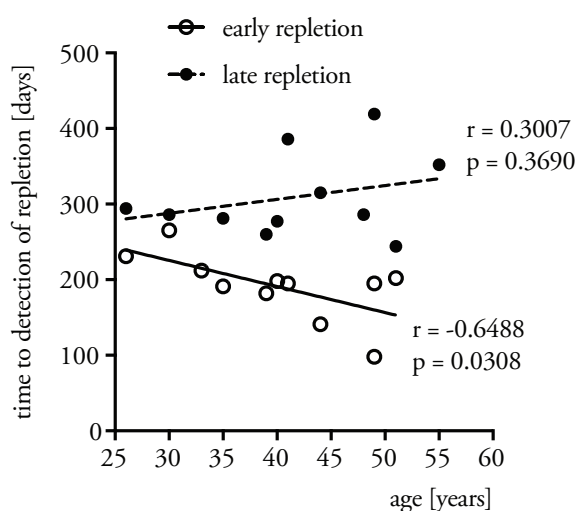


Figure 30. Correlation between the time to detection of CD20<sup>+</sup> cells repletion and age. The figure shows the time in days past between last anti-CD20 therapy administration and the detection of CD20<sup>+</sup> T cells at early repletion and of CD20<sup>+</sup> B cells at late repletion alongside with patients' age. (n = 11, linear regression, Pearson r)

In addition, the correlation to patient's age with the frequency of CD20<sup>+</sup> T cell population was interesting. Figure 31 shows a positive correlation between CD20<sup>+</sup> T<sub>H</sub> cell frequency of all living PBMCs and age. When observing the cell frequencies within the cell populations, one can see, that the frequencies of both cell populations positively correlate with age. When separating male and female, one can see within the CD20<sup>+</sup> T<sub>C</sub> cells a positive correlation with age only among the male patients (n = 5, r = 0.9808, p = 0.0032), within the CD20<sup>+</sup> T<sub>H</sub> cells a non-significant positive correlation with age only among the female patients (n = 6, r = 0.7851, p = 0.0643; data not shown).

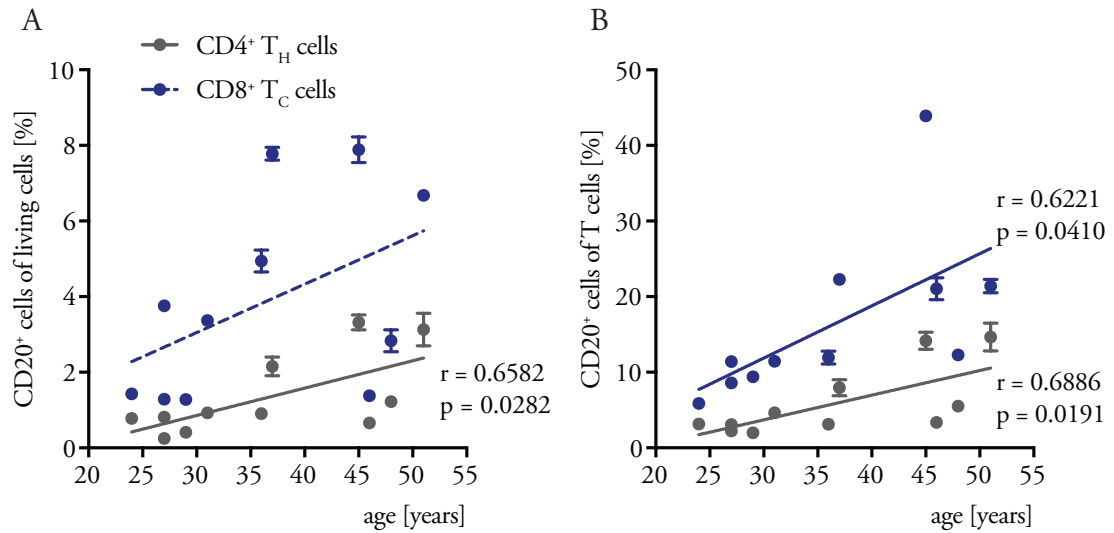


Figure 31. Correlation between frequencies of CD20<sup>+</sup> T cells and age. The figure shows the frequencies of CD20<sup>+</sup> T<sub>H</sub> and T<sub>C</sub> cells expressed as % of all living PBMCs (A) and of CD4<sup>+</sup>/8<sup>+</sup> cells (B) alongside with patients' age. Data is presented as mean ± standard error of mean (n = 11, linear regression, Pearson r; A – T<sub>C</sub>: p = 0.1391 not shown in figure).

## 4 Discussion

This dissertation aimed to characterize the effects of anti-CD20 mediated B cell depletion on CD20<sup>+</sup> B and T cells and on other immune cell populations in MS patients during depletion and repletion.

Here, I was able to demonstrate that

1. the repleting B cells replete pre-dominantly in a transitional and mature naïve phenotype, yet more activated, pro-inflammatory and with more potent co-stimulation capacities.
2. the small CD20<sup>+</sup> T cell population, which is also depleted upon anti-CD20 therapy, doesn't show phenotype differences upon repletion, yet replete faster than the B cells.
3. the remaining T cells, and especially the CD4<sup>+</sup> T<sub>H</sub> cells, show a loss of effector functions upon anti-CD20 therapy.
4. myeloid cells, on the other hand, vary in their reaction to the treatment, and show only little phenotype differences.
5. Patients' EDSS correlated with two main B cell subpopulations: naïve and memory B cells.
6. Regarding the question of patient selection for the treatment, patients could be classified into two distinct groups according to their B cell phenotype before anti-CD20 therapy.

### **Aim 1: Direct effects of anti-CD20 depletion on CD20<sup>+</sup> cells:**

B cells replete more activated after anti-CD20 depletion. Rituximab as a mean for CD20 depletion is not firstly used in MS, it is also applied in many other autoimmune diseases, such as rheumatoid arthritis, primary Sjögren's syndrome, anti-neutrophil cytoplasmic antibody (ANCA) associated vasculitis and different glomerulonephritis, as a mean to achieve clinical remission (Gürcan et al. 2009; Jayne 2010). As shown in this dissertation, the repleting B cells show a different phenotype than the ones before depletion. The repleting B cells are mostly transitional but also mature naïve B cells. The transitional B cells are the most mature B cells capable of migrating from the bone marrow into the periphery, indicating a repletion based on a new differentiation from the bone marrow. These cells show a more activated phenotype when compared with their phenotype before depletion. This is seen firstly in the elevated expression of the activation markers CD25, CD69 and CD95 (FAS). These finding come to some extent as a surprise. For example, CD25 is expressed by all B cells, but known to be expressed predominantly within the memory B cell pool. Brisslert et al. (2006) and Amu et al. (2007) have shown, that CD25<sup>+</sup> B cells in healthy controls as well as in patients with rheumatoid arthritis and systemic lupus erythematosus are pre-dominantly memory B cells (CD27<sup>+</sup>), morphologically larger and more granulated, proliferate to a greater extent as a response to IL-2, and are more efficient APCs than CD25<sup>-</sup> B cells. Nevertheless, In context with the phenotypical analysis above, I do not believe that the higher expression of CD25 is due to an elevated frequency of memory B cells in the repleting pool, but reflective of the fact that naïve, regrowing B cells are being activated in the process of re-population. This general observation confirms earlier experimental study by Häusler et al. (2018) showing that in the context of peripheral

activation, B cells reappear with an enhanced pro-inflammatory molecular arsenal. As shown in Figure A2, the patients with a naïve B cell phenotype before treatment showed a slightly elevated CD25 expression in comparison to the patients with a memory/balanced B cell phenotype. Secondly, the higher CD40 and CD86 expression indicate more potent co-stimulation capacities, which match the findings above. Similar results were also found by Leandro et al. (2006), Roll et al. (2006) and Pers et al. (2007) who have investigated the B cell repopulation after CD20 depletion with rituximab in other autoimmune diseases (rheumatoid arthritis, primary Sjögren's syndrome and others), and by Häusler et al. (2018), who investigated this re-population in EAE mice. On the other hand, Maurer et al. (2016) have found, that after a successful CD20 depletion, the remaining memory B cells who escaped depletion tend to undergo clonal expansion, and the patients replete therefore with a memory B cell phenotype. This could be explained by the findings of Häusler et al. (2018) who have shown, that anti-CD20 therapy has a limited efficiency on B cell depletion in the secondary lymphatic organs and in the bone marrow, where the remaining CD20<sup>+</sup> B cells also showed a large CD27<sup>+</sup> proportion.

With regard to the repletion phenotype, Leandro et al. (2006) have also found, that the patients with rheumatoid arthritis who relapsed during B cell repletion tended to replete with a higher frequency of memory B cells. This raises the issue of depletion efficiency, which according to Leandro (2013) is variable even when treated with the same dose. Reff et al. (1994) have shown, that a dosage dependent depletion exists, and that even though all B cells in peripheral blood were depleted, there was not a sufficient depletion in secondary lymphatic organs. Therefore, a sufficient dose which will prevent the survival of CD27<sup>+</sup> memory B cells should be in my opinion chosen in order to prevent unwanted relapses during B cell repletion, as Kim et al. (2011) found.

The CD20<sup>+</sup> T cells phenotype doesn't change upon anti-CD20 depletion. The existence and depletion potential of CD20<sup>+</sup> T cells (and NK cells) is already known. This small population counts 5-10% of T cells, and 5-6% of living PBMCs. A study performed by Storie et al. (1995) in healthy controls showed that the CD20<sup>dim</sup> expression was restricted to CD20<sup>+</sup> T cells, whereas all CD20<sup>+</sup> B cells were CD20<sup>bright</sup>. They have also found, that the majority of these cells are CD8<sup>+</sup> and CD45RO<sup>+</sup>. I have found similar results, indicating a CD8 dominance among the CD20<sup>+</sup> T cells, and a majority of CD45RO expression, but only among the CD4<sup>+</sup> cells, indicating a memory phenotype. The majority of the CD8<sup>+</sup> cells were CD45RA<sup>+</sup>, indicating either a naïve phenotype, but could also indicate a terminally differentiated phenotype. Like Leandro et al. (2006) I have also found no differences in their phenotype at repletion.

In different individuals, CD20<sup>+</sup> T cells show different dominance. Different studies to this theme present contradiction. Leandro et al. (2006) and von Essen et al. (2019) found a CD4 dominance, Schuh et al. (2016) and Gingele et al. (2018) found like me a CD8 dominance.

This raises the question: do certain people show a different CD20<sup>+</sup> T cell phenotype, and if so, why?

CD20<sup>+</sup> T cells replete faster than B cells and show increased frequency with age. I confirmed the results of the above mentioned studies in other autoimmune diseases, that the CD20<sup>+</sup> T cells, and especially the CD8<sup>+</sup> population, replete faster than the B cells. Schuh et al. (2016) have found, that in several MS patients, relapses occurred after administration of anti-CD20 therapy at time of CD20<sup>+</sup> T cell repletion, yet in B cell absence. This raises not only the question of the pathogenetic role of these cells in disease development, but also raises the question of therapy intervals. Could those patients having a relapse at CD20<sup>+</sup> T cell repletion present a unique pathogenesis involving CD20<sup>+</sup> T cells? Could they be identified? If so, they could be candidate to an earlier depletion than other patients. This faster repletion raises questions on its own: do these cells differentiate like the B cells in the bone marrow and when mature enough migrate into the periphery, or do they differentiate in the periphery from CD20<sup>-</sup> T cells, and if so why?

Regarding these questions, Schuh et al. (2016) also showed that the CD20<sup>+</sup> T cells express the CD20 antigen after transcription and translation, indicating an endogen up-regulation of this marker. They were also able to find them in human primary (thymus and bone marrow) and secondary (adenoid) lymphatic tissue, in the thymus only within the mature, CD4<sup>+</sup> or CD8<sup>+</sup> medullary T cell population. The question remains: do these cells have a specific role and are consequently a distinct population with a distinct role? Storie et al. (1995) have found like me that the frequency of the CD20<sup>+</sup> T cell compartment increases with age, and cannot be found for example in cord blood. This raises again the question of origin of these cells, since the capacity of the bone marrow to produce more naïve cells decreases with age.

### **Aim 2: Indirect effects of anti CD20 depletion on CD20<sup>-</sup> cells:**

CD4<sup>+</sup> and CD8<sup>+</sup> T cells react alike to anti-CD20 depletion and show loss in effector function. It is interesting to see, that both T cell populations, T<sub>H</sub> and T<sub>C</sub> cells, react similarly over time to B cell depletion, yet the T<sub>H</sub> cells seem to be more affected than the others, most likely due to their close interaction with the B cells. Both show firstly a decrease in terminally differentiated cells (the T<sub>H</sub> larger than T<sub>C</sub>), which could be explained through the increase in frequency of L-selectin positive cells which is seen at depletion and further at late repletion. This means that the T cells have a higher adhesion and rolling potential and therefore a higher migration potential. This could have two meanings: (1) a higher migration in the periphery and CNS and therefore increase in CNS inflammation or (2) a higher migration into the secondary lymphatic organs, mobilizing T cells away from the CNS, which in turn could have a positive effect on CNS inflammation. Sadly, we only analyzed the rolling potential of the T cells through L-selectin and not the actual migration capacity through integrin  $\alpha 4\beta 1$  (very late antigen-4), which is essential for T cell migration through the BBB into the CNS.

This increase in frequency of L-selectin expression, presented as decrease in frequency of terminally differentiated T cells, in the CD4<sup>+</sup> compartment accompanied with slight increase in frequency of T<sub>EM</sub> cells, shows a decrease in the frequency of overall T cells with the highest immediate effector function, which also nest in the periphery and not in secondary lymphoid organs. This accompanied increased respectively constant frequency of CD4<sup>+</sup> respectively CD8<sup>+</sup> T<sub>EM</sub> cells could indicate a higher potential for myeloid cells' activation. The T<sub>EM</sub> show a high effector function expressed among others in IFN- $\gamma$  secretion, which in turn activates macrophages, NK cells and other T cells.

Myeloid cells vary in their reaction to anti-CD20 depletion. The myeloid cells, as unspecific APCs seem to be less effected than the T cells from B cell absence. They show differences in activation, antigen presentation and cytokine secretion, but those changes normalize at B cell repletion, suggesting one of two things: (1) the myeloid cells do take the role of the B cells in their absence (better antigen presentation, more IL-6 secretion), yet "give it back" at B cell re-appearance, (2) the B cells regulate myeloid cells' activation, and it therefore normalizes upon naïve B cell repletion. Lehmann-Horn et al. (2011) investigated the influence of anti-CD20 depletion on CD11b<sup>+</sup> APCs in EAE mice and in patients. They have found, that in B cell depleted mice the remaining CD11b<sup>+</sup> cells produced more TNF- $\alpha$  after depletion than before, and concluded that naïve B cells regulate APCs in an anti-inflammatory manner. They have also found, that compared to untreated control patients some B cell depleted patients presented a higher frequency of myeloid cells secreting TNF- $\alpha$ , and the overall samples of the treated patients were also distributed over a wider range of values, reflecting a greater variability in the myeloid cells' reaction to anti-CD20 depletion.

In addition, Hauser et al. (2008), Clifford et al. (2011), Memon et al. (2018) and others have found, when compared with placebo groups, no higher risk of malignancies, opportunistic and serious infections (requiring hospitalization) not only among MS patients treated with rituximab but also among patients with other autoimmune diseases, for example rheumatoid arthritis. This could be explained due to the only small changes in CD8<sup>+</sup> T cells' and myeloid cells' phenotype, maintaining a stable immune reaction against pathogens and against malignant cells, meaning that B cell depletion does not cause a significant immunosuppression.

### **Aim 3: Individualized MS therapy**

MS patients show with increasing age an increase in B cell count in peripheral blood, which only correlates with female patients. Morbach et al. (2010) have characterized the changes in B cells and in the B cell sub-populations from infancy to adulthood in healthy individuals, and so created reference values for these parameters. They have found, that the B cell count in peripheral blood of healthy individuals increases until the age of approximately 26 years of age, and then stabilizes until the age of 50. The MS patients in this study show generally a lower B cell count (reference for age of 26-50: 199 [169-271] cells/ $\mu$ l blood), yet most still

within the norm (100-500 cells/ $\mu$ l blood). This contradicts the findings of Habib et al. (2015), which have found an increase in CD19<sup>+</sup> B cell counts in MS patients when compared to healthy controls. Moreover, the B cell count of the patients in this study positive correlates with age in total, and when looked at the value distribution between the two genders, one can only see a positive correlation only among the women, and not among the men. This is an interesting observation, for MS is known to affect more women than men. This is surprising, since in general the B cell compartment does not show a significant gender specific distribution (Kverneland et al. 2016). I thus hypothesize that the observed association relates to MS or autoimmunity in general. It is known that certain B cells sub-populations are more frequent in elderly women with autoimmune disorders than in young women, or men of any age. At this point, I can only speculate that the increase of the B cell counts with increasing age in women relates to an expansion of the reported B cell population (Rubtsova et al. 2012).

MS patients show two main B cell phenotypes: memory/balanced and naïve type. The two main B cell populations seen in peripheral blood are naïve and memory B cells. Duddy et al. (2007) have shown a more activated and pro-inflammatory profile, among others via secretion of pro-inflammatory cytokines, in memory than in naïve B cells, which almost exclusively secrete IL-10. This reinforces the findings of Souto-Carneiro et al. (2009) and Kappos et al. (2014). The former showed, that rheumatoid arthritis patients have decreased memory B cell frequency in peripheral blood compared with healthy controls, since they accumulate in the synovial tissue, contributing to the inflammation. The memory B cell frequency in peripheral blood of these patients increases after treatment with anti-TNF- $\alpha$ -mAb infliximab since TNF- $\alpha$  regulates this migration into the inflamed tissue. Because of therapy success in rheumatoid arthritis, it is assumed, that memory B cells contribute to the inflammation in the synovial tissue. The latter showed, that inhibiting the B cell differentiation with ataccept causes a relative increase in memory B cells and/or reduction in regulatory B cells, and by doing so worsens the clinical activity of MS. The involvement of memory B cell in MS pathogenesis points out even further when looking at the works of Hyrich (2004) and Titelbaum et al. (2005). Both reported of rheumatoid arthritis patients with no history of neurologic diseases showing both MS clinic and MRI activity consistent with demyelination after therapy with etanercept and infliximab. This raises the question: is there a marker only expressed by memory B cells, who could be used as a target for a memory B cell depletion?

I have found in all but one patient a strong correlation between the naïve and memory B cell frequencies and the EDSS score (which should be in light of the small number of patients addressed very cautiously), which led me as presented to classify all patients into two groups according to the dominant B cell population before therapy administration: memory/balanced type (which could be further classified in memory and in balanced type) and naïve type. As those cells differ in their phenotype, this raises the question: should some patient groups not be depleted? Surprisingly, I have found the patients with

memory/balanced type to present a lower EDSS score than the other patients (demonstrating clinical meaning), yet large differences in T cell phenotype in the CD4<sup>+</sup> and CD8<sup>+</sup> compartment, which might not be beneficial for the patients (increase in CD62L expression) and in my opinion negative changes in myeloid cells phenotype (more IL-6 and TNF- $\alpha$ , constant yet minor IL-10 secretion). On the other hand, the patients with naïve type show only changes in CD8<sup>+</sup> T cells, unspecific changes in myeloid cells' antigen presentation and in my opinion positive changes in myeloid cells cytokine secretion (less IL-6 and TNF- $\alpha$ , constant increasing IL-10 secretion). Nevertheless, these negative changes in T cells of the patients with memory/balance type could also be positive. The increase in CD62L expression could mean as explained above more migration potential into the secondary lymphatic organs, mobilizing T cells away from the CNS and losing effector functions. A constant expression of this marker after depletion, as shown in the patients with naïve type could indicate a persistence of these effector functions and migration potential. As explained above, the naïve B cells also regulate myeloid APCs in an anti-inflammatory manner, and therefore their depletion might not be beneficial for the patients.

Nevertheless, all patients profited from the anti-CD20 therapy, since they did not develop new MRI lesions, didn't deteriorate in their EDSS score or had any relapses after therapy administration, even though they had different B cell phenotypes, meaning that these differences are not relevant for the indication for an anti-CD20 therapy. Yet some wonder, if patients should be constantly depleted of B cells, or whether an effect has been achieved through the depletion, which then can be maintained with a subsequent therapy, maintaining the clinical benefit.

According to the studies mentioned above and the changes described, the two patient groups should receive in case of therapy cessation in my opinion different immune therapies, since their T cells react differently to anti-CD20 depletion. The patients with memory/balanced type, whose T cells lose effector functions and migrate into the secondary lymphatic organs should receive a therapy that would leave those cells there, and away from the CNS. This could be, for example, Fingolimod, a sphingosine-1-phosphate receptor modulator keeping lymphocytes in the lymph nodes, and so preventing them from causing an inflammation in the CNS. The patients with naïve type, whose T cells show a persistence of effector functions should maybe receive a migration inhibiting therapy, in order to prevent further migration into the CNS. This could be, for example, natalizumab, an  $\alpha$ 4-integrin-mAb interfering with lymphocyte migration into the CNS, or a proliferation inhibitor, for example cladribine, a purine analogue which prevents the proliferation of rapid proliferating cells.

This raises further questions: (1) how come some patients show almost no change in T cell phenotype, and a persistence of effector functions despite clinical benefit? Could one identify a different B cell role in those patients compared to the others? (2) some patients don't profit from an anti-CD20 therapy. Could one identify them? How do their T cells react to the anti-CD20 therapy?

## 5 Summary

This study was performed in order to better understand the effects of anti-CD20 depletion on the immune system of Multiple Sclerosis patients in light of the therapy success. Patients treated with the anti-CD20 antibody rituximab, as an off-label therapy option, and ocrelizumab, as approved therapy, for relapsing-remitting Multiple Sclerosis almost don't have new relapses or new magnetic resonance imaging lesions. Yet the long-term consequences of such therapy are still unknown. Taken together, I demonstrated not only the changes in B cell phenotype upon repletion, but also long-lasting changes in T cell phenotype as a response to B cell depletion and repletion. I was able to classify all patients into two main groups based on their B cell phenotype before depletion, and to show, that the T cells of these groups differ in their response to anti-CD20 depletion. I also suggested follow-up treatment options for every group, according to the changes in their T cell phenotype upon therapy, in case of treatment cessation.

Yet some questions remain open, and need to be further clarified. This study was designed mostly to investigate changes in antigen presenting cells' function of myeloid cells, and with very few T cell panels only. In my opinion a similar study should be performed with more T cell markers, which would be able to clarify the migration potential of these cells upon repletion. Furthermore, the CD20<sup>+</sup> T cells could be further classified, and analyzed, in order to exclude disease activity. Such study should be in my opinion performed with more patients, in order to have enough patients with the three possible B cells phenotypes: naïve, balanced and memory type. Only then one could better analyze the differences in T cell phenotype upon anti-CD20 depletion dependent from the initial B cell phenotype.

When such differences are defined, and a possible follow up therapy is identified, one could try to cease therapy with anti-CD20 antibody, and start a maintenance therapy with, as suggested in the discussion, Fingolimod/natalizumab or cladribine.

## 6 Supplement

### 6.1 Certificate – TBNK classification



# ZERTIFIKAT

Ringversuch vom 21.03.2018

Sie haben die Anforderungen des Ringversuchs mit den folgenden Untersuchungen erfüllt

#### Hämatologie 10 - Immunphänotypisierung 01 (213):

Gültigkeitsdauer 12 Monate:

B-Lymphozyten

CD4 pos. Lymphozyten mit CD3-Expression (%)

CD4 pos. Lymphozyten mit CD3-Expression (/nl)

CD8 pos. Lymphozyten mit CD3-Expression

NK-Zellen ohne CD3-Expression

T-Lymphozyten

(R) diese Untersuchung unterliegt den RiLiBÄK

Teilnehmer:

6429

Dr. med. Lutz Binder  
Universitätsmedizin Göttingen  
Georg-August-Universität  
UMG-Labor  
Robert-Koch Str. 40  
37075 Göttingen

Düsseldorf, 19.04.2018

Prof. Dr. med. Michael Spannagl  
(Leiter der Referenzinstitution)



Prof. Dr. med. Wolfgang Kern  
(Ringversuchsleiter)

## 6.2 Correlation between naïve and memory B cell frequencies and age

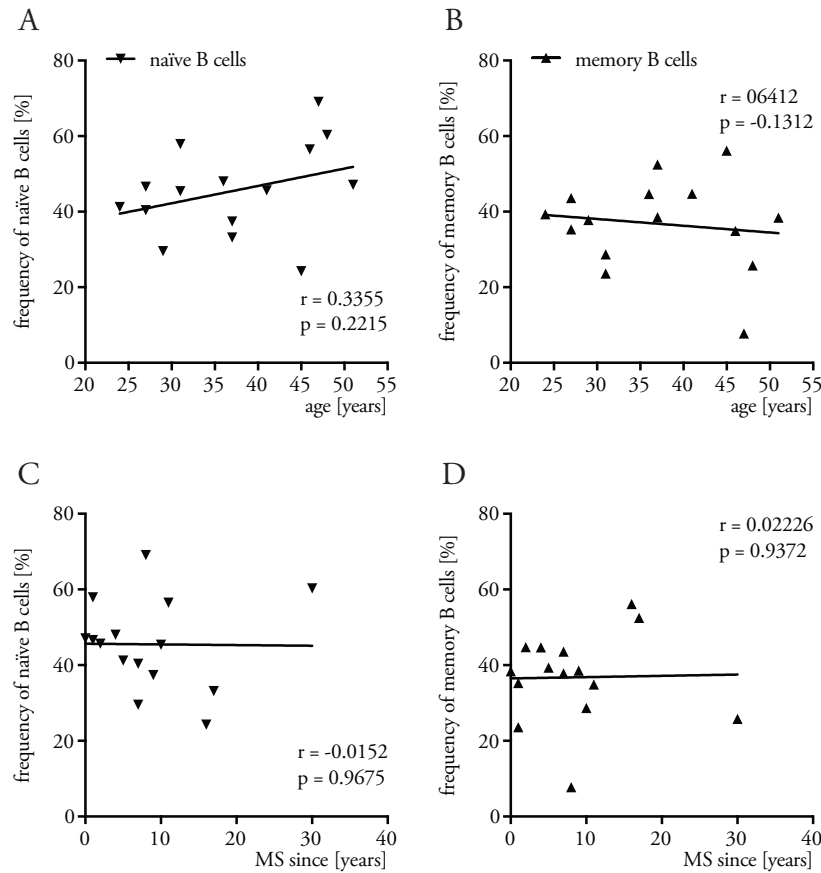


Figure A1. Correlation between naïve and memory B cell frequencies and age. The figure shows the frequency of naïve (A), memory (B) B cells expressed as % of CD19<sup>+</sup> cells, both before depletion, and the ratio naïve/memory (C) and patients' age at time of first administration of anti-CD20 therapy (n = 15, linear regression, Pearson r).

## 6.3 Data to different B cell activation, APC function and cytokine phenotype among the two patient groups

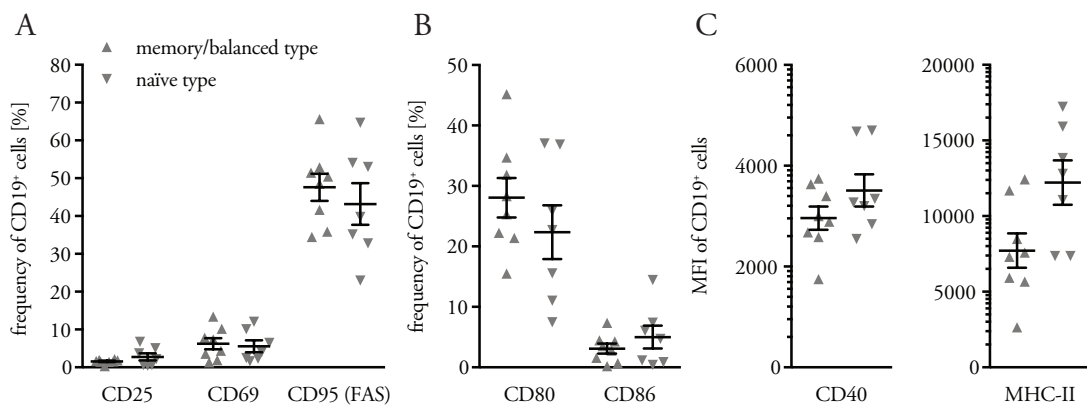


Figure A2. Differences in B cell activation phenotype between memory/balanced and naïve type. The figure shows the frequencies of (A) CD25<sup>+</sup>, CD69<sup>+</sup>, and CD95 (FAS)<sup>+</sup>, (B) CD80<sup>+</sup> and

CD86<sup>+</sup> cells expressed as % of CD19<sup>+</sup> B cells and (C) MFIs of CD40 and MHC-II of CD19<sup>+</sup> B cells all upon CpG stimulation [2 µg/ml] before B cell depletion. Data to frequencies of CD40<sup>+</sup> and MHC-II<sup>+</sup> B cells, as shown in Figure 7, demonstrate a ubiquitous expression of said surface antigens. Data is presented as mean ± standard error of mean (n = 8/7; unpaired t-test/Mann-Whitney-U-Test: ns unless otherwise stated).

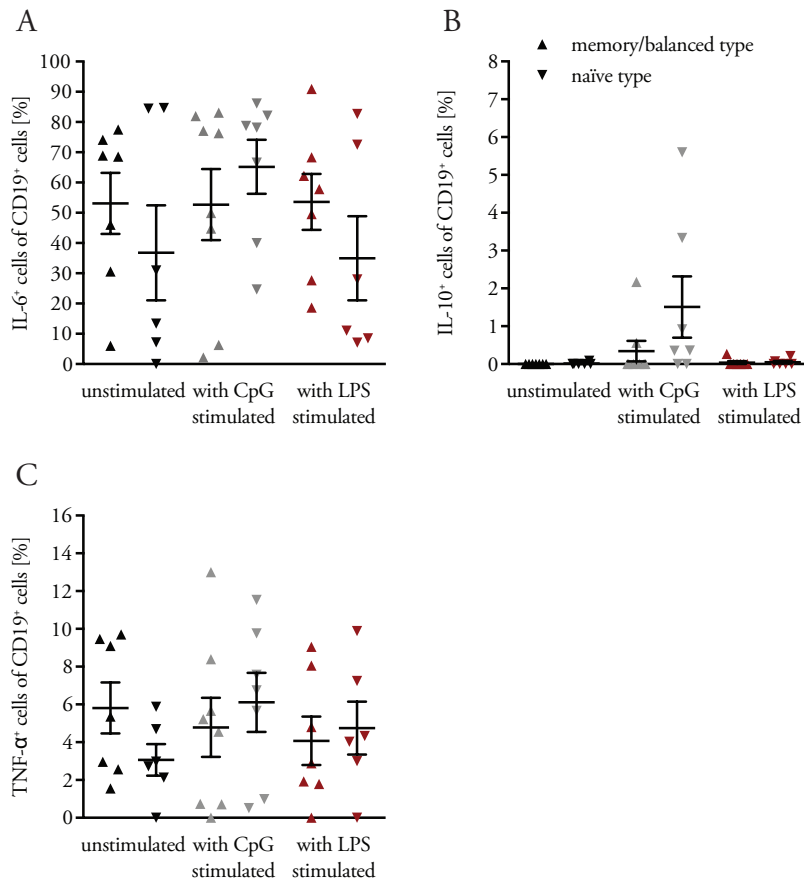


Figure A3. Differences in B cell cytokine phenotype between memory/balanced and naïve type. The figure shows the frequencies of IL-6<sup>+</sup> (A), IL-10<sup>+</sup> (B) and TNF-α<sup>+</sup> (C) expressed as % of CD19<sup>+</sup> B cells unstimulated, upon CpG [1 µg/ml] and LPS [500 pg/ml] stimulation as shown in Table 11 before B cell depletion. Data is presented as mean ± standard error of mean (n = 8/7; unpaired t-test/Mann-Whitney-U-Test: ns unless otherwise stated).

## 6.4 Data to different cell phenotypes among the two patient groups

### 6.4.1 Data to CD4<sup>+</sup> T<sub>H</sub> cells

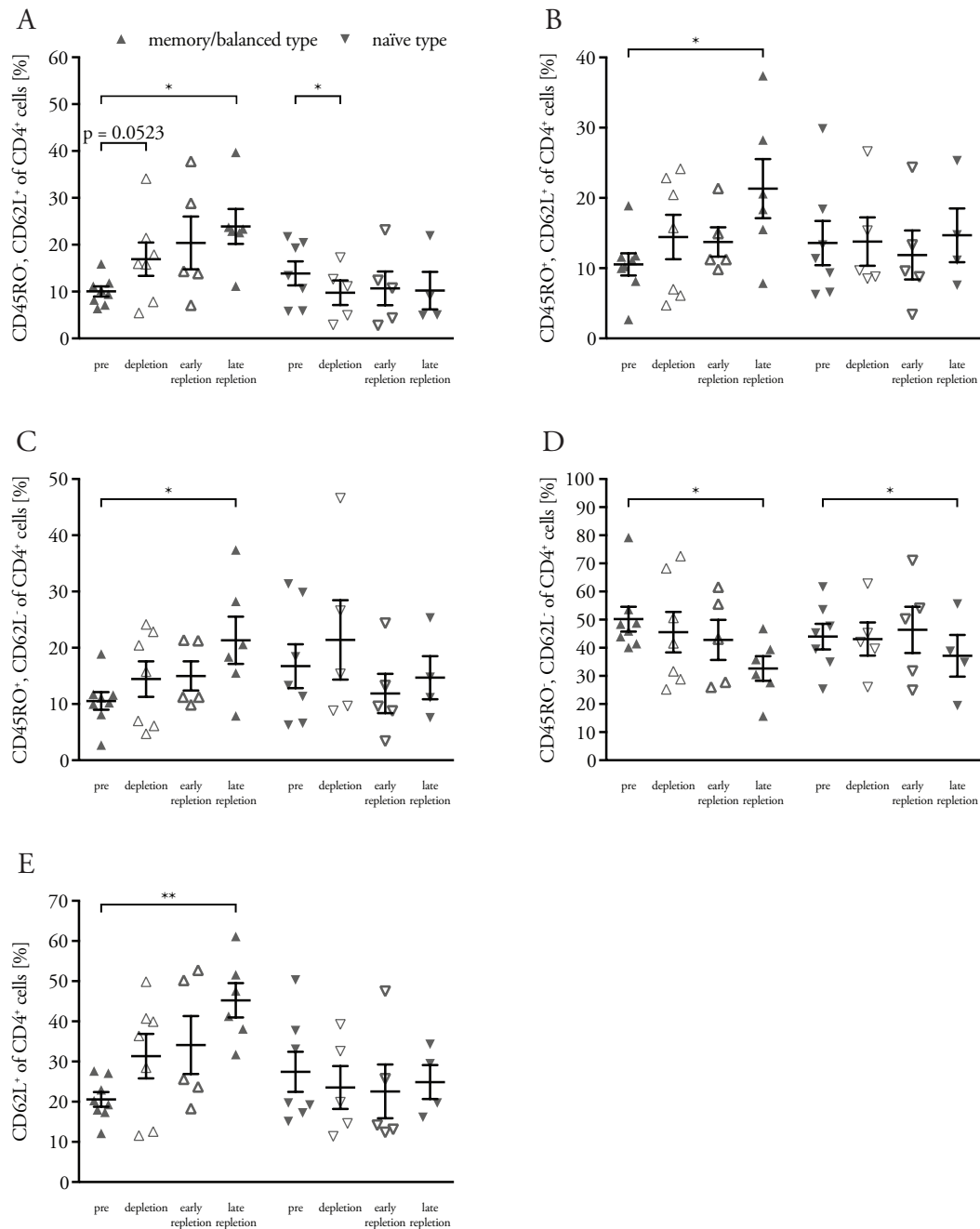


Figure A4. Differences in CD4<sup>+</sup> T<sub>H</sub> cells maturation and CD62L expression phenotype between memory/balanced and naïve type. The figure shows the frequencies of naïve (A), central memory (B), effector memory (C) and terminally differentiated (D) T<sub>H</sub> cells as well as frequencies of CD62L<sup>+</sup> T<sub>H</sub> cells (E) expressed as % of CD4<sup>+</sup> cells through four selected samples representing four selected time points for every patient. Data is presented as mean ± standard error of mean (n = 8/7/5/6, n = 7/5/5/4; paired t-test/Wilcoxon matched-pairs signed rank test: ns unless otherwise stated).

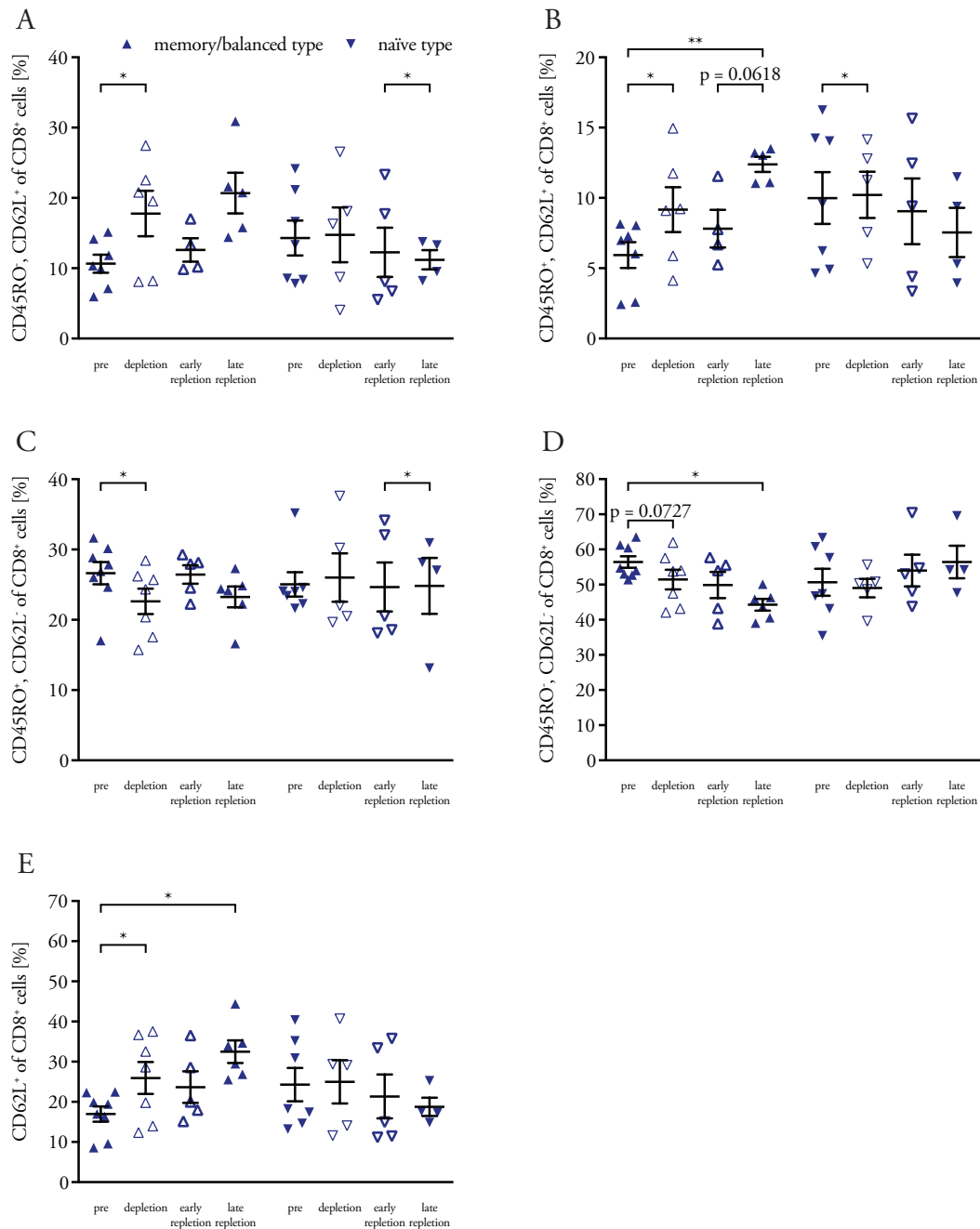
6.4.2 Data to CD8<sup>+</sup> T<sub>C</sub> cells

Figure A5. Differences in CD8<sup>+</sup> T<sub>C</sub> cells maturation and CD62L expression phenotype between memory/balanced and naïve type. The figure shows the frequencies of naïve (A), central memory (B), effector memory (C) and terminally differentiated (D) T<sub>C</sub> cells as well as frequencies of CD62L<sup>+</sup> T<sub>C</sub> cells (E) expressed as % of CD8<sup>+</sup> cells through four selected samples representing four selected time points for every patient. Data is presented as mean  $\pm$  standard error of mean (n = 8/7/5/6, n = 7/5/5/4; paired t-test/Wilcoxon matched-pairs signed rank test: ns unless otherwise stated; memory/balanced type: T<sub>N</sub> pre-late repletion p = 0.0333, T<sub>EM</sub> pre-late repletion p = 0.0314, all after Bonferroni-Holm correction: ns).

### 6.4.3 Data to CD14<sup>+</sup> myeloid cells

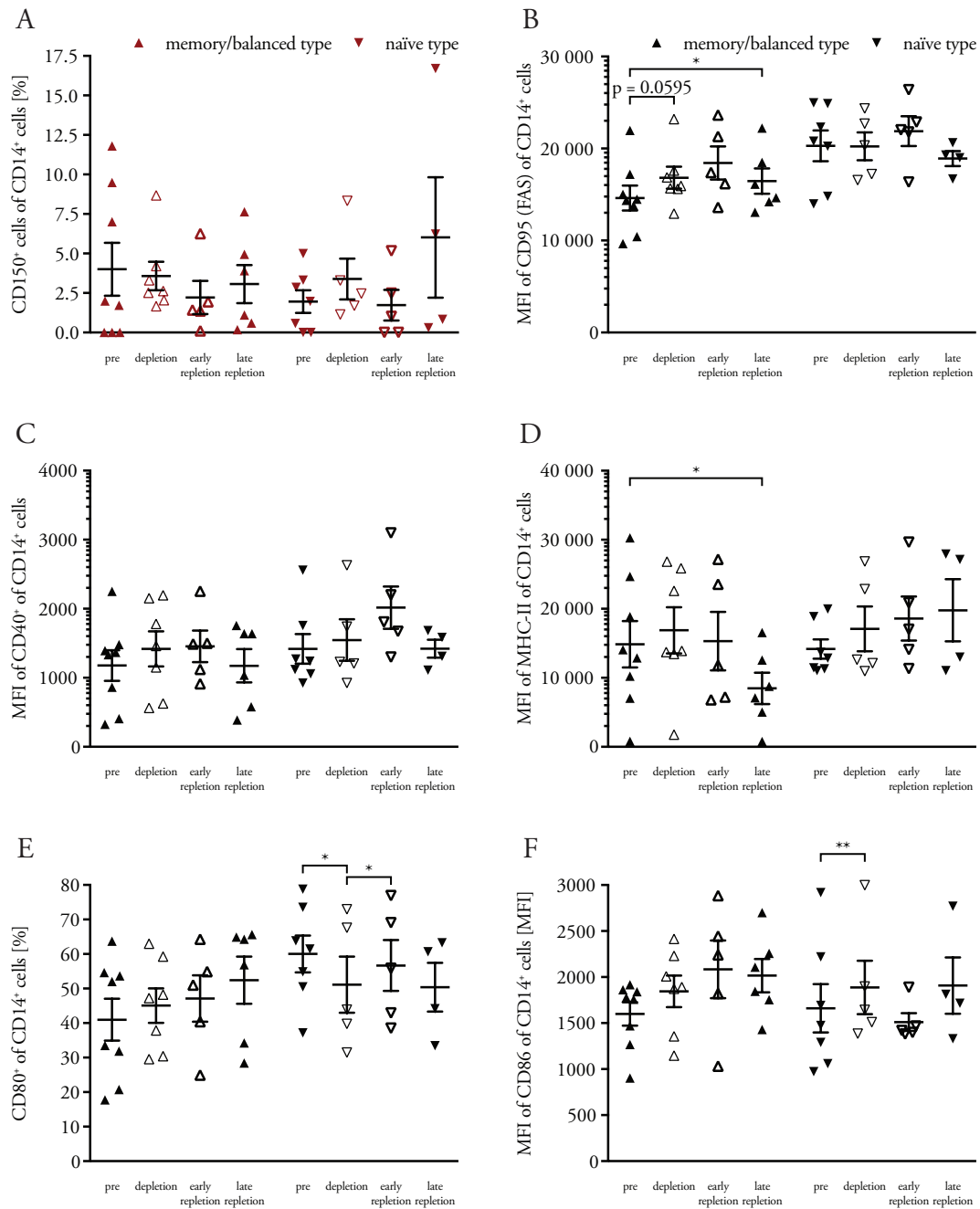


Figure A6. Differences in CD14<sup>+</sup> myeloid cells activation and APC phenotype between memory/balanced and naïve type. The figure shows the frequencies of CD150<sup>+</sup> (A) myeloid cells upon LPS stimulation [100 pg/ml] as shown in Table 11, and CD80<sup>+</sup> (E) myeloid cells both expressed as % of CD14<sup>+</sup> cells, MFIs of CD95 (FAS)<sup>+</sup> (B), CD40<sup>+</sup> (C) and MHC-II<sup>+</sup> (D) and CD86<sup>+</sup> (F) myeloid cells through four selected samples representing four selected time points for every patient. Data is presented as mean  $\pm$  standard error of mean (n = 8/7/5/6, n = 7/5/5/4; paired t-test/Wilcoxon matched-pairs signed rank test: ns unless otherwise stated).

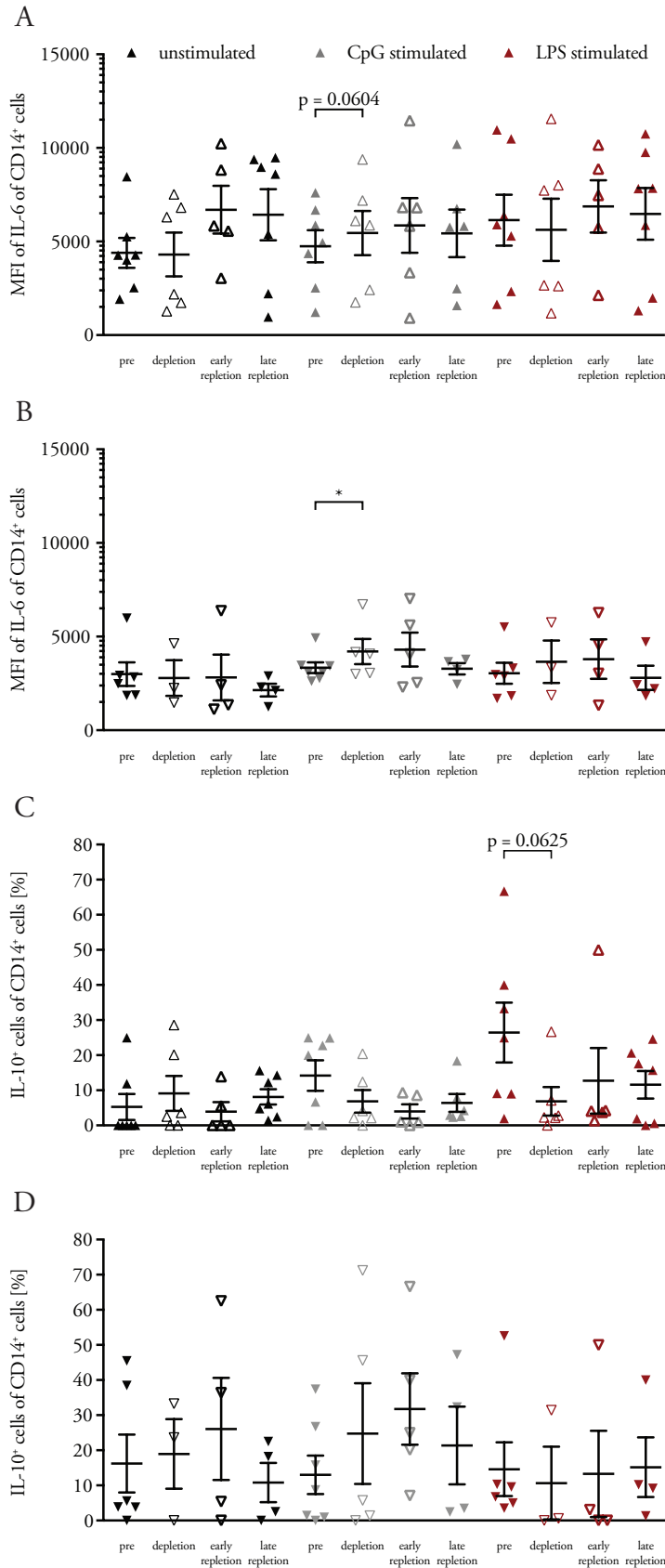


Figure A7. Differences in CD14<sup>+</sup> myeloid cells cytokine phenotype between memory/balanced and naïve type I. The figure shows the MFIs of IL-6<sup>+</sup> (A, B) and frequencies of IL-10<sup>+</sup> (C, D) myeloid cells expressed as % of CD14<sup>+</sup> cells unstimulated, upon CpG [1 µg/ml] and LPS [500 pg/ml] stimulation as shown in Table 11 through four selected samples representing four selected time points

for every patient. Figures A, C show the data for the patients with memory/balanced type, B, D for naïve type. Data is presented as mean  $\pm$  standard error of mean ( $n = 7/6/5/6,7$ ,  $n = 7,6/5,3/5,4/4$ ; paired t-test/Wilcoxon matched-pairs signed rank test: ns unless otherwise stated).

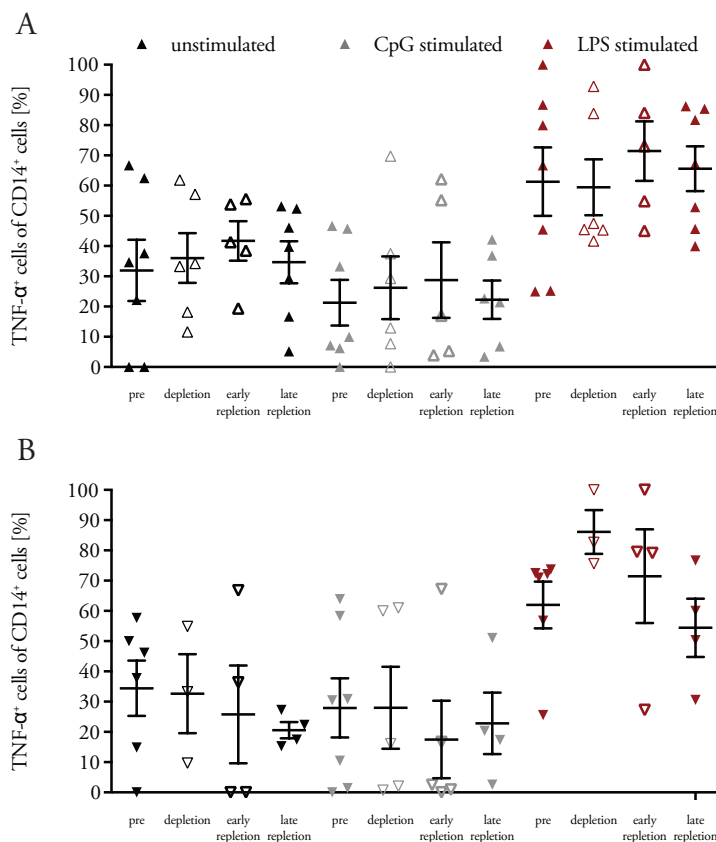


Figure A8. Differences in CD14<sup>+</sup> myeloid cells cytokine phenotype between memory/balanced and naïve type II. The figure shows the frequencies of TNF- $\alpha$ <sup>+</sup> myeloid cells expressed as % of CD14<sup>+</sup> cells unstimulated, upon CpG [1  $\mu$ g/ml] and LPS [500 pg/ml] stimulation as shown in Table 11 through four selected samples representing four selected time points for every patient. Figure A show the data for the patients with memory/balanced type, B for naïve type. Data is presented as mean  $\pm$  standard error of mean ( $n = 7/6/5/6,7$ ,  $n = 7,6/5,3/5,4/4$ ; paired t-test/Wilcoxon matched-pairs signed rank test: ns unless otherwise stated).

## 7 References

- Agrawal S, Gupta S (2011): TLR1/2, TLR7, and TLR9 signals directly activate human peripheral blood naive and memory b cell subsets to produce cytokines, chemokines, and hematopoietic growth factors. *J Clin Immunol* **31**, 89–98
- Ai W, Li H, Song N, Li L, Chen H (2013): Optimal method to stimulate cytokine production and its use in immunotoxicity assessment. *Int J Environ Res Public Health* **10**, 3834–3842
- Amu S, Tarkowski A, Dörner T, Bokarewa M, Brisslert M (2007): The human immunomodulatory cd25 + b cell population belongs to the memory b cell pool: Immunomodulatory CD25+ memory B cells. *Scand J Immunol* **66**, 77–86
- Arenas-Ramirez N, Woytschak J, Boyman O (2015): Interleukin-2: Biology, design and application. *Trends Immunol* **36**, 763–777
- Ascherio A, Munger KL (2007): Environmental risk factors for multiple sclerosis. Part I: The role of infection. *Ann Neurol* **61**, 288–299
- Ascherio A, Munger K (2016): Epidemiology of multiple sclerosis: From risk factors to prevention-an update. *Semin Neurol* **36**, 103–114
- Ascherio A, Munger KL, Lennette ET, Spiegelman D, Hernán MA, Olek MJ, Hankinson SE, Hunter DJ (2001): Epstein-Barr virus antibodies and risk of multiple sclerosis: A prospective study. *JAMA* **286**, 3083–3088
- Bach J-F (2002): The effect of infections on susceptibility to autoimmune and allergic diseases. *N Engl J Med* **347**, 911–920
- Banks WA, Kastin AJ, Gutierrez EG (1994): Penetration of interleukin-6 across the murine blood-brain barrier. *Neurosci Lett* **179**, 53–56
- Bar-Or A (2003): Analyses of all matrix metalloproteinase members in leukocytes emphasize monocytes as major inflammatory mediators in multiple sclerosis. *Brain* **126**, 2738–2749
- Barr TA, Shen P, Brown S, Lampropoulou V, Roch T, Lawrie S, Fan B, O'Connor RA, Anderton SM, Bar-Or A, et al. (2012): B cell depletion therapy ameliorates autoimmune disease through ablation of IL-6-producing B cells. *J Exp Med* **209**, 1001–1010
- Barun B, Bar-Or A (2012): Treatment of multiple sclerosis with anti-CD20 antibodies. *Clin Immunol Orlando Fla* **142**, 31–37
- Bastard JP, Jardel C, Delattre J, Hainque B, Bruckert E, Oberlin F (1999): Evidence for a link between adipose tissue interleukin-6 content and serum. *Circulation* **99**, 2221–2222
- Beltran E, Obermeier B, Moser M, Coret F, Simo-Castello M, Bosca I, Perez-Mirallas F, Villar LM, Senel M, Tumani H, et al. (2014): Intrathecal somatic hypermutation of IgM in multiple sclerosis and neuroinflammation. *Brain J Neurol* **137**, 2703–2714
- Berer K, Mues M, Koutrolas M, Rasbi ZA, Boziki M, Johnner C, Wekerle H, Krishnamoorthy G (2011): Commensal microbiota and myelin autoantigen cooperate to trigger autoimmune demyelination. *Nature* **479**, 538
- Bielekova B, Sung M-H, Kadom N, Simon R, McFarland H, Martin R (2004): Expansion and functional relevance of high-avidity myelin-specific CD4+ T cells in multiple sclerosis. *J Immunol* **172**, 3893–3904

- Bittner S, Ruck T, Wiendl H, Grauer OM, Meuth SG (2017): Targeting B cells in relapsing–remitting multiple sclerosis: From pathophysiology to optimal clinical management. *Ther Adv Neurol Disord* 10, 51–66
- Brisslert M, Bokarewa M, Larsson P, Wing K, Collins LV, Tarkowski A (2006): Phenotypic and functional characterization of human CD25+ B cells. *Immunology* 117, 548–557
- Brodin P, Jovic V, Gao T, Bhattacharya S, Angel CJL, Furman D, Shen-Orr S, Dekker CL, Swan GE, Butte AJ, et al. (2015): Variation in the human immune system is largely driven by non-heritable influences. *Cell* 160, 37–47
- Browne P, Chandraratna D, Angood C, Tremlett H, Baker C, Taylor BV, Thompson AJ (2014): Atlas of multiple sclerosis 2013: A growing global problem with widespread inequity. *Neurology* 83, 1022–1024
- Brück W, Gold R, Lund BT, Oreja-Guevara C, Prat A, Spencer CM, Steinman L, Tintoré M, Vollmer TL, Weber MS, et al. (2013): Therapeutic decisions in multiple sclerosis: Moving beyond efficacy. *JAMA Neurol* 70, 1315–1324
- Buckner JH (2010): Mechanisms of impaired regulation by CD4+CD25+FOXP3+ regulatory T cells in human autoimmune diseases. *Nat Rev Immunol* 10, 849–859
- Buljevac D, Hop WCJ, Reedeker W, Janssens ACJW, van der Meché FGA, van Doorn PA, Hintzen RQ (2003): Self reported stressful life events and exacerbations in multiple sclerosis: Prospective study. *BMJ* 327, 646
- Cambiaggi C, Scupoli MT, Cestari T, Gerosa F, Carra G, Tridente G, Accolla RS (1992): Constitutive expression of CD69 in interspecies T-cell hybrids and locus assignment to human chromosome 12. *Immunogenetics* 36, 117–120
- Cantorna MT, Snyder L, Lin Y-D, Yang L (2015): Vitamin D and 1,25(OH)<sub>2</sub>D regulation of T cells. *Nutrients* 7, 3011–3021
- Cao Y, Goods BA, Raddassi K, Nepom GT, Kwok WW, Love JC, Hafler DA (2015): Distinct inflammatory profiles of myelin-reactive T cells from patients with multiple sclerosis. *Sci Transl Med* 7, 287ra74
- Carswell R: *Pathological anatomy: Illustrations of the elementary forms of disease*. Longman, Orme, Brown, Green and Longman 1838
- Clifford DB, Ances B, Costello C, Rosen-Schmidt S, Andersson M, Parks D, Perry A, Yerra R, Schmidt R, Alvarez E, Tyler KL (2011): Rituximab-associated progressive multifocal leukoencephalopathy in rheumatoid arthritis. *Arch Neurol* 68, 1156–1164
- Compston A, Coles A (2008): Multiple sclerosis. *The Lancet* 372, 1502–1517
- Compston A, Confavreux C, Lassmann H, McDonald I, Miller D, Noseworthy J, Smith K, Wekerle H (Hrsg.): *McAlpine's multiple sclerosis (fourth edition)*. Churchill Livingstone, Edinburgh 2006
- Cotran RS, Kumar V, Collins T, Robbins SL: *Robbins pathologic basis of disease*. Saunders, Philadelphia 1999
- Cross AH, Stark JL, Lauber J, Ramsbottom MJ, Lyons J-A (2006): Rituximab reduces B cells and T cells in cerebrospinal fluid of multiple sclerosis patients. *J Neuroimmunol* 180, 63–70

- Dantzer R, O'Connor JC, Freund GG, Johnson RW, Kelley KW (2008): From inflammation to sickness and depression: When the immune system subjugates the brain. *Nat Rev Neurosci* **9**, 46–56
- Dua T, Rompani P, World Health Organization, Multiple Sclerosis International Federation (Hrsg.): Atlas: Multiple sclerosis resources in the world, 2008. World Health Organization, Geneva, Switzerland 2008
- Duddy M, Niino M, Adatia F, Hebert S, Freedman M, Atkins H, Kim HJ, Bar-Or A (2007): Distinct effector cytokine profiles of memory and naive human B cell subsets and implication in multiple sclerosis. *J Immunol* **178**, 6092–6099
- Elliott C, Lindner M, Arthur A, Brennan K, Jarius S, Hussey J, Chan A, Stroet A, Olsson T, Willison H, et al. (2012): Functional identification of pathogenic autoantibody responses in patients with multiple sclerosis. *Brain* **135**, 1819–1833
- Farina C, Theil D, Semlinger B, Hohlfeld R, Meinel E (2004): Distinct responses of monocytes to Toll-like receptor ligands and inflammatory cytokines. *Int Immunol* **16**, 799–809
- Feinstein A, Freeman J, Lo AC (2015): Treatment of progressive multiple sclerosis: What works, what does not, and what is needed. *Lancet Neurol* **14**, 194–207
- Fischer HJ, Finck TLK, Pellkofer HL, Reichardt HM, Lühder F (2019): Glucocorticoid therapy of multiple sclerosis patients induces anti-inflammatory polarization and increased chemotaxis of monocytes. *Front Immunol* **10**, 1200
- Friese MA, Schattling B, Fugger L (2014): Mechanisms of neurodegeneration and axonal dysfunction in multiple sclerosis. *Nat Rev Neurol* **10**, 225
- Frischer JM, Bramow S, Dal-Bianco A, Lucchinetti CF, Rauschka H, Schmidbauer M, Laursen H, Sorensen PS, Lassmann H (2009): The relation between inflammation and neurodegeneration in multiple sclerosis brains. *Brain* **132**, 1175–1189
- Gardiner-Garden M, Frommer M (1987): CpG islands in vertebrate genomes. *J Mol Biol* **196**, 261–282
- Genain CP, Cannella B, Hauser SL, Raine CS (1999): Identification of autoantibodies associated with myelin damage in multiple sclerosis. *Nat Med* **5**, 170–175
- Gingele S, Jacobus T, Konen F, Hümmert M, Sühs K-W, Schwenkenbecher P, Ahlbrecht J, Möhn N, Müschen L, Bönig L, et al. (2018): Ocrelizumab depletes CD20+ T cells in multiple sclerosis patients. *Cells* **8**, 12
- Gürçan HM, Keskin DB, Stern JNH, Nitzberg MA, Shekhani H, Ahmed AR (2009): A review of the current use of rituximab in autoimmune diseases. *Int Immunopharmacol* **9**, 10–25
- Habib J, Deng J, Lava N, Tyor W, Galipeau J (2015): Blood B cell and regulatory subset content in multiple sclerosis patients. *J Mult Scler* **21**, 2
- Haghikia A, Hohlfeld R, Gold R, Fugger L (2013): Therapies for multiple sclerosis: Translational achievements and outstanding needs. *Trends Mol Med* **19**, 309–319
- Hauser SL, Waubant E, Arnold DL, Vollmer T, Antel J, Fox RJ, Bar-Or A, Panzara M, Sarkar N, Agarwal S, et al. (2008): B-cell depletion with rituximab in relapsing-remitting multiple sclerosis. *N Engl J Med* **358**, 676–688

- Häusler D, Häusser-Kinzel S, Feldmann L, Torke S, Lepennetier G, Bernard CCA, Zamvil SS, Brück W, Lehmann-Horn K, Weber MS (2018): Functional characterization of reappearing B cells after anti-CD20 treatment of CNS autoimmune disease. *Proc Natl Acad Sci* 115, 9773–9778
- Hawker K, O'Connor P, Freedman MS, Calabresi PA, Antel J, Simon J, Hauser S, Waubant E, Vollmer T, Panitch H, et al. (2009): Rituximab in patients with primary progressive multiple sclerosis: Results of a randomized double-blind placebo-controlled multicenter trial. *Ann Neurol* 66, 460–471
- Hayes CE, Hubler SL, Moore JR, Barta LE, Praska CE, Nashold FE (2015): Vitamin D actions on CD4(+) T cells in autoimmune disease. *Front Immunol* 6, 100
- Hellings N, Barée M, Verhoeven C, D'hooghe MB, Medaer R, Bernard CCA, Raus J, Stinissen P (2001): T-cell reactivity to multiple myelin antigens in multiple sclerosis patients and healthy controls. *J Neurosci Res* 63, 290–302
- Hernan MA, Olek MJ, Ascherio A (2001): Cigarette smoking and incidence of multiple sclerosis. *Am J Epidemiol* 154, 69–74
- Hohlfeld R, Dornmair K, Meinel E, Wekerle H (2016): The search for the target antigens of multiple sclerosis, part 2: CD8+ T cells, B cells, and antibodies in the focus of reverse-translational research. *Lancet Neurol* 15, 317–331
- Holmes N (2006): CD45: all is not yet crystal clear. *Immunology* 117, 145–155
- Hyrich KL (2004): Anti-tumour necrosis factor therapy in rheumatoid arthritis: An update on safety. *Ann Rheum Dis* 63, 1538–1543
- International Multiple Sclerosis Genetics Consortium (IMSGC), Wellcome Trust Case Control Consortium 2 (WTCCC2), International IBD Genetics Consortium (IIBDGC), Beecham AH, Patsopoulos NA, Xifara DK, Davis MF, Kempainen A, Cotsapas C, Shah TS, et al. (2013): Analysis of immune-related loci identifies 48 new susceptibility variants for multiple sclerosis. *Nat Genet* 45, 1353–1360
- Jayne D (2010): Role of rituximab therapy in glomerulonephritis: Table 1. *J Am Soc Nephrol* 21, 14–17
- Ji Q, Castelli L, Goverman JM (2013): MHC class I-restricted myelin epitopes are cross-presented by Tip-DCs that promote determinant spreading to CD8+ T cells. *Nat Immunol* 14, 254–261
- Kabat EA, Freedman DA (1950): A study of the crystalline albumin, gamma globulin and total protein in the cerebrospinal fluid of 100 cases of multiple sclerosis and in other diseases. *Am J Med Sci* 219, 55–64
- Kamburova EG, Koenen HJPM, Borgman KJE, ten Berge IJ, Joosten I, Hilbrands LB (2013): A single dose of rituximab does not deplete B cells in secondary lymphoid organs but alters phenotype and function: Rituximab alters B cells in human lymph nodes. *Am J Transplant* 13, 1503–1511
- Kappos L, Hartung H-P, Freedman MS, Boyko A, Radü EW, Mikol DD, Lamarine M, Hyvert Y, Freudensprung U, Plitz T, van Beek J (2014): Atacicept in multiple sclerosis (ATAMS): A randomised, placebo-controlled, double-blind, phase 2 trial. *Lancet Neurol* 13, 353–363
- Kawabe T, Naka T, Yoshida K, Tanaka T, Fujiwara H, Suematsu S, Yoshida N, Kishimoto T, Kikutani H (1994): The immune responses in CD40-deficient mice: Impaired immunoglobulin class switching and germinal center formation. *Immunity* 1, 167–178

- Kebir H, Ifergan I, Alvarez JI, Bernard M, Poirier J, Arbour N, Duquette P, Prat A (2009): Preferential recruitment of interferon- $\gamma$ -expressing TH17 cells in multiple sclerosis. *Ann Neurol* **66**, 390–402
- Kim S-H, Kim W, Li XF, Jung I-J, Kim HJ (2011): Repeated treatment with rituximab based on the assessment of peripheral circulating memory B cells in patients with relapsing neuromyelitis optica over 2 years. *Arch Neurol* **68**, 1412–1420
- Kim S-H, Huh S-Y, Lee SJ, Joung A, Kim HJ (2013): A 5-year follow-up of rituximab treatment in patients with neuromyelitis optica spectrum disorder. *JAMA Neurol* **70**, 1110
- Kohn LA, Hao Q-L, Sasidharan R, Parekh C, Ge S, Zhu Y, Mikkola HKA, Crooks GM (2012): Lymphoid priming in human bone marrow begins prior to CD10 expression with up-regulation of L-selectin. *Nat Immunol* **13**, 963–971
- Kouwenhoven M, Teleshova N, Ozenci V, Press R, Link H (2001): Monocytes in multiple sclerosis: Phenotype and cytokine profile. *J Neuroimmunol* **112**, 197–205
- Kowarik MC, Cepok S, Sellner J, Grummel V, Weber MS, Korn T, Berthele A, Hemmer B (2012): CXCL13 is the major determinant for B cell recruitment to the CSF during neuroinflammation. *J Neuroinflammation* **2**, 93
- Kozovska ME, Hong J, Zang YCQ, Li S, Rivera VM, Killian JM, Zhang JZ (1999): Interferon beta induces T-helper 2 immune deviation in MS. *Neurology* **53**, 1692
- Krumbholz M, Theil D, Derfuss T, Rosenwald A, Schrader F, Monoranu C-M, Kalled SL, Hess DM, Serafini B, Aloisi F, et al. (2005): BAFF is produced by astrocytes and up-regulated in multiple sclerosis lesions and primary central nervous system lymphoma. *J Exp Med* **201**, 195–200
- Krumbholz M, Theil D, Cepok S, Hemmer B, Kivisäkk P, Ransohoff RM, Hofbauer M, Farina C, Derfuss T, Hartle C, et al. (2006): Chemokines in multiple sclerosis: CXCL12 and CXCL13 up-regulation is differentially linked to CNS immune cell recruitment. *Brain* **129**, 200–211
- Kuhlmann T, Lingfeld G, Bitsch A, Schuchardt J, Brück W (2002): Acute axonal damage in multiple sclerosis is most extensive in early disease stages and decreases over time. *Brain* **125**, 2202–2212
- Kurtzke JF (1983): Rating neurologic impairment in multiple sclerosis: An expanded disability status scale (EDSS). *Neurology* **33**, 1444–1452
- Kverneland AH, Streitz M, Geissler E, Hutchinson J, Vogt K, Boës D, Niemann N, Pedersen AE, Schlickeiser S, Sawitzki B (2016): Age and gender leucocytes variances and references values generated using the standardized ONE-Study protocol: Age and gender leucocytes variances and references values using ONE-study protocol. *Cytometry A* **89**, 543–564
- Lang HLE, Jacobsen H, Ikemizu S, Andersson C, Harlos K, Madsen L, Hjorth P, Sondergaard L, Svejgaard A, Wucherpfennig K, et al. (2002): A functional and structural basis for TCR cross-reactivity in multiple sclerosis. *Nat Immunol* **3**, 940–943
- Lanzavecchia A (1985): Antigen-specific interaction between T and B cells. *Nature* **314**, 537–539
- Lassmann H, Raine CS, Antel J, Prineas JW (1998): Immunopathology of multiple sclerosis: Report on an international meeting held at the Institute of Neurology of the University of Vienna. *J Neuroimmunol* **86**, 213–217
- Leandro MJ (2013): B-cell subpopulations in humans and their differential susceptibility to depletion with anti-CD20 monoclonal antibodies. *Arthritis Res Ther* **15**, S3

- Leandro MJ, Cambridge G, Ehrenstein MR, Edwards JCW (2006): Reconstitution of peripheral blood B cells after depletion with rituximab in patients with rheumatoid arthritis. *Arthritis Rheum* 54, 613–620
- Lehmann-Horn K, Schleich E, Hertenberg D, Hapfelmeier A, Kümpfel T, von Bubnoff N, Hohlfeld R, Berthele A, Hemmer B, Weber MS (2011): Anti-CD20 B-cell depletion enhances monocyte reactivity in neuroimmunological disorders. *J Neuroinflammation* 8, 146
- Levin LI, Munger KL, O'Reilly EJ, Falk KI, Ascherio A (2010): Primary infection with the Epstein-Barr virus and risk of multiple sclerosis. *Ann Neurol* 67, 824–830
- Liao W, Lin J-X, Leonard WJ (2011): IL-2 Family Cytokines: New insights into the complex roles of IL-2 as a broad regulator of T helper cell differentiation. *Curr Opin Immunol* 23, 598–604
- Liu F, Bardhan K, Yang D, Thangaraju M, Ganapathy V, Waller JL, Liles GB, Lee JR, Liu K (2012): NF- $\kappa$ B directly regulates fas transcription to modulate Fas-mediated apoptosis and tumor suppression. *J Biol Chem* 287, 25530–25540
- LL 31 2012 Diagnose und Therapie der Multiplen Sklerose. <https://www.dgn.org/leitlinien/2333-ll-31-2012-diagnose-und-therapie-der-multiplen-sklerose#therapie>; Zugriff am 25.02.2019
- Lublin FD, Reingold SC, National Multiple Sclerosis Society (USA) Advisory committee on clinical trials of new agents in multiple sclerosis\* (1996): Defining the clinical course of multiple sclerosis: Results of an international survey. *Neurology* 46, 907–911
- Lucchinetti C, Brück W, Parisi J, Scheithauer B, Rodriguez M, Lassmann H (2000): Heterogeneity of multiple sclerosis lesions: Implications for the pathogenesis of demyelination. *Ann Neurol* 47, 707–717
- Lucchinetti CF, Brück W, Rodriguez M, Lassmann H (1996): Distinct patterns of multiple sclerosis pathology indicates heterogeneity on pathogenesis. *Brain Pathol Zurich Switz* 6, 259–274
- Mahad DJ, Ziabreva I, Campbell G, Lax N, White K, Hanson PS, Lassmann H, Turnbull DM (2009): Mitochondrial changes within axons in multiple sclerosis. *Brain J Neurol* 132, 1161–1174
- Mahnke YD, Brodie TM, Sallusto F, Roederer M, Lugli E (2013): The who's who of T-cell differentiation: Human memory T-cell subsets. *Eur J Immunol* 43, 2797–2809
- Marrosu MG, Muntoni F, Murru MR, Costa G, Pischedda MP, Pirastu M, Sotgiu S, Rosati G, Cianchetti C (1992): HLA-DQB1 genotype in Sardinian multiple sclerosis: Evidence for a key role of DQB1 \*0201 and \*0302 alleles. *Neurology* 42, 883–886
- Martin M del P, Cravens PD, Winger R, Kieseier BC, Cepok S, Eagar TN, Zamvil SS, Weber MS, Frohman EM, Kleinschmidt-Demasters BK, et al. (2009): Depletion of B lymphocytes from cerebral perivascular spaces by rituximab. *Arch Neurol* 66, 1016–1020
- Martyn CN, Cruddas M, Compston DA (1993): Symptomatic Epstein-Barr virus infection and multiple sclerosis. *J Neurol Neurosurg Psychiatry* 56, 167–168
- Maurer MA, Tuller F, Gredler V, Berger T, Lutterotti A, Lünemann JD, Reindl M (2016): Rituximab induces clonal expansion of IgG memory B-cells in patients with inflammatory central nervous system demyelination. *J Neuroimmunol* 290, 49–53
- Melzer N, Meuth SG (2014): Disease-modifying therapy in multiple sclerosis and chronic inflammatory demyelinating polyradiculoneuropathy: Common and divergent current and future strategies. *Clin Exp Immunol* 175, 359–372

- Memon AB, Javed A, Caon C, Srivastawa S, Bao F, Bernitsas E, Chorostecki J, Tselis A, Seraji-Bozorgzad N, Khan O (2018): Long-term safety of rituximab induced peripheral B-cell depletion in autoimmune neurological diseases. *PLoS One* **13**, e0190425
- Mikaeloff Y, Caridade G, Tardieu M, Suissa S, on behalf of the KIDSEP study group (2007): Parental smoking at home and the risk of childhood-onset multiple sclerosis in children. *Brain* **130**, 2589–2595
- Miron VE, Boyd A, Zhao J-W, Yuen TJ, Ruckh JM, Shadrach JL, van Wijngaarden P, Wagers AJ, Williams A, Franklin RJM, French-Constant C (2013): M2 microglia/macrophages drive oligodendrocyte differentiation during CNS remyelination. *Nat Neurosci* **16**, 1211–1218
- Molnarfi N, Schulze-Topphoff U, Weber MS, Patarroyo JC, Prod'homme T, Varrin-Doyer M, Shetty A, Linington C, Slavin AJ, Hidalgo J, et al. (2013): MHC class II-dependent B cell APC function is required for induction of CNS autoimmunity independent of myelin-specific antibodies. *J Exp Med* **210**, 2921–2937
- Moore KW, de Waal Malefyt R, Coffman RL, O'Garra A (2001): Interleukin-10 and the interleukin-10 receptor. *Annu Rev Immunol* **19**, 683–765
- Morbach H, Eichhorn EM, Liese JG, Girschick HJ (2010): Reference values for B cell subpopulations from infancy to adulthood. *Clin Exp Immunol* **162**, 271–279
- Mosser DM, Zhang X (2008): Interleukin-10: new perspectives on an old cytokine. *Immunol Rev* **226**, 205–218
- Mundt S, Mrdjen D, Utz SG, Greter M, Schreiner B, Becher B (2019): Conventional DCs sample and present myelin antigens in the healthy CNS and allow parenchymal T cell entry to initiate neuroinflammation. *Sci Immunol* **4**, eaau8380
- Münz C, Lünemann JD, Getts MT, Miller SD (2009): Antiviral immune responses: Triggers of or triggered by autoimmunity? *Nat Rev Immunol* **9**, 246–258
- Niedel JE, Kuhn LJ, Vandenbark GR (1983): Phorbol diester receptor copurifies with protein kinase C. *Proc Natl Acad Sci U S A* **80**, 36–40
- Obermeier B, Mentele R, Malotka J, Kellermann J, Kümpfel T, Wekerle H, Lottspeich F, Hohlfeld R, Dormair K (2008): Matching of oligoclonal immunoglobulin transcriptomes and proteomes of cerebrospinal fluid in multiple sclerosis. *Nat Med* **14**, 688
- Olerup O, Hillert J (1991): HLA class II-associated genetic susceptibility in multiple sclerosis: a critical evaluation. *Tissue Antigens* **38**, 1–15
- Owen JA, Punt Jenni, Stranford SA, Jones PP, Kuby Janis: *Kuby immunology*. W.H. Freeman, New York 2013
- Pers J-O, Daridon C, Bendaoud B, Devauchelle V, Berthou C, Saraux A, Youinou P (2007): B-Cell depletion and repopulation in autoimmune diseases. *Clin Rev Allergy Amp Immunol* **34**, 50–55
- Qin Y, Duquette P, Zhang Y, Talbot P, Poole R, Antel J (1998): Clonal expansion and somatic hypermutation of V(H) genes of B cells from cerebrospinal fluid in multiple sclerosis. *J Clin Invest* **102**, 1045–1050
- Quintana FJ, Patel B, Yeste A, Nyirenda M, Kenison J, Rahbari R, Fetco D, Hussain M, O'Mahony J, Magalhaes S, et al. (2014): Epitope spreading as an early pathogenic event in pediatric multiple sclerosis. *Neurology* **83**, 2219–2226

- Ramagopalan SV, Morris AP, Dyment DA, Herrera BM, DeLuca GC, Lincoln MR, Orton SM, Chao MJ, Sadovnick AD, Ebers GC (2007): The inheritance of resistance alleles in multiple sclerosis. *PLoS Genet* **3**, 1607–1613
- Ramirez-Ortiz ZG, Specht CA, Wang JP, Lee CK, Bartholomeu DC, Gazzinelli RT, Levitz SM (2008): Toll-Like Receptor 9-dependent immune activation by unmethylated CpG motifs in *aspergillus fumigatus* DNA. *Infect Immun* **76**, 2123–2129
- Ransohoff RM, Engelhardt B (2012): The anatomical and cellular basis of immune surveillance in the central nervous system. *Nat Rev Immunol* **12**, 623–635
- Reff ME, Camer K, Chambers KS, Chinn PC, Leonard JE, Raab R, Newman RA, Hanna N, Anderson DR (1994): Depletion of B cells in vivo by a chimeric mouse human monoclonal antibody to CD20. *Blood* **83**, 435–445
- Roll P, Palanichamy A, Kneitz C, Dorner T, Tony H-P (2006): Regeneration of B cell subsets after transient B cell depletion using anti-CD20 antibodies in rheumatoid arthritis. *Arthritis Rheum* **54**, 2377–2386
- Rothfield L, Pearlman-Kothencz M (1969): Synthesis and assembly of bacterial membrane components. A lipopolysaccharide-phospholipid-protein complex excreted by living bacteria. *J Mol Biol* **44**, 477–492
- Rubtsova K, Marrack P, Rubtsov AV (2012): Age-associated B cells: Are they the key to understanding why autoimmune diseases are more prevalent in women? *Expert Rev Clin Immunol* **8**, 5–7
- Sakaguchi S, Sakaguchi N, Asano M, Itoh M, Toda M (1995): Immunologic self-tolerance maintained by activated T cells expressing IL-2 receptor alpha-chains (CD25). Breakdown of a single mechanism of self-tolerance causes various autoimmune diseases. *J Immunol Baltim Md* **155**, 1151–1164
- Sallusto F, Geginat J, Lanzavecchia A (2004): Central memory and effector memory T cell subsets: Function, generation, and maintenance. *Annu Rev Immunol* **22**, 745–763
- Sathaliyawala T, Kubota M, Yudanin N, Turner D, Camp P, Thome JJC, Bickham KL, Lerner H, Goldstein M, Sykes M, et al. (2013): Distribution and compartmentalization of human circulating and tissue-resident memory T cell subsets. *Immunity* **38**, 187–197
- Sawcer S, Franklin RJM, Ban M (2014): Multiple sclerosis genetics. *Lancet Neurol* **13**, 700–709
- Schneider P (2005): The role of APRIL and BAFF in lymphocyte activation. *Curr Opin Immunol* **17**, 282–289
- Schuh E, Berer K, Mulazzani M, Feil K, Meinel I, Lahm H, Krane M, Lange R, Pfannes K, Subklewe M, et al. (2016): Features of human CD3+CD20+ T cells. *J Immunol* **197**, 1111–1117
- Serafini B, Rosicarelli B, Magliozzi R, Stigliano E, Aloisi F (2004): Detection of ectopic B-cell follicles with germinal centers in the meninges of patients with secondary progressive multiple sclerosis. *Brain Pathol* **14**, 164–174
- Sorensen PS, Blinkenberg M (2016): The potential role for ocrelizumab in the treatment of multiple sclerosis: current evidence and future prospects. *Ther Adv Neurol Disord* **9**, 44–52
- Souto-Cameiro MM, Mahadevan V, Takada K, Fritsch-Stork R, Nanki T, Brown M, Fleisher TA, Wilson M, Goldbach-Mansky R, Lipsky PE (2009): Alterations in peripheral blood memory B cells in patients with active rheumatoid arthritis are dependent on the action of tumour necrosis factor. *Arthritis Res Ther* **11**, R84

- Storie I, Wilson GA, Granger V, Barnett D, Reilly JT (1995): Circulating CD20dim T-lymphocytes increase with age: Evidence for a memory cytotoxic phenotype. *Clin Lab Haematol* 17, 323–328
- Surh CD, Sprent J (2008): Homeostasis of naive and memory T cells. *Immunity* 29, 848–862
- Svenningsson A, Bergman J, Dring A, Vågberg M, Birgander R, Lindqvist T, Gilthorpe J, Bergenheim T (2015): Rapid depletion of B lymphocytes by ultra-low-dose rituximab delivered intrathecally. *Neurol Neuroimmunol Neuroinflammation* 2, e79
- Theil D, Farina C, Meinel E (2005): Differential expression of CD150 (SLAMF) on monocytes and macrophages in chronic inflammatory contexts: abundant in Crohn's disease, but not in multiple sclerosis. *J Clin Pathol* 58, 110–111
- Thompson AJ, Banwell BL, Barkhof F, Carroll WM, Coetzee T, Comi G, Correale J, Fazekas F, Filippi M, Freedman MS, et al. (2018): Diagnosis of multiple sclerosis: 2017 revisions of the McDonald criteria. *Lancet Neurol* 17, 162–173
- Titelbaum DS, Degenhardt A, Kinkel RP (2005): Anti-tumor necrosis factor alpha-associated multiple sclerosis. *AJNR Am J Neuroradiol* 26, 1548–1550
- Trapp BD, Peterson J, Ransohoff RM, Rudick R, Mörk S, Bö L (1998): Axonal Transection in the Lesions of Multiple Sclerosis. *N Engl J Med* 338, 278–285
- Underhill DM, Ozinsky A (2002): Toll-like receptors: Key mediators of microbe detection. *Curr Opin Immunol* 14, 103–110
- Vieira PL, Heystek HC, Wormmeester J, Wierenga EA, Kapsenberg ML (2003): Glatiramer acetate (Copolymer-1, Copaxone) promotes Th2 cell development and increased IL-10 production through modulation of dendritic cells. *J Immunol* 170, 4483–4488
- von Essen MR, Ammitzbøll C, Hansen RH, Petersen ERS, McWilliam O, Marquart HV, Damm P, Sellebjerg F (2019): Proinflammatory CD20+ T cells in the pathogenesis of multiple sclerosis. *Brain* 142, 120–132
- Wajant H (2002): The Fas signaling pathway: More than a paradigm. *Science* 296, 1635
- Weber MS, Hemmer B, Cepok S (2011): The role of antibodies in multiple sclerosis. *Biochim Biophys Acta BBA - Mol Basis Dis* 1812, 239–245
- Weinshenker BG, Bass B, Rice GP, Noseworthy J, Carriere W, Baskerville J, Ebers GC (1989): The natural history of multiple sclerosis: a geographically based study. I. Clinical course and disability. *Brain J Neurol* 112 (Pt 1), 133–146
- Wucherpfennig KW, Sethi D (2011): T cell receptor recognition of self and foreign antigens in the induction of autoimmunity. *Semin Immunol* 23, 84–91
- Ziegler SF, Ramsdell F, Alderson MR (1994): The activation antigen CD69. *Stem Cells Dayt Ohio* 12, 456–465
- Zoghi S, Amirghofran Z, Nikseresht A, Ashjzadeh N, Kamali-Sarvestani E, Rezaei N (2011): Cytokine secretion pattern in treatment of lymphocytes of multiple sclerosis patients with fumaric acid esters. *Immunol Invest* 40, 581–596

## Acknowledgments

Firstly, I would like to thank Martin Weber, my supervisor, who gave me the opportunity to work in his research group. I am grateful for all his guidance, scientific expertise, personal teaching, help and support. With his help I have learned to develop my own ideas and theories.

I thank Fred Lühder for his help and constructive criticism during my progress report meetings and after. I especially thank him for not accepting anything but perfect.

I thank the members of the Weber research group for their help and advice. I specially wish to thank Katja Grondey and Jan Traub who instructed and assisted me in both methods and experiments, and Sebastian Torke, whose advice helped me with my paper. Furthermore I wish to thank Jasmin Ochs and Julian Koch for their assistance.

Further I wish to thank Silke Häusser-Kinzel, whose advice helped me to better argue my theories and hypotheses.

I wish to thank Cynthia Bunker, Heidi Berns and Bernd Zirk for their support.

I thank the Gerhard C. Stark Stiftung for their support and endorsement.

I thank my parents, who always encouraged and helped me to achieve my dreams.

This work is dedicated to Wolfgang Brück, without whom nothing is possible, and with whom everything is.

## **Curriculum vitae**

For data protection reasons I wish not to publish my résumé in the electronic version of my work.